UC San Diego
UC San Diego Electronic Theses and Dissertations

Title

Beyond the name : p75 neurotrophin receptor as a regulator of hepatic stellate cell differentiation in liver repair

Permalink

https://escholarship.org/uc/item/1wv4j99s

Author

Passino, Melissa Ann

Publication Date

2007

Peer reviewed|Thesis/dissertation

UNIVERSITY OF CALIFORNIA, SAN DIEGO

Beyond the name: p75 neurotrophin receptor as a regulator of
hepatic stellate cell differentiation in liver repair

A Dissertation submitted in partial satisfaction of the requirements for the degree

Doctor of Philosophy

in

Biomedical Sciences

by

Melissa Ann Passino

Committee in charge:

      Professor Katerina Akassoglou, Chair
      Professor Kim E. Barrett
      Professor Russell F. Doolittle
      Professor Palmer W. Taylor
      Professor Anthony Wynshaw-Boris

2007

The Dissertation of Melissa Ann Passino is approved, and it is acceptable in quality and form for publication on microfilm:

_____

_____

_____

_____

_____
Chair

University of California, San Diego

2007

DEDICATION

This thesis is dedicated to my mother and to my grandparents, whose ultimate examples of strength, sacrifice, and perseverance have provided lasting repercussions for which I am forever indebted.

TABLE OF CONTENTS

LIST OF ABBREVIATIONS

aa	amino acid(s)
Ad	adenovirus
AEC	3-amino-9-ethylcarbazole
ANOVA	analysis of variance
AP-1	activator protein-1
αSMA	α-smooth muscle actin
AT-1	angiotensin receptor
BDNF	brain derived neurotrophic factor
BrdU	5-bromo-2'-deoxyuridine
BSA	bovine serum albumin
CCl_4	carbon tetrachloride
cDNA	complementary deoxyribonucleic acid
C/EBP	CCAAT/enhancer binding protein
CNS	central nervous system
Col1α1	collagen I α1 gene
CRD	cysteine-rich domain
CREB	cAMP response element-binding protein
Cy3	cyanine 3
DAPI	4',6-Diamidine-2'-phenylindole
ddH_2O	double deionized water
DMEM	Dulbecco's Modified Eagle's Medium

DMSO	dimethyl sulfoxide
DNA	deoxyribonucleic acid
DTT	dithiothreitol
ECD	extracellular domain
ECL	enhanced chemiluminescence
ECM	extracellular matrix
EDTA	ethylenediaminetetraacetic acid
EGTA	ethylene glycol-bis(2-aminoethylether)-*N,N,N',N'*-tetraacetic acid
ELISA	enzyme-linked immunosorbent assay
ERK	extracellular signal-regulated kinase
F_1	first filial generation
FBS	fetal bovine serum
Fc	Fc fragment of immunoglobulin G
FITC	fluorescein isothiocyanate
FL	full length
FLAG	8 amino acid FLAG peptide tag
FPLC	fast performance liquid chromatography
Fwd	forward/sense primer
GAPDH	glyceraldehyde-3-phosphate dehydrogenase
GFAP	glial fibrillary acidic protein
Gly-Pro-Arg	glycine-proline-arginine peptide
GTPase	guanosine triphosphatase

[^{3}H]	tritium/tritiated
HBSS	Hanks' balanced salt solution
HCl	hydrochloride/hydrochloric acid
HEK	human embryonic kidney
Hepes	N-(2-Hydroxyethyl)piperazine-N'-(2-ethanesulfonic acid)
HGF	hepatocyte growth factor
HPRT	hypoxanthine-guanine phosphoribosyltransferase
HSC	hepatic stellate cell
ICAM	intracellular adhesion molecule
ICD	intracellular domain
IgG	immunoglobulin G
IL	interleukin
i.p.	intraperitoneally
JNK	c-Jun N-terminal kinase
K_d	dissociation constant
KSCN	potassium thiocyanate
Lenti	lentivirus
MAG	myelin-associated glycoprotein
MMP	matrix metalloproteinase
MOI	multiplicity of infection
mRNA	messenger ribonucleic acid
NaBr	sodium bromide

NaCl	sodium chloride
NaOAc	sodium acetate
NaOH	sodium hydroxide
NCAM	neural cell adhesion molecule
NF-κB	nuclear factor-κB
NGF	nerve growth factor
NGFR	nerve growth factor receptor
NogoR	Nogo receptor
NRAGE	neurotrophin receptor-interacting MAGE homolog
NRIF	neurotrophin receptor interacting factor
NT	neurotrophin
OmGP	oligodendrocyte-myelin glycoprotein
p75^{NTR}	p75 neurotrophin receptor
PAGE	polyacrylamide gel electrophoresis
PBS	phosphate buffered saline
PCR	polymerase chain reaction
PDGF	platelet-derived growth factor
PET	polyethylene terephthalate
PFA	paraformaldehyde
PHx	partial hepatectomy
PI3 kinase	phosphatidyl inositol 3 kinase
plg	plasminogen gene
PMSF	phenylmethanesulfonyl fluoride

PNS	peripheral nervous system
PPAR	peroxisome proliferator-activated receptor
PrP	prion protein
PVDF	polyvinyl difluoride
Rev	reverse/antisense primer
RNA	ribonucleic acid
RT	reverse transcription
SD	standard deviation
SDS	sodium dodecyl sulfate
SEM	standard error of the mean
shRNA	short hairpin ribonucleic acid
siRNA	small interfering ribonucleic acid
SRF	serum response factor
TBS	Tris buffered saline
TBS-T	Tris buffered saline with Tween-20
TCA	trichloroacetic acid
TGFβ-1	transforming growth factor β-1
TIMP	tissue inhibitor of metalloproteinases
TNFR	tumor necrosis factor receptor
TR	truncated
Trk	tropomyosin-related kinase
wt	wild-type

LIST OF FIGURES

LIST OF TABLES

ACKNOWLEDGMENTS

technical assistance with Biacore binding experiments and molecular biology, respectively.

Lastly I would like to thank Sara Epperson, Jennie Bever, Jeremy Babendure, Anne Valle, Larry Brunton, and all of my other friends in the Pharmacology department and BMS graduate program, as well as all of my family members, especially my sister Katie, for their continual and unconditional moral support, without which I would have never made it through graduate school. "The best thing you've ever done for me is to help me take my life less seriously, it's only life, afterall."

VITA

Education

2007   Ph.D., Biomedical Sciences
University of California, San Diego

2001   B.A., Biochemistry (Magna Cum Laude)
Tufts University, Medford, Massachusetts

Research Fellowships and Awards

2006   Ray Thomas Edwards Foundation Travel Award,
Society for Neuroscience 36th Annual Meeting

2006   Young Investigators' Bursary Award,
European Association for the Study of the Liver

Sept. 2001 – Aug. 2005   Pharmacology Training Grant Fellow

2001   Phi Beta Kappa Society, lifetime member

2001   Audrey Butvay Gruss Science Award

2001   T.H. Carmichael and E.L. Carmichael Prize Scholarship
in Physiology

2000   R.M. Karapetoff Cobb Chemistry Award

2000   Howard Hughes Summer Undergraduate Fellow

2000   Golden Key National Honor Society, lifetime member

Publications

1. **Passino MA**, Adams RA, Sikorski SL, Akassoglou K. Regulation of hepatic stellate cell differentiation by the neurotrophin receptor $p75^{NTR}$. *Science*, in press. (Data from Chapter 3.)

2. **Passino MA**, Schachtrup C, Akassoglou K. Binding of fibrinogen fragment D to $p75^{NTR}$ causes neuronal apoptosis. (Data from Chapter 4, in preparation.)

3. **Passino MA**, Sachs BD, Akassoglou K. The biological functions of p75^{NTR}: intracellular signaling pathways as novel targets for drug discovery. *Drug Discov. Today*, in preparation.

4. Sachs BD, McCall JR, Wallace DA, Zhang J, **Passino MA**, Schachtrup C, Baillie GS, Klussmann E, Lynch MJ, Sikorski SL, Nuriel T, Tsigelny I, Houslay MD, Chao MV, Akassoglou K. p75 neurotrophin receptor regulates tissue fibrosis through inhibition of plasminogen activation via a PDE4/cAMP/PKA pathway. *J Cell Biol.*, submitted.

5. Adams RA, **Passino MA**, Sachs BD, Nuriel T, Akassoglou K. Fibrin mechanisms and functions in nervous system pathology. *Mol. Interv.*, 2004, 4(3): 163-176.

Abstracts

1. **Passino M**, Sikorski S, Akassoglou K. p75 neurotrophin receptor promotes liver repair via regulation of hepatic stellate cell differentiation: a novel function for non-neuronal p75^{NTR}. Society for Neuroscience 36th Annual Meeting, Atlanta, GA, October 2006. Poster presentation.

2. **Passino M**, Sikorski S, Akassoglou K. Loss of p75 neurotrophin receptor exacerbates the effects of plasminogen deficiency. International Society for Fibrinolysis and Proteolysis 18th International Congress, San Diego, CA, August 2006. Oral presentation.

3. **Passino M**, Sikorski S, Akassoglou K. p75 neurotrophin receptor promotes liver regeneration via regulation of hepatic stellate cell differentiation. European Association for the Study of the Liver 41st Annual Meeting, Vienna, Austria, April 2006. Oral presentation.

4. **Passino M**, Sikorski S, Akassoglou K. Loss of p75 neurotrophin receptor exacerbates the effects of plasminogen deficiency. Gordon Research Conference for Plasminogen Activation & Extracellular Proteolysis, Ventura, CA, February 2006. Poster and oral presentations.

ABSTRACT OF THE DISSERTATION

Beyond the name: p75 neurotrophin receptor as a regulator of

hepatic stellate cell differentiation in liver repair

by

Melissa Ann Passino

Doctor of Philosophy in Biomedical Sciences

University of California, San Diego, 2007

Professor Katerina Akassoglou, Chair

Although the p75 neurotrophin receptor ($p75^{NTR}$) has been primarily studied as a regulator of cell survival and apoptosis in the nervous system, $p75^{NTR}$ also exhibits widespread expression in non-neuronal tissues which can be upregulated after tissue injury. However, the biological significance of injury-induced, non-neuronal expression of $p75^{NTR}$ remains enigmatic. In human fibrotic and cirrhotic liver disease, $p75^{NTR}$ is upregulated exclusively by hepatic stellate cells (HSCs), liver cells with neuroendocrine characteristics that can differentiate to activated matrix-producing

myofibroblasts after liver injury. The work performed for my dissertation studies has led to the discovery of a novel function for p75$^{\text{NTR}}$ in the regulation of HSC differentiation which can support a repair-promoting crosstalk between HSCs and hepatocytes after liver injury. In the *plg-/-* mouse model of liver injury, loss of p75$^{\text{NTR}}$ resulted in exacerbated liver pathology and inhibited HSC activation *in vivo*. *In vitro*, *p75$^{\text{NTR}}$-/-* HSCs failed to differentiate, and adenoviral delivery of *p75$^{\text{NTR}}$* restored activation in *p75$^{\text{NTR}}$-/-* HSCs, suggesting that p75$^{\text{NTR}}$ is necessary for HSC differentiation. HSC differentiation was neurotrophin-independent, and expression of the intracellular domain of p75$^{\text{NTR}}$ alone was sufficient to promote HSC activation. *p75$^{\text{NTR}}$-/-* HSCs exhibited loss of Rho activation compared to wild-type HSCs, and restoration of Rho activity completely rescued the differentiation of *p75$^{\text{NTR}}$-/-* HSCs. Moreover, inhibition of p75$^{\text{NTR}}$-mediated Rho activation prevented activation of wild-type HSCs, suggesting that p75$^{\text{NTR}}$ signaling through Rho promotes HSC differentiation. Additionally, we found p75$^{\text{NTR}}$-mediated HSC activation is necessary for liver repair, as the loss of p75$^{\text{NTR}}$ resulted in diminished liver cell proliferation in the *plg-/-* mouse, as well as decreased levels of hepatocyte growth factor (HGF) in the liver. In co-culture, *p75$^{\text{NTR}}$-/-* HSCs were unable to promote hepatocyte proliferation to the extent of wild-type HSCs, but hepatocyte proliferation was recovered by addition of HGF. Overall, the results of our studies suggest that p75$^{\text{NTR}}$ expression and Rho activation in HSCs is necessary for their differentiation to repair-supporting, HGF-secreting cells, which in turn can promote the hepatocyte proliferation necessary for liver repair after injury or disease.

Chapter 1: Introduction

This thesis focuses on the characterization of a novel biological function and new ligand for the neurotrophin receptor p75 (p75^{NTR}). In order to understand the significance and rationale behind the search for novel functions and ligands for p75^{NTR}, this chapter provides a summary of the relevant literature on p75^{NTR}, including its functions and signaling mechanisms, as well as information on p75^{NTR} as it relates to liver injury specifically as well as in tissue fibrosis in general.

1. p75^{NTR}

1.1. p75^{NTR} historical background

After the discovery of the neurotrophic factor nerve growth factor (NGF) in the 1950s by Rita Levi-Montalcini [1], studies focused on finding the receptor through which NGF can exert its neurotrophic actions on neurons. Research led to the cloning of the nerve growth factor receptor (NGFR) in 1986 by Dan Johnson [2]. Since its cloning, however, the function of the NGFR has expanded. The receptor has been found to bind not only NGF but all neurotrophins, including brain derived neurotrophic factor (BDNF), neurotrophin-3 (NT-3), and neurotrophin-4 (NT-4) [3]. Thus, due its pan-neurotrophin binding abilities and its apparent molecular mass of 75 kDa, NGFR is now known as the p75 neurotrophin receptor, or p75^{NTR}.

Based on sequence analysis, p75^{NTR} is classified as a member of the tumor necrosis factor receptor (TNFR) superfamily. Like the other members of the TNFR superfamily, p75^{NTR} is a single transmembrane-spanning protein with an

amino-terminal extracellular domain and carboxy-terminal intracellular domain. The extracellular domain has been crystallized [4] and consists of four cysteine-rich domains (CRDs) which are involved in ligand binding and contain an N-linked glycosylation site, followed by a stalk domain that is involved in the sorting of p75^{NTR}. The intracellular domain of p75^{NTR} contains a juxtamembrane adaptor protein-binding region, followed by a death domain which is involved in apoptotic signaling (Fig. 1) [5].

1.2. p75^{NTR} expression and function

1.2.1. Nervous system

p75^{NTR} is highly expressed in a variety of tissues during embryonic development [6]. After birth, p75^{NTR} expression declines in most tissues, however after injury p75^{NTR} can be re-expressed in many adult tissues (Table 1). As p75^{NTR} was first discovered for its ability to bind nerve growth factor and thus be a regulator of neuronal survival, p75^{NTR} expression and function have been most extensively studied in the nervous system. In the nervous system, p75^{NTR} is expressed by a variety of neuronal cell types, including cortical and hippocampal neurons in the brain, and sensory and motor neurons in the spinal cord. p75^{NTR} is also expressed by glial cells, including oligodendrocytes in the central nervous system (CNS) and Schwann cells in the peripheral nervous system (PNS) (for reviews, see [3], [7]). p75^{NTR} expression is upregulated in the nervous system in a wide variety of injuries and diseases, including

brain trauma, spinal cord injury, axotomy, ischemic injury, seizure, multiple sclerosis, and Alzheimer's disease [7].

Numerous studies have been performed *in vitro* using cultured cells in a quest to define the specific functions of $p75^{NTR}$. $p75^{NTR}$ was originally discovered for its role in neurotrophin-mediated promotion of neuronal survival [2]. Seemingly contradictory to its survival-promoting function, $p75^{NTR}$ is also able to induce apoptotic cell death in culture [8]. Additionally, $p75^{NTR}$ has been shown to regulate neurite extension in cultured neuronal cells [9], which could potentially have important implications in nerve regeneration after injury. It has also been suggested that $p75^{NTR}$ may play a role in cell cycle progression through its interaction with the transcriptional repressor zinc finger protein SC1 [10].

Specific functions of $p75^{NTR}$ in the nervous system have been also been identified *in vivo* through knockout and transgenic mouse studies. The first $p75^{NTR}$ null mouse was generated by Lee and colleagues, and surprisingly the only major phenotype exhibited was defects in sensory nerve development [11]. Interestingly, $p75^{NTR}$ mutant mice expressing a pro-apoptotic truncated form of the receptor [12] also exhibited defects in the peripheral nervous system sensory neurons [13], further suggesting a role for $p75^{NTR}$ in nervous system development. A transgenic mouse line overexpressing the intracellular domain of $p75^{NTR}$ in neurons revealed a ligand-independent role for $p75^{NTR}$ in promoting neuronal apoptosis [14]. Injury models performed on $p75^{NTR}$ null mice have revealed potential functions for the receptor in pathological circumstances. Beattie *et al.* observed that in a spinal cord injury model, $p75^{NTR}$ null mice exhibited less apoptosis of oligodendrocytes [15]. Additionally,

Scott *et al.* noted that p75^{NTR} null mice had greater neuronal sprouting after spinal cord injury [16]. Taken together, these results suggest that p75^{NTR} plays a detrimental role in preventing recovery after spinal cord injury by causing death of oligodendrocytes, the myelinating cells of the CNS, as well as preventing neurite outgrowth from damaged neurons. In an animal model of multiple sclerosis, conflicting reports exist about the function of p75^{NTR}. Copray *et al.* reported that p75^{NTR} null mice show exacerbated symptoms, suggesting that p75^{NTR} is playing a protective role in multiple sclerosis [17]. However, work performed by Soilu-Hanninen *et al.* showed mice treated with p75^{NTR} antisense oligonucleotides to knockdown p75^{NTR} expression fared better than control-treated mice, suggesting p75^{NTR} expression is harmful in multiple sclerosis [18]. Both groups attribute their results to p75^{NTR} functioning in brain endothelial cells, however they disagree as to whether p75^{NTR} is beneficial or detrimental to endothelial cell-mediated blood-brain barrier integrity. From these initial studies characterizing p75^{NTR} in the nervous system, it is clear that p75^{NTR} has several functions and plays an important role in nervous system injury and disease.

1.2.2. Non-nervous system

In addition to the nervous system, a number of papers have been published describing the expression of p75^{NTR} in tissues outside of the nervous system, including the liver, kidney, pancreas, skeletal muscle, and cells of the immune system (Table 1). However, the function of p75^{NTR} in non-neuronal tissues is not well characterized.

Despite the knowledge of widespread expression of p75^{NTR} in non-nervous system tissue, less than a handful of studies have been performed to examine the function of p75^{NTR} in non-neuronal cells, and prior to our studies, the only functions for p75^{NTR} that had been examined in non-neuronal cells were cell survival and apoptosis. Trim *et al.* observed hepatic stellate cell apoptosis *in vitro* upon treatment with high exogenous concentrations of NGF [19]. More recently, Reddypalli *et al.* proposed that NGF via p75^{NTR} can promote myoblast survival and proliferation [20]. Both of these studies assert that their observed results are mediated by p75^{NTR} as the cell types studied lack expression of TrkA, the other receptor for NGF, however these studies do not use any form of genetic depletion or gene knockdown to demonstrate that their results are specifically p75^{NTR}-mediated.

The most evidence for a biological function of non-neuronal p75^{NTR} *in vivo* comes from studies of the vascular system. Kraemer demonstrated that in p75^{NTR} null mice there was reduced apoptosis of vascular smooth muscle cells after carotid artery injury, suggesting that p75^{NTR} can promote smooth muscle cell apoptosis [21]. Additionally, p75^{NTR} mutant mice expressing a pro-apoptotic truncated form of the protein [12] exhibit blood vessel abnormalities [13], suggesting a role for p75^{NTR} in vascular system development. The only other *in vivo* evidence for p75^{NTR} function outside of the nervous system comes from the skin and lung. Botchkarev showed that p75^{NTR} null mice exhibit greater hair growth due to decreased apoptosis of hair follicle keratinocytes, suggesting that p75^{NTR}-mediated keratinocyte death may play a role in hair loss [22]. In an asthma model, p75^{NTR} null mice are less susceptible to airway inflammation caused by neurotrophin-mediated neuroimmune response [23].

However, this is attributed to decreased hyperreactivity of p75^{NTR}-expressing nerve fibers in the lung as opposed to a resident lung cell response. Thus despite the numerous papers showing the widespread expression of p75^{NTR} outside of the nervous system, *in vivo* evidence of the potential functions of non-neuronal p75^{NTR} only exists for just a few of the tissues in which p75^{NTR} is expressed.

1.3. p75^{NTR} signaling: a complex story

There have been numerous studies performed to elucidate the function of p75^{NTR} by investigating its signaling properties [3, 7, 24]. These studies have revealed that p75^{NTR} signaling is quite complex: it can bind to several physiological and pathological ligands, interact with different co-receptors, undergo intramembrane proteolysis, and can initiate a number of different intracellular signaling cascades, all together contributing to the variety of functions that p75^{NTR} can possess.

1.3.1. The many ligands of p75^{NTR}

Although p75^{NTR} was originally discovered because of its function as an NGF receptor, research over the past 15 years has uncovered several additional ligands that have the ability to bind to the extracellular domain of p75^{NTR}. In addition to the original neurotrophin ligand NGF, all other known neurotrophins (BDNF, NT-3, NT-4) can bind to p75^{NTR} with similar nanomolar affinities (Fig. 2) [25]. Several studies have shown that the neurotrophins are present as homodimers, and in dimeric form are able to interact with the second and third cysteine-rich domains (CRD2 and CRD3) of

p75^{NTR} [4]. Binding of neurotrophins to p75^{NTR} can elicit a multitude of cellular functions, including cell death, survival, and cell cycle progression [5]. However, mature proteolytically-processed neurotrophins are unable to effectively elicit a p75^{NTR}-mediated cell death response as would be predicted by the death domain of p75^{NTR}. In 2001, work by Lee *et al.* provided the first evidence for the binding of the unprocessed precursor form of neurotrophins, the proneurotrophins, to p75^{NTR} and showed that the high affinity binding of proNGF to p75^{NTR} is able to potently elicit apoptosis in neurons, oligodendrocytes, and a vascular smooth muscle cell line in culture [26]. As both neurotrophins and proneurotrophins are normally present in tissue, it is believed that these ligands are important in normal physiological processes that are mediated by p75^{NTR}.

In addition to the traditional neurotrophin-related ligands, several pathological ligands for p75^{NTR} have been identified (Fig. 2) [27]. Yaar *et al.* showed that β-amyloid can bind to p75^{NTR} with nanomolar affinity and that treatment with aggregated β-amyloid can cause apoptosis of p75^{NTR}-expressing cells, suggesting a potential role for p75^{NTR} in Alzheimer's disease [28]. Della-Bianca *et al.* observed that a peptide derived from prion protein (PrP 106-126) can bind to p75^{NTR} and induce apoptosis in a neuronal cell line, identifying p75^{NTR} as a potential mediator of cell death associated with prion-related diseases [29]. Additionally, the binding of rabies virus glycoprotein to p75^{NTR} was described by Tuffereau *et al.*, who proposed that binding of the virus to p75^{NTR} could provide a means by which rabies virus can infect motor and sensory neurons [30]. Because p75^{NTR} upon neurotrophin binding can be internalized into the cell, some believe that binding of pathological ligands to p75^{NTR}

represents a mechanism by which these ligands can "hijack" transport systems and gain access to the intracellular milieu [27].

1.3.2. Co-receptors of p75^{NTR}

To add further complexity to p75^{NTR} signaling, research over the past several years has shown that p75^{NTR} can act as or may require a co-receptor to exert biological effects in cells (Fig. 3). The concept that p75^{NTR} may act as a co-receptor first came about when a discrepancy was observed in binding affinity between neurotrophins binding to the cell surface versus neurotrophins binding to isolated p75^{NTR} protein. In the early 1990s a second type of receptor with the ability to bind neurotrophins was discovered, the tropomyosin-related kinases, or Trks. The Trks consist of three related Trk proteins, TrkA, TrkB, and TrkC, belonging to the receptor tyrosine kinase superfamily and each having its own binding specificity for a particular neurotrophin. Like p75^{NTR}, each Trk receptor has the ability to bind its specific neurotrophin ligand with nanomolar affinity ($K_d \sim 10^{-9}$ M). However, in cells that co-express both p75^{NTR} and Trk, neurotrophins are able to bind with sub-nanomolar affinity ($K_d \sim 10^{-11}$ M), suggesting that p75^{NTR} and Trk interact to form high affinity neurotrophin binding sites on cells [3]. It was considered that p75^{NTR} enhances the ability of Trk receptors to bind and respond to the subpicomolar concentrations of neurotrophins that exist in tissues, and for reasons still unclear promote Trk-mediated signaling involved in neuronal cell survival and while suppressing its own p75^{NTR}-mediated apoptosis signaling pathways. However, this concept was recently challenged by a study that

determined that a tripartite complex of p75^{NTR}, Trk, and NGF is not structurally plausible [31].

While the survival-promoting function of p75^{NTR} occurs when it is partnered with Trks, the apoptotic effects of proneurotrophins through p75^{NTR} require a different co-receptor, Sortilin [26]. Sortilin belongs to the VSP10 family of transmembrane proteins, which are involved in endosomal and lysosomal vesicle trafficking from the trans golgi network [24]. Sortilin can bind proneurotrophins independently of p75^{NTR}, but both p75^{NTR} and Sortilin expression are required to induce proneurotrophin-mediated apoptosis. Although the signaling cascades activated in p75^{NTR}/Sortilin-mediated apoptosis have yet to be elucidated, prior studies investigating the role of p75^{NTR} in apoptosis have discovered roles for the intracellular adaptor proteins NRIF and NRAGE, the small GTPase Rac, and the kinase JNK in promoting mitochondrial-mediated caspase activation that can lead to apoptosis.

In addition to its roles in mediating cell death and survival, p75^{NTR} also plays a role in neuronal cell growth, a key process in nerve regeneration after injury, where it is involved in controlling the inhibition of neurite process extension. In neurite growth inhibition, p75^{NTR} forms a complex with another distinct set of proteins, the Nogo receptor (NogoR) and LINGO-1. NogoR had been previously characterized as the receptor for myelin-based proteins Nogo, MAG, and OmGP, which are known to inhibit neurite outgrowth. However, because NogoR is a GPI-linked protein and contains no intracellular region through which signaling can occur, research was performed to find a transmembrane receptor that could couple to NogoR and mediate intracellular signaling events that lead to the inhibition of neurite outgrowth.

Yamashita *et al.* showed that MAG-induced growth inhibition was attenuated in neurons from p75^{NTR} null mice [32], suggesting that p75^{NTR} is potentially involved in NogoR-mediated inhibition of neurite outgrowth. Subsequent research revealed that indeed p75^{NTR} and NogoR form a complex on the cell surface [33, 34]. The current proposed mechanism by which p75^{NTR}/NogoR can inhibit neurite outgrowth involves NogoR binding to myelin-based proteins Nogo, MAG, and OmGP, leading to the proteolytic cleavage of the intramembrane region of p75^{NTR} by α- and γ-secretase and causing subsequent activation of the small GTPase Rho [35]. Studies by Yamashita and colleagues helped to elucidate the mechanism by which p75^{NTR} can alter Rho activation within cells [9, 36]. In the absence of p75^{NTR} activation, Rho is found in the cytosol bound to its endogenous protein inhibitor Rho-GDI, causing Rho to be inactive. When p75^{NTR} is activated after binding of myelin proteins to the NogoR complex, Rho-GDI is sequestered and binds to the intracellular domain of p75^{NTR}. This causes a dissociation of Rho from Rho-GDI, releasing active Rho into the cytoplasm and allowing it to initiate downstream signaling that ultimately causes a rigidifying of the cytoskeleton, thus preventing neurite extension. Recent research has identified LINGO-1 as a third essential component in the p75^{NTR}/NogoR complex [37]. LINGO-1 is transmembrane protein whose function is yet unknown, but the intracellular domain of LINGO-1 was shown to be necessary in order to cause neurite growth inhibition through the p75^{NTR}/NogoR/LINGO-1 complex. While the Trk proteins, Nogo, and LINGO-1 may share some common structural features, protein sequence places Sortilin in a completely different class of proteins. That all of these proteins are able to bind to and interact with p75^{NTR} is intriguing, and begs the

question of how many other proteins may act as co-receptors of p75^{NTR}, and how these interactions can influence p75^{NTR} function.

1.3.3. Ligand-independent functions of p75^{NTR}

To further complicate the story of p75^{NTR} signaling, in addition to having several physiological and pathological ligands, p75^{NTR} can function and signal independently of ligand binding. Studies by Rabizadeh *et al.* [8] and Majdan *et al.* [14] have shown that p75^{NTR} may signal in a ligand-independent manner in neuronal cells to induce apoptosis. Additionally, Roux *et al.* observed that p75^{NTR} can promote cell survival in a ligand-independent and Trk-independent manner through the PI3 kinase-mediated activation of Akt [38]. Yamashita *et al.* found that overexpression of p75^{NTR} alone, in the absence of any type of ligand, could promote the activation of Rho [9]. In all of these studies, expression of the intracellular domain (ICD) of p75^{NTR} alone could exert a signaling event and biological effect in the absence of a ligand. Since p75^{NTR} is not constitutively expressed in all tissues, and its expression is upregulated at sites of tissue injury, its expression itself could function as the signal to trigger a signaling pathway. Recent studies have shown that either high glucose levels [39] or hypo-osmolar stress [40] can upregulate p75^{NTR} expression *in vitro*. However, it is completely unknown what mechanisms are involved in causing the upregulation of p75^{NTR} after injury *in vivo*, and remains one of the most elusive questions facing the p75^{NTR} field.

As it is evident from the overwhelming amount of data that exists, p75^{NTR} function and signaling are complex and some believe that what we currently know about p75^{NTR} is merely the tip of the iceberg. The questions that face the p75^{NTR} field currently include whether there are other functions for p75^{NTR}, whether other co-receptors and other ligands exist, and what role p75^{NTR} plays outside of the nervous system. As p75^{NTR} is expressed in the liver after injury and in liver disease, it is of interest to determine the function of this receptor in the liver and what role it plays in liver pathology.

2. p75^{NTR} and liver disease and regeneration

2.1. p75^{NTR} in the liver

In normal healthy liver p75^{NTR} is expressed at low levels [19]. Upon liver injury, p75^{NTR} expression is upregulated in liver tissue. Upregulation of p75^{NTR} in the liver has been documented in both human cirrhotic liver disease and in animal models of toxic liver injury [19, 41]. The p75^{NTR}-immunopositive cells in the liver were determined to be hepatic stellate cells (HSCs), based on their peri-sinusoidal localization, spindle morphology, and immunoreactivity for α-smooth muscle actin (αSMA), a cytoskeletal stress fiber whose expression in the liver parenchyma is restricted to differentiated HSCs. While Trim and colleagues have shown a potential role for NGF in promoting HSC apoptosis [19, 42], the role of p75^{NTR} in HSC function and liver physiology and pathology is not fully understood.

2.2. Functions of HSCs

The hepatic stellate cell was first identified in 1876 by Karl von Kupffer who originally sought to identify nerve fibers in the liver. Staining of the liver with gold chloride, a histochemical dye used to label axons, not only stained nerves, but also star-shaped cells in the hepatic sinusoid that Kupffer termed "*Sternzellen*" [43]. In 1951 Toshio Ito first described perisinusoidal lipid-containing cells in the liver, which he called "*Fettspeicherungszellen*" (fat-storing cells) [44]. It was not until 1971 that Kenjiro Wake proved that von Kupffer's *Sternzellen* and Ito's fat-storing cells were one in the same [45], and are now known more commonly as hepatic stellate cells (HSCs). HSCs comprise about 5-8% of the cells in the liver [46]. In the healthy liver, HSCs (also sometimes still referred to as Ito cells or lipocytes) are in a quiescent state and one of their major functions is retinol (vitamin A) storage. However, upon liver injury or disease, HSCs undergo differentiation to what has been termed an "activated" state. The process of HSC differentiation from a quiescent to an activated state involves the loss of retinol-storing lipid droplets, a change in cell morphology to a myofibroblast-like appearance, and expression of factors involved in fibrogenesis [46]. Because of their role in liver fibrosis, HSCs, their functions, and the molecular mediators involved have been extensively studied.

2.2.1. HSC differentiation

HSC differentiation is a hallmark of fibrotic liver disease of different etiologies, such as viral hepatitis and chronic alcohol consumption [47]. After liver

injury or disease, quiescent HSCs undergo differentiation to an activated form, which is indicated by their increased proliferation and overall changes in cell morphology and gene and protein expression to a myofibroblast-like state. Myofibroblasts are characterized by the presence of specific cytoskeletal stress fibers, including αSMA, as well as by their upregulated expression and secretion of pro-fibrogenic factors such as transforming growth factor β (TGFβ), extracellular matrix (ECM) proteins including collagens I and III, the ECM remodeling enzymes matrix metalloproteinases (MMPs), and their inhibitors, the tissue inhibitors of matrix metalloproteinases (TIMPs) [48]. Initially after liver injury, HSC activation is beneficial as activated HSCs provide a provisional ECM scaffold for proliferating hepatocytes, as well as secreting growth factors, most importantly hepatocyte growth factor (HGF) [49], that promote hepatocyte proliferation necessary for liver repair. However, during chronic liver injury or disease, HSCs remain activated and collagen deposition becomes excessive, leading to liver fibrosis [50]. Understanding the molecular mechanisms that initiate and regulate HSC activation are critical so that we may begin to develop treatments that manipulate HSC activation in chronic liver disease.

Currently, a major cytokine known to be involved in HSC activation is TGFβ. Liver injury initiates an inflammatory response in the liver, causing certain liver cells as well as infiltrating inflammatory cells to secrete TGFβ [51]. TGFβ binding to TGFβ receptors on HSCs initiates signaling through the Smad family of transcriptional activators, stimulating collagen I mRNA and protein expression [52], as well as regulating organization of cytoskeletal stress fibers [53]. Activated HSCs also upregulate their own expression of TGFβ, initiating an autocrine signaling loop

that serves to perpetuate HSC activation. The importance of TGFβ in HSC activation has been confirmed *in vivo*, as TGFβ null mice show minimal αSMA and collagen expression after acute liver injury, suggesting that TGFβ is necessary for promoting HSC activation [54].

Because HSCs undergo the loss of their lipid-containing vesicles during activation, recent research has proposed a mechanism of adipogenic regulation of HSC differentiation [55]. To maintain their lipocyte state, quiescent HSCs display pro-adipogenic signaling, including activity of adipogenic transcription factors PPARγ and C/EBP and expression of adipocyte-specific genes adipsin and resistin [56]. Upon activation HSCs undergo loss of pro-adipogenic signaling, including decreased expression and activity of PPARγ, as well as initiating anti-adipogenic signaling, such as expression of PPARβ and secretion of leptin [56, 57]. The targeting of HSCs' adipogenic properties has been of much interest for its potential therapeutic value, and indeed research has shown that stimulation of PPARγ activity *in vivo* can ameliorate liver fibrosis by decreasing HSC activation and ECM deposition in the liver [58].

HSC activation is characterized by drastic changes in gene expression, so it is not surprising that several transcription factors and other factors involved in controlling gene expression have been implicated in the regulation of HSC differentiation. In addition to the transcription factors already discussed (the Smads, PPARγ, and C/EBP), there is also evidence for the involvement of NF-κB, AP-1, CREB, Foxf1, and several nuclear hormone receptors in regulating HSC differentiation [59]. Additionally, recent studies have shown that chromatin repression due to CpG methylation can regulate HSC activation in an epigenetic

fashion [60]. Unfortunately, targeting of proteins directly involved in transcriptional regulation is not an ideal therapeutic approach, as these factors are not specific to only HSCs, but are present and active in many cell types throughout the body.

In addition to the factors already mentioned, there are references scattered throughout the HSC literature identifying various other factors that may potentially play a role in HSC activation. For example, similar to myofibroblasts in other tissues and diseases, HSC function can be regulated by angiotensin II signaling via the AT-1 receptor [61], as well as by changes in intracellular calcium signaling [62, 63]. Additionally, HSC activation has been shown to be regulated both by hormones (estradiol) [64] and neurotransmitters (norepinephrine) [65]. Other factors implicated in HSC differentiation include the cytokines IL-6 [66] and IL-1α [67], the cell surface protein CD38 [68], the carbohydrate-binding lectin Galectin-3 [69], and two injury/disease-related conditions: oxidative stress [66] and hepatocyte apoptotic body engulfment [70]. In addition, recent data from microarray analysis to examine gene expression differences between activated and quiescent HSCs have implicated Bmp and Wnt signaling pathways as potentially playing a role in HSC activation [71, 72]. Based on the volume of data, one would be inclined to believe that HSC differentiation is a complex process; whether these additional factors play important roles in HSC activation and how they fit in with the currently known mechanisms remains to be understood.

In addition to blocking the activation of HSCs, some believe that reversing HSC activation (i.e. promoting HSC de-differentiation to the quiescent lipocyte state) may be a plausible therapeutic option for treating liver fibrosis. Currently, there are

two focal areas for which there is evidence of playing a role in the reversal of HSC differentiation: extracellular matrix composition/structure and adipogenic factors. A role for the ECM in regulating HSC activation has been identified for over a decade [73]. Work by Gaça *et al.* showed that culture-activated HSCs that were re-plated on Matrigel matrix were able to revert to a non-activated phenotype, suggesting a role for matrix-dependent deactivation of HSCs [74]. As already described, there is mounting evidence for the concept of adipogenic regulation of HSC activation state. Recent studies by the Tsukamoto lab have shown that either ectopic expression of PPARγ or treatment with adipocyte differentiation mixture (isobutylmethylxanthine, dexamethasone, and insulin) can cause culture-activated HSCs to de-differentiate into a quiescent state [56, 75]. While these *in vitro* studies seem to be promising, whether HSC de-differentiation actually occurs *in vivo* remains to be proven.

2.2.2. HSC proliferation and apoptosis

While HSC differentiation remains a primary area of focus in the liver fibrosis field, many groups also study the functions of HSC proliferation and apoptosis with the hopes of identifying other potential therapeutic targets. In healthy liver, quiescent HSCs lie in a non-proliferative state. After injury, HSCs begin to differentiate as well as proliferate. Currently the most potent factor that induces HSC proliferation is PDGF [76]. PDGF binding to PDGF receptors on HSCs initiates the activation of several well-known mitogenic signaling cascades, including the Ras/ERK pathway and the PI3 kinase/Akt/p70^{S6} kinase pathway [76]. While controlling the proliferation

of activated HSCs may help to slow the progression of liver fibrosis, it does not help in the reversal or cure of liver disease because some activated HSCs are still present and thus continue to secrete matrix and contribute to fibrotic scarring. With this in mind, research has focused on finding factors that can induce apoptosis of activated HSCs in order to remove the fibrogenic cells altogether. Many factors have been proposed to induce HSC apoptosis, including TNF receptor superfamily ligands TNFα, Fas ligand, and NGF; TIMP-1 antagonists to promote matrix degradation; and the fungal toxin gliotoxin [77]. Although triggering apoptosis in HSCs would appear to be a promising therapeutic target for liver disease, recent work has shown that in chronic liver disease human HSCs are resistant to apoptosis due to their overexpression of the anti-apoptotic protein Bcl-2 [77]. Thus, therapies aimed at inducing apoptosis of activated HSCs may not be as effective as previously thought. Because of this, specific targeting of HSC activation becomes increasingly important in the development of therapeutics to treat chronic liver disease.

2.3. HSCs in liver injury and regeneration

Persistent HSC activation during chronic liver injury or disease is the cause of fibrosis and ultimately irreversible cirrhosis, as activated HSCs secrete collagen and other ECM components that lead to the fibrotic scarring of liver tissue. Because of their critical role in liver fibrosis, HSCs are the key target in the development of therapeutics for liver disease. Although the majority of the HSC literature focuses on their role as promoters of liver fibrosis, a few recent studies have demonstrated that

HSCs are actually necessary and important for the initiation of liver repair. Liver injury causes inflammatory and oxidative stress responses that lead to hepatocyte necrosis and apoptosis. In order for liver repair to occur, crosstalk between the remaining hepatocytes and other cells of the liver, including HSCs, Kupffer cells, and endothelial cells, must take place to promote proliferation and migration of the remaining hepatocyte population [49]. The presence of HSCs and their ability to differentiate has been shown to be critical for liver repair and regeneration [78]. Uyama *et al.* showed that HSC secretion of hepatocyte growth factor (HGF) promotes hepatocyte proliferation *in vitro* [79]. *In vitro* and *in vivo* studies by Mabuchi and colleagues revealed that in the regenerating liver, activated but not quiescent HSCs are intimately associated with regenerating hepatocyte clusters through cell-to-cell contacts [80, 81]. Additional evidence for the importance of HSC activation in liver regeneration comes from the work of Kalinichenko *et al.*, who showed that mice heterozygous for the transcription factor *Foxf1* have impaired liver regeneration after injury due to defective HSC activation [82]. These recent discoveries have shown a positive role for HSCs after liver injury, an important one that must be kept in mind when developing new therapeutics aimed at manipulating HSC function in liver disease.

It is clear that the hepatic stellate cell is an important cell in contributing to liver disease. As already mentioned, p75^{NTR} expression is highly upregulated during HSC activation, however its role in HSC biology is unclear. Elucidation of the

function of p75^{NTR} in HSC biology will help to evaluate the therapeutic potential of targeting p75^{NTR} in liver disease.

3. p75^{NTR} and fibrinogen/fibrin in disease and injury

I have just described how p75^{NTR} may play a new function in liver; now I will describe how p75^{NTR} may play a role in fibrotic disease in general and how p75^{NTR} may interact with a new pathological ligand to mediate its effects.

3.1. Fibrinogen/fibrin in disease and injury

Vascular damage is a hallmark of many injuries and disease states. Additionally, disease and injury-related inflammation can compromise vascular integrity and cause the vasculature to become leaky. In these instances, molecules in the blood that are normally contained within the blood vessels can extravasate into the surrounding injured or diseased tissue. One of the major molecules found in the blood is the clotting protein fibrinogen. Fibrinogen is a soluble 340 kDa dimeric glycoprotein synthesized by the liver and secreted into the plasma. Each monomeric subunit is composed of three nonidentical polypeptide chains, designated Aα, Bβ, and γ, that are linked together by disulfide bonds. Upon initiation of the coagulation cascade, the serine protease thrombin cleaves peptides from the N-terminal regions of the Aα and Bβ chains. The cleavage of these peptides, termed fibrinopeptide A and fibrinopeptide B, exposes polymerization sites and initiates the formation of a polymer consisting of noncovalently linked protofibrils, which, upon binding of activated

coagulation factor XIII, form an insoluble fibrin clot (Fig. 4) [83]. The clotting functions of fibrinogen have historically been well recognized. However, in addition to the clotting that occurs after injury, fibrinogen may also leak into the surrounding tissues after vascular damage or inflammation. The presence of fibrinogen or fibrin deposits within tissues has been documented for many disease states and after injury. In the nervous system, fibrin deposits are found in plaques in the brains of patients with multiple sclerosis [84], as well as in the PNS after sciatic nerve injury [85, 86]. Fibrin is also found in atherosclerotic lesions [87], in the lung after sepsis [88], in the liver after toxic liver injury [89], in the kidney in patients with glomerulonephritis [90], and is also found deposited in the breast tissue of women with breast cancer [91].

While the clotting functions of fibrinogen have been well documented, the role that fibrinogen and fibrin may play in pathological conditions such as tissue fibrosis is less well understood. In the clotting process, fibrinogen binds to integrin $\alpha IIb\beta3$ receptors on adjacent platelets, functioning as a molecular bridge between cells to create the matrix "net" that serves as the building block of clot formation. In addition to the mechanical role of the fibrinogen-$\alpha IIb\beta3$ integrin interaction, fibrinogen/fibrin can also bind to a number of other receptors and promote intracellular signaling. Other fibrinogen/fibrin receptors include the $\alpha5\beta1$, $\alpha v\beta3$, and Mac-1 integrins, and the cell adhesion molecules ICAM-1 and VE-cadherin [92]. These receptors are found on a variety of cell types within tissues, and fibrinogen/fibrin binding to these receptors can regulate major signaling pathways and mediate various cellular responses ranging from angiogenesis to inflammation and propagation of infection [92]. Whether

fibrinogen/fibrin can bind other receptors and regulate other pathological processes remains to be discovered.

3.2. The relationship between p75^{NTR} and fibrinogen/fibrin

As already discussed, p75^{NTR} expression is normally at low levels in adult tissues, but after injury p75^{NTR} expression can be upregulated in many tissues in the body. Additionally, p75^{NTR} is also upregulated in a variety of diseases associated with fibrosis, such as multiple sclerosis [93], stroke [94], spinal cord injury [15], peripheral nerve injury [86], atherosclerosis [95], lung inflammation [96], liver fibrosis and cirrhosis [19, 41], and cancer [97, 98]. Because of the correlation between p75^{NTR} expression and fibrin deposition after tissue injury, it is of interest to determine whether any interactions occur between p75^{NTR} and fibrinogen/fibrin, and how these two proteins are related in pathogenesis. Previous work performed by Akassoglou and colleagues has shown that fibrin inhibits sciatic nerve regeneration after injury, induces expression of p75^{NTR} in Schwann cells, and causes the cells to arrest in a non-myelinating state [86]. Additional work in our lab by Sachs *et al.* has shown that p75^{NTR} inhibits the degradation of fibrin after tissue injury [99]. In addition to the physiological neurotrophin and proneurotrophin ligands, p75^{NTR} can also bind several pathological ligands associated with disease and infection. Fibrinogen/fibrin can bind to a number of receptors and regulate a variety of cell functions associated with disease and injury [92]. Thus, it is of extreme interest to determine if p75^{NTR} and fibrinogen/fibrin interact in a receptor-ligand manner to regulate disease pathology.

Identification of a $p75^{NTR}$/fibrinogen interaction and determining the importance of this interaction in pathogenesis would be beneficial in developing a novel therapeutic target for the treatment of fibrosis and pathologies of various etiologies.

4. Rationale, aims, and significance

Despite the fact that $p75^{NTR}$ was cloned over two decades ago, numerous studies into the functions of $p75^{NTR}$ have yielded conflicting results, and top researchers in the field admit that the many functions of $p75^{NTR}$ remain enigmatic. One fact that is consistent for $p75^{NTR}$ is that its expression is upregulated after injury and onset of disease. Because of this, we believe that $p75^{NTR}$ may play an important role in disease, and thus our lab is interested in pursuing research aimed at elucidating the functions of $p75^{NTR}$ during pathogenesis. This includes identifying novel functions for $p75^{NTR}$ both in the nervous system and outside of the nervous system, as well as finding new pathological ligands that bind to $p75^{NTR}$ and may play a role in promoting disease pathogenesis.

The goal of my dissertation research is to address the role of $p75^{NTR}$ in tissue fibrosis, more specifically the following points:

1. $p75^{NTR}$ expression is highly upregulated in liver fibrosis and cirrhosis.

The first part of my dissertation addresses the question:

What is the role of $p75^{NTR}$ in the liver?

To address this question, I will determine the function of $p75^{NTR}$ in the hepatic stellate cell, the liver cell type that expresses $p75^{NTR}$, and examine how loss of $p75^{NTR}$ expression affects liver injury and repair.

2. **Preliminary data from our lab provides evidence for an interaction between p75^{NTR} and fibrinogen/fibrin.**

The second part of my dissertation addresses the question:

Do p75^{NTR} and fibrinogen/fibrin interact in a receptor-ligand manner to regulate disease pathology?

To address this question, I will determine if the interaction between p75^{NTR} and fibrinogen/fibrin is a direct interaction, and if so, characterize the interaction between p75^{NTR} and fibrinogen/fibrin by determining a dissociation constant (K_d) for the binding interaction.

Because p75^{NTR} expression is specifically upregulated in tissues during disease and after injury, we believe that p75^{NTR} may play an important role in pathogenesis. Elucidation of the specific functions of p75^{NTR} in disease and identification of novel pathological ligands for p75^{NTR} are important in evaluating this receptor's potential as a therapeutic target in the treatment of a wide variety of diseases.
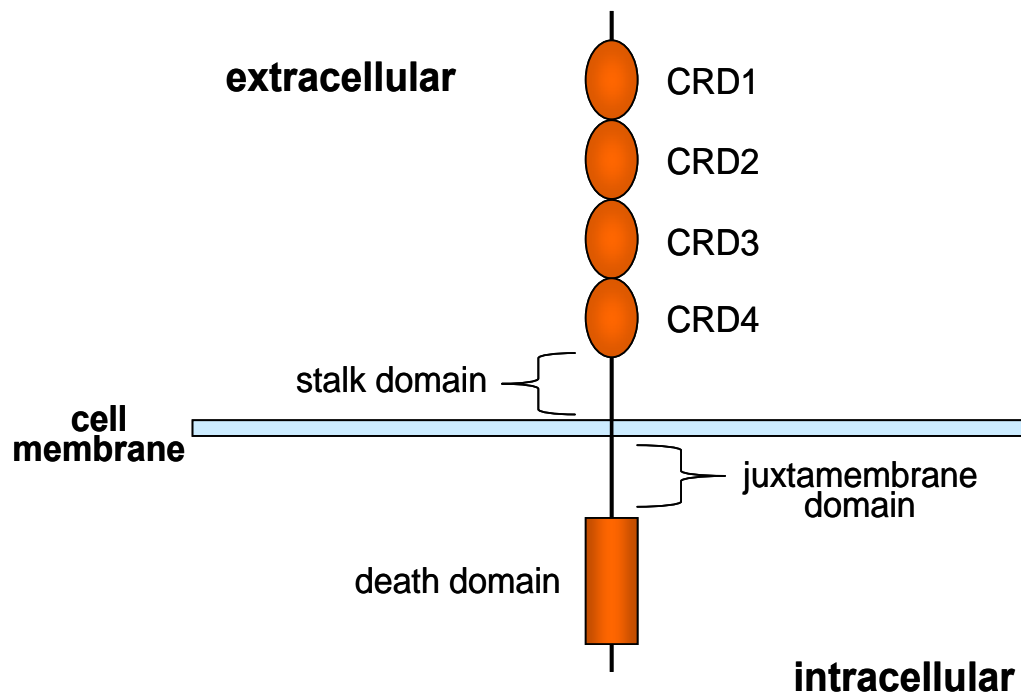
Figure 1. Schematic of the p75^{NTR} protein.

Cartoon representation of p75^{NTR}. p75^{NTR} is a single transmembrane-spanning protein with an amino-terminal extracellular domain and carboxy-terminal intracellular domain. The extracellular domain consists of four cysteine-rich domains (CRDs) which are involved in ligand binding, followed by a stalk domain that is involved in the sorting of p75^{NTR}. The intracellular domain of p75^{NTR} contains a juxtamembrane adaptor protein-binding domain, followed by a death domain which is involved in apoptotic signaling.
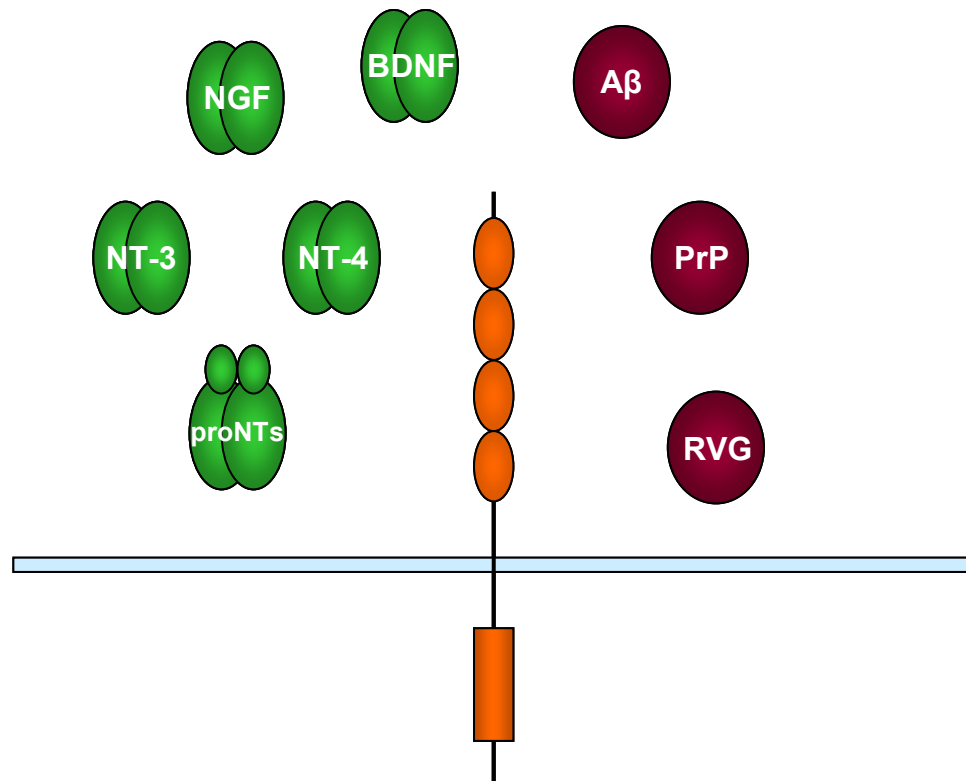
Figure 2. Ligands of p75^NTR.

Cartoon representation of p75^NTR and its known ligands. p75^NTR (orange) can bind to several physiological and pathological ligands. The known physiological ligands (green) for p75^NTR are the neurotrophins nerve growth factor (NGF), brain derived neurotrophic factor (BDNF), neurotrophin-3 (NT-3), and neurotrophin-4 (NT-4), as well as the proneurotrophins (proNTs), the precursor forms of the neurotrophins. The known pathological ligands (dark red) of p75^NTR include β-amyloid (Aβ), prion protein peptide 106-126 (PrP), and rabies virus glycoprotein (RVG).
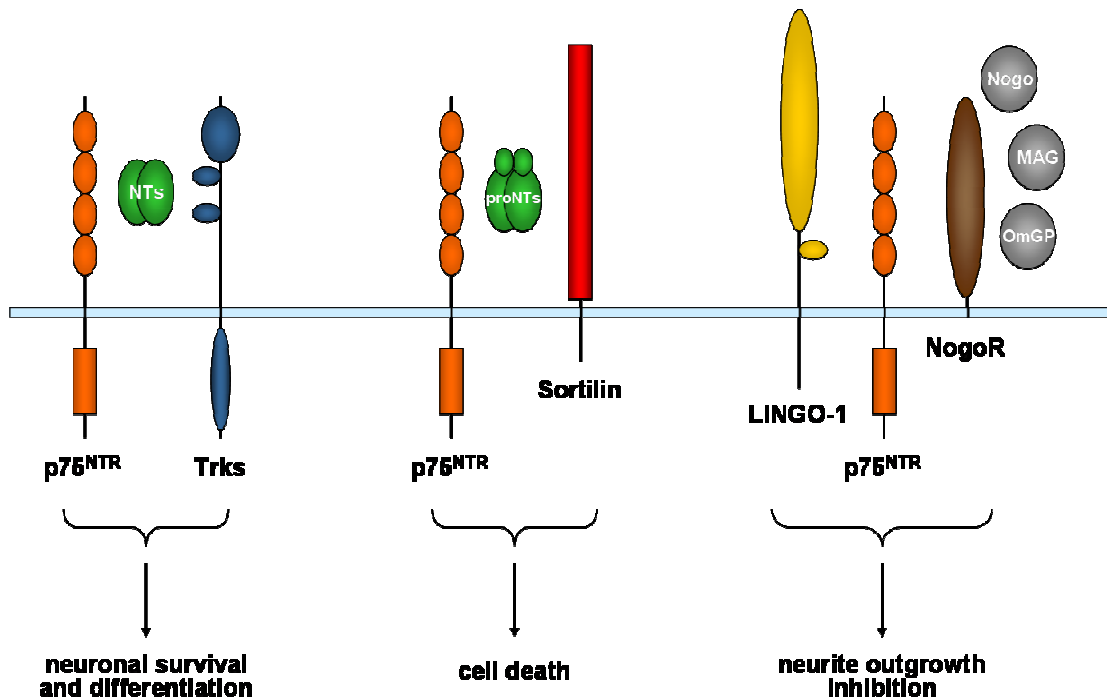
Figure 3. Co-receptors of p75^{NTR}.

Cartoon representation of p75^{NTR} and its known co-receptors. p75^{NTR} (orange) can interact with Trk receptors (blue), and upon binding of mature neurotrophins (NTs) (green) can promote neuronal survival and differentiation. p75^{NTR} can also interact with Sortilin (red) to create a high-affinity binding site for proneurotrophins (proNTs) (green), leading to cell death signaling. Additionally, p75^{NTR} can act as a co-receptor for the Nogo receptor (NogoR) (brown), a receptor that binds the myelin-based proteins Nogo, myelin-associated glycoprotein (MAG), and oligodendrocyte myelin glycoprotein (OmGP) (gray). p75^{NTR} and NogoR interact with a third receptor, LINGO-1 (yellow), to inhibit neurite outgrowth in neurons.
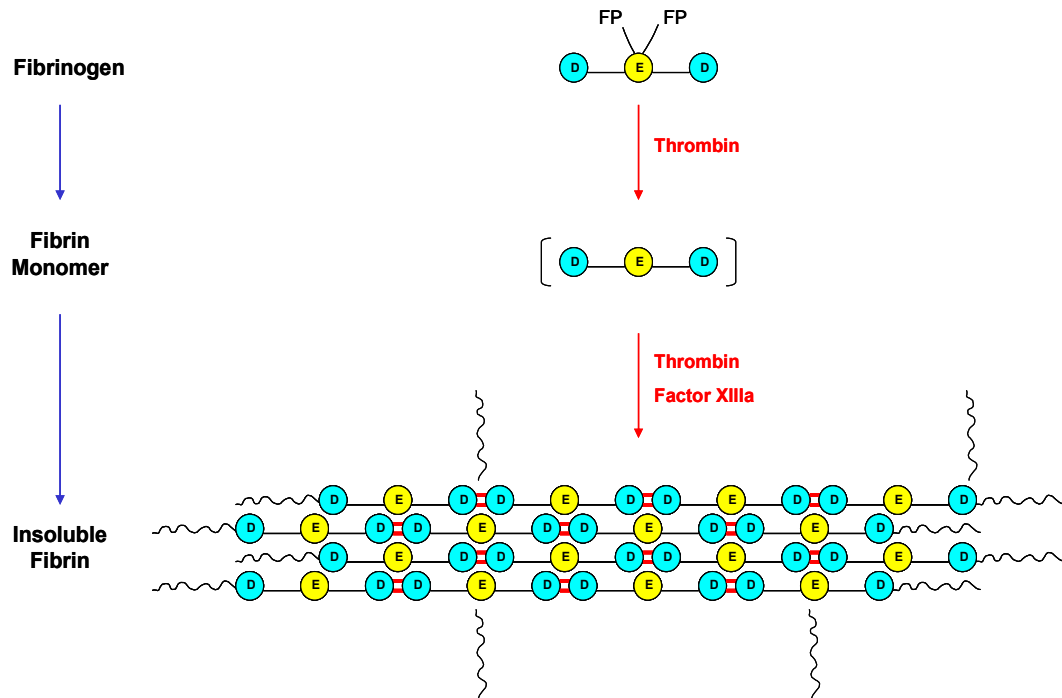
Figure 4. Fibrin polymerization.

Cartoon representation of fibrin polymerization. After initiation of the coagulation cascade, the soluble blood protein fibrinogen (top) undergoes cleavage by the serine protease thrombin, which removes the fibrinopeptides (FP) A and B to form a soluble fibrin monomer (center). Further cleavage by thrombin and additional cross-linking by activated Factor XIII (Factor XIIIa) create the insoluble fibrin meshwork (bottom) that is responsible for clot formation. D (blue), D domain of fibrinogen; E (yellow), E domain of fibrinogen.

Table 1. p75^{NTR} expression in tissue.

Tissue	Cell type	References
Nervous system tissue		
Central Nervous System	Neurons	[3, 7]
	Oligodendrocytes	[100]
	Endothelial cells	[17]
Peripheral Nervous System	Schwann cells	[101]
	Neurons	[3, 7]
Non-nervous system tissue		
Liver	Hepatic stellate cells	[19, 41]
Lung	Neurons	[102]
	Pulmonary artery branches	
Kidney	Glomerulus	[103]
Pancreas	Peri-islet Schwann cells	[104]
	Pancreatic stellate cells	[19]
	Ductal cells	[105]
Gut	Enteric nervous system (neurons and glia)	[106, 107]
Immune System	Dendritic cells	[108]
	Mast cells	[109, 110]
	Monocytes	[111]
	Macrophages	[112]
	Eosinophils	[113, 114]
	Medullary thymic epithelial cells	[115]
Skeletal Muscle	Myoblasts	[20]
	Satellite cells	[116]
Vasculature	Vascular smooth muscle cells	[21, 95]
Eye	Conjunctival fibroblasts	[117]
Skin	Hair follicle keratinocytes	[22]
Breast	Myoepithelial cells	[118]
Placenta	Trophoblast cells	[119]
Gonads	Prostate epithelium	[120]
	Testis epithelium, spermatocytes	[121]

Chapter 2. Materials and Methods

1. p75^{NTR} and the liver

1.1. Animals

Plg-/- mice and *p75^{NTR}-/-* mice were obtained from The Jackson Laboratories. *Plg-/-* mice and *p75^{NTR}-/-* mice were bred to obtain a double heterozygous first generation (F$_1$). Double heterozygous F$_1$ mice were then bred to obtain *plg-/-p75^{NTR}-/-* mice. In experiments, *plg+/+p75^{NTR}+/+*, *plg-/-p75^{NTR}+/+*, and *plg+/+p75^{NTR}-/-* littermates were used as controls. Mice were fed standard chow and had access to food and water *ad libitum*. All animal procedures were performed under the guidelines set by the University of California San Diego Institutional Animal Care and Use Committee and are in accordance with those set by the National Institutes of Health.

1.2. Liver imaging and histology

Whole liver images were obtained by a Zeiss Stemi 2000-C stereoscope using an AxioCam HRc camera and AxioVision software (Carl Zeiss, Inc.). Liver cryosections (10 μm) were used for Hematoxylin staining and immunostaining.

For immunochemical detection of p75^{NTR}, liver cryosections were fixed in ice cold 4% paraformaldehyde (PFA) for 30 minutes, then rinsed with phosphate buffered saline (PBS) three times. Peroxidase activity was quenched by incubation with 1.8% hydrogen peroxide in PBS for 10 minutes at room temperature. After rinsing three

times with PBS, sections were blocked with antibody diluent [3% bovine serum albumin (BSA)/0.1% Triton X-100/PBS] + 3% goat serum for 30 minutes at room temperature. Slides were then rinsed again three times with PBS and incubated with primary antibody (rabbit anti-p75^{NTR}, 1:500, gift of M.V. Chao, New York University) in antibody diluent overnight at 4°C. Slides were washed 3 times for 5 minutes each in PBS, incubated with secondary antibody (biotin-conjugated goat anti-rabbit IgG, 1:300, Vector Laboratories) in antibody diluent for 30 minutes at room temperature, then washed with PBS 3 times for 5 minutes each. Bound antibody was visualized by using the avidin-biotin-peroxidase complex (Vectastain Elite ABC kit; Vector Laboratories) according to manufacturer's instructions with 3-amino-9-ethylcarbazole (AEC) (Sigma) as a chromogen. Slides were rinsed with ddH$_2$O and mounted with Mowiol mounting medium.

For immunochemical detection of fibrin or desmin, liver cryosections were fixed in ice cold methanol for 7 minutes, then rinsed with PBS two times. For desmin immunostaining, the tissue was permeabilized with 0.1% Triton X-100/PBS for 1 hour at room temperature. After rinsing two times with PBS, sections were blocked with antibody diluent + 3% serum (horse for fibrin; goat for desmin) for 30 minutes at room temperature. Slides were incubated with primary antibody [sheep anti-fibrin(ogen), 1:100, US Biological; rabbit anti-desmin, 1:50, Santa Cruz Biotechnology] overnight at 4°C. For double confocal immunofluorescence rabbit anti-desmin (1:50) and goat anti-p75^{NTR} (1:100, Santa Cruz) were used. Slides were washed 3 times for 5 minutes each in PBS, incubated with secondary antibody [cyanine 3 (Cy3)-conjugated donkey anti-sheep IgG; fluoroscein isothiocyanate

(FITC)-conjugated goat anti-rabbit IgG; Cy3-conjugated donkey anti-goat IgG; all 1:100, Jackson ImmunoResearch) in antibody diluent for 30 minutes at room temperature, washed again with PBS 3 times for 5 minutes each, and finally mounted with SlowFade Gold Antifade Reagent (Invitrogen) + 4',6-Diamidine-2'-phenylindole (DAPI) (1 μg/mL). Images were obtained using an Axioplan 2 microscope (Zeiss) and AxioCam HRc camera. To quantitate the number of desmin-positive cells, 4 images per tissue section were obtained with the 20X objective and the number of desmin-positive cells per field were counted.

To examine liver cell proliferation *in vivo*, mice were injected intraperitoneally (i.p.) with 100 mg/kg 5-bromo-2'-deoxyuridine (BrdU) (Calbiochem) daily for 3 days and sacrificed on the fourth day. Cryosections were stained using the BrdU Immunohistochemistry System (Calbiochem) according to manufacturer's protocol. To quantitate BrdU labeling, 5 images per tissue section were obtained with the 10X objective and number of BrdU-positive nuclei per field were counted.

1.3. Detection of fibrin in liver tissue

Fibrin was isolated from liver tissue and detected by western blot as described in Weiler-Guettler *et al.* [122], with modifications. Fifty mg of previously snap-frozen liver tissue was homogenized in extraction buffer [10 mM sodium phosphate buffer, pH 7.5, with 0.1 M ε–aminocaproic acid (Sigma), 5 mM ethylenediaminetetraacetic acid (EDTA) (Fisher), protease inhibitors (Protease Inhibitor Cocktail Set III, Calbiochem; 1:100), and 10 U heparin/mL. After agitation at 4°C for 14 hours,

particulate material (including fibrin) was collected by centrifugation at 10,000x*g* for 10 minutes, resuspended in extraction buffer without protease inhibitors, centrifuged again, and the final pellet was resuspended in 3 M urea. After agitation at 37°C for 2 hours, the samples were vortexed, then centrifuged at 14,000x*g* for 15 minutes. The sediment was dissolved in 2X reducing sodium dodecyl sulfate (SDS) sample buffer [120 mM Tris, pH 6.8, 20% glycerol, 4% SDS, and 200 mM dithiothreitol (DTT)], subjected to SDS-polyacrylamide gel electrophoresis (PAGE) (8% gel) and transferred to polyvinyl difluoride (PVDF) membrane (Immobilon-P, Millipore Corp.) by electroblotting. Fibrin β chains (~54 kDa) were detected with mouse anti-human fibrin antibody (mAb NYB T2G1, Accurate Chemical & Scientific Corp.; 1:500), followed by a peroxidase-labeled anti-mouse IgG and chemiluminescence system (ECL, Amersham Biosciences).

1.4. RNA extraction and real-time reverse transcription-polymerase chain reaction (RT-PCR)

RNA was isolated from liver tissue and cultured cells using the RNeasy Mini Kit (Qiagen) according to manufacturer's instructions. RNA was reverse transcribed to cDNA using the GeneAmp RNA PCR Core Kit (Applied Biosystems) according to manufacturer's instructions using random hexamer primers. Real-time PCR analysis was performed using the Opticon DNA Engine 2 (MJ Research) and the Quantitect SYBR Green PCR kit (Qiagen) using 1.5 µL of cDNA template in a 25 µL reaction. PCR efficiencies of the primers were calculated by serial dilution of template and no

significant differences in efficiency were found between the target genes and the housekeeping genes. Results were analyzed with the Opticon 2 Software using the comparative C_T method as described [123]. Data were expressed as $2^{-\Delta\Delta C_T}$ for the experimental gene of interest normalized against the housekeeping gene and presented as fold change versus the relevant control. The following primers were used:

αSMA [124]:	Fwd 5' AAC GCC TTC CGC TGC CC 3'
	Rev 5' CGA TGC CCG CTG ACT CC 3'
col1α1 [125]:	Fwd 5' CCT GCC TGC TTC GTG TAA ACT 3'
	Rev 5' TTG GGT TGT TCG TCT GTT TCC 3'
TGFβ-1 [126]:	Fwd 5' CCG CAA CAA CGC AAT CTA TG 3'
	Rev 5' GCC CTG TAT TCC GTC TCC TT 3'
GAPDH:	Fwd 5' CAA GGC CGA GAA TGG GAA G 3'
	Rev 5' GGC CTC ACC CCA TTT GAT GT 3'
HPRT [127]:	Fwd 5' GTT AAG CAG TAC AGC CCC AAA 3'
	Rev 5' AGG GCA TAT CCA ACA ACA AAC TT 3'

1.5. HSC isolation

Primary hepatic stellate cells were isolated as described in Schnabl *et al.* [52] with modifications. Briefly, mice (2-4 months age) were anesthetized with 0.7 mL 2.5% Avertin injected i.p. and livers were perfused *in situ* through the inferior vena cava with warm perfusion solution [50 mL Hanks' balanced salt solution without Ca^{2+} or Mg^{2+} (HBSS; Invitrogen)], followed by pronase solution [1 mg pronase

(Calbiochem) per gram body weight in 40 mL DMEM/F12 medium (Invitrogen) + 1% penicillin/streptomycin (Invitrogen) + 0.25 µg/mL Amphotericin B (Invitrogen)], and finally collagenase solution [5 mg collagenase type IV (Sigma) per mouse in 50 mL DMEM/F12 + 1% penicillin/streptomycin + 0.25 µg/mL Amphotericin B]. After perfusions, the liver was removed and washed in warm HBSS. The livers of 3-4 mice were pooled, minced with scalpels, triturated with a 10 mL syringe, mixed with warm DMEM (Invitrogen) +1% penicillin/streptomycin + 0.25 µg/mL Amphotericin B to 35 mL, and shaken at 37°C for 10 minutes. The homogenate was then filtered through 2 layers of sterile gauze, cold HBSS added to 50 mL, centrifuged at 50xg at 4°C for 2 minutes, and the supernatant was collected. The pellet was washed 2 more times and supernatants collected. The supernatants were pooled and centrifuged at 500xg at 4°C for 7 minutes. The pellets were resuspended in cold HBSS, pooled, and mixed with 40% iodixanol (OptiPrep; Greiner Bio-One) in HBSS to achieve 17.5% iodixanol concentration. Five mL of 11.5% iodixanol in HBSS was layered on top of the cell solution, followed by 2 mL of HBSS. The gradient was centrifuged at 1400xg for 20°C for 17 minutes, and the HSCs were collected from between the HBSS layer and 11.5% iodixanol layer. HSCs were washed 3 times in 10 mL cold HBSS with centrifugation at 500xg at 4°C for 5 minutes. HSCs were resuspended in HSC medium [DMEM + 10% fetal bovine serum (FBS; Invitrogen) + 1% penicillin/streptomycin + 0.25 µg/mL Amphotericin B] and plated on 10 cm non-tissue culture-treated plates. Cells were passed 1:2 when confluent by lifting with 0.25% trypsin + 0.02% EDTA in PBS and scraping with a cell scraper (Falcon).

1.6. αSMA immunocytochemistry

HSC activation was assessed by immunochemical detection of αSMA, a cytoskeletal stress fiber only present in myofibroblasts, as described in Swaney *et al.* [128], with modifications. HSCs (day 14-21, passage 2-4) were seeded on poly-D-lysine-coated (Sigma; 50 μg/mL) 8 well chamber slides (Nunc), 15,000 cells/well, and incubated for 2-3 days. Cells were washed with PBS, fixed with 4% PFA, permeabilized with 0.3% Triton X-100/PBS for 10 minutes, then blocked with 5% BSA/0.1% Triton X-100/PBS for 10 minutes. Slides were incubated with mouse anti-αSMA antibody (Sigma; 1:1000 in PBS) for 1 hour at 37°C, washed with 0.1% Triton X-100/PBS, and blocked as described above. FITC-conjugated anti-mouse IgG (Vector Laboratories; 1:200 in PBS) was added for 1 hour at 37°C, the slide was washed with PBS, and then mounted with ProLong Gold Antifade Reagent (Invitrogen) + DAPI (1 μg/mL). For quantitation of percentage of activated cells, images were obtained, and the total number of cells (DAPI+ nuclei) and αSMA+ cells were counted, with the % activated cells equal to the αSMA+ cells/total number of cells. For quantitation of activated cell size, the area of αSMA+ cells was calculated using AxioVision software (Carl Zeiss, Inc.). For quantitation 16 fields/genotype were counted for each condition. Results are from five separate experiments performed in duplicates.

1.7. Immunoblots

Wild-type and $p75^{NTR}$-/- HSCs (day 8, passage 2) were lysed with cell lysis buffer supplemented with protease inhibitor cocktail and the lysates were cleared by centrifuging at 13,000xg for 5 minutes. Protein concentration of cleared lysates was determined by Bradford protein assay. Samples were prepared in 1X reducing SDS sample buffer (1 μg for αSMA; 20 μg for collagen I), boiled for 5 minutes, then separated by 8% SDS-PAGE gel electrophoresis and transferred to PVDF membrane by electroblotting. After blocking in 5% nonfat milk in TBS-T (25 mM Tris, pH 7.4, 137 mM NaCl, 3 mM KCl, 1% Tween-20) for 1 hour at room temperature, membranes were incubated overnight with primary antibody diluted in 5% BSA in TBS-T (mouse anti-αSMA, 1:1000, Sigma; rabbit anti-collagen I, 1:1000, Rockland Immunochemicals; mouse anti-β tubulin, 1:1000, Sigma). Blots were washed 3 times for 5 minutes each with TBS-T, incubated with peroxidase-labeled secondary antibodies diluted in 5% nonfat milk in TBS-T for 1 hour at room temperature (goat anti-mouse IgG, 1:10,000, Santa Cruz Biotechnology; goat anti-rabbit IgG, 1:5000, Cell Signaling Technology), washed again, followed by detection with chemiluminescence (ECL, Amersham Biosciences).

1.8. Adenovirus-mediated gene expression in HSCs

Freshly isolated wild-type and $p75^{NTR}$-/- HSCs were seeded onto poly-D-lysine-coated 8 well chamber slides, 200,000 cells/well. The following day (day 1), the medium was changed to fresh HSC medium. On day 2, the cells were washed

once with serum-free DMEM and then treated with adenovirus in DMEM + 2% FBS as follows: Ad p75^{NTR} FL, containing the full length rat p75^{NTR} gene, 200 MOI [38]; Ad p75^{NTR} ICD, containing the intracellular domain of the rat p75^{NTR} gene, 10 MOI [38]; Ad Rho, containing constitutively active RhoA (L63Rho), 10 MOI [129]; or Ad control (empty vector), 10 or 200 MOI. After 16 hours with adenovirus, the medium was changed to fresh DMEM + 10% FBS, and the medium was replaced every other day thereafter. On day 7, cells were stained for αSMA as described.

1.9. Lentivirus-mediated RNA interference in HSCs

To knockdown *p75^{NTR}* expression in wt HSCs, short hairpin RNA (shRNA) against mouse *p75^{NTR}* was expressed using a lentiviral vector system (BLOCK-iT™ Lentiviral RNAi Expression System; Invitrogen). Briefly, short hairpin DNA oligos (sequence depicted in Fig. 13) were synthesized based on a previously published small interfering RNA sequence against mouse *p75^{NTR}* [130] and cloned into the pENTR/U6 Entry Construct vector. An LR recombination reaction was performed to insert the U6 promoter/mouse *p75^{NTR}* shRNA oligo/Pol III terminus cassette from the pENTR/U6 Entry Construct vector into the pLenti6/BLOCK-iT™-DEST vector. The vector generated, pLenti6/BLOCK-iT™ mouse *p75^{NTR}* shRNA vector, was cotransfected with ViraPower™ virus packaging mix using Lipofectamine™ 2000 (Invitrogen) into human embryonic kidney 293FT cells to produce virus. Supernatants containing lentivirus were harvested three days post-transfection and centrifuged at 3000 rpm for 5 minutes to pellet debris. Subsequently, 4 mL of supernatant was centrifuged at

50,000x*g* for 1.5 hours at 4°C to pellet virus, and the lentivirus pellet was resuspended in 150 μL of PBS. Freshly isolated wt HSCs were either seeded onto poly-D-lysine-coated 8 well chamber slides, 200,000 cells/well. The following day (day 1), the medium was changed to fresh HSC medium. On day 2, the cells were treated with lentivirus (20 μL in PBS) in DMEM + 10% FBS. After 24 hours with lentivirus, the medium was changed to fresh DMEM + 10% FBS, and the medium was replaced every other day thereafter. αSMA immunostaining was performed on day 10 as described.

1.10. Assessing the role of Trk and neurotrophins on HSC differentiation

Wild-type HSCs were isolated and seeded on 8 well chamber slides (100,000 cells/well) as described above. Media was changed and treatments were added every other day starting on day 1. Cells were treated with DMSO (Fisher), K252a, an inhibitor of Trk receptors (10 nM; Calbiochem), goat IgG (2 μg/mL; Jackson ImmunoResearch), goat anti-NGF, an NGF neutralizing antibody (2 μg/mL; Sigma), human IgG Fc fragment (1 or 20 μg/mL; Jackson ImmunoResearch), Fc-p75^{NTR}, a pan-neurotrophin neutralizing agent (20 μg/mL; Alexis Biochemicals), or Fc-TrkB, a BDNF neutralizing agent (1 μg/mL; R&D Systems). On day 7, cells were stained for αSMA as described.

1.11. Assessing HSC apoptosis and proliferation *in vitro*

Wild-type and *p75^{NTR}*-/- HSCs (day 9-21, passage 2-4) were seeded in 96 well plates, 10,000 cells/well, and incubated overnight. The following day, the media was replaced with fresh HSC media with or without NGF (100 ng/mL; PeproTech). To determine extent of apoptosis, cells were incubated for 24 hours with treatment, then apoptosis was assessed using an ELISA that measures DNA fragmentation (Cell Death Detection ELISA^{PLUS} kit; Roche) according to manufacturer's instructions. To determine the extent of proliferation, cells were incubated for 48 hours with treatment, with BrdU (10 μM) added 24 hours into the treatment. Cell proliferation, as determined by BrdU incorporation into DNA, was assessed using an ELISA (colorimetric BrdU Cell Proliferation ELISA; Roche) according to manufacturer's protocol.

1.12. Assessing liver cell apoptosis *in vivo*

Liver cryosections were permeabilized (without fixation) with 0.1% Triton X-100 in TBS-T for 20 minutes at room temperature, then washed 3 times for 5 minutes each with TBS-T. Sections were incubated with CaspACE FITC-VAD-FMK In Situ Marker, a fluorescently-labeled pan-caspase inhibitor that irreversibly binds to activated caspases *in situ* (20 μM; Promega), diluted in TBS-T for 1 hour at room temperature, washed 5 times for 5 minutes each with TBS-T, and mounted with SlowFade Gold Antifade Reagent (Invitrogen) + DAPI (1 μg/mL).

1.13. Phospho-cofilin immunocytochemistry

Rho activity in HSCs was assessed by immunochemical detection of phosphorylated cofilin, a downstream target in the Rho activation pathway. Cells were washed once with Tris buffered saline (TBS), then fixed with cold methanol for 10 minutes at ⁻20°C. Cells were washed 3 times for 5 minutes each with TBS, then incubated with freshly prepared 0.1% sodium borohydride in TBS for 5 minutes at room temperature. Cells were washed again 3 times for 5 minutes each with TBS, then blocking solution (10% goat serum, 1% BSA in PBS) was added for 1 hour at room temperature. Cells were washed once for 5 minutes with TBS, then incubated with rabbit anti-phospho-cofilin diluted in 1% BSA in TBS (1:50; Cell Signaling Technology) overnight at 4°C. After washing 3 times for 5 minutes each with TBS, cells were incubated with Cy3-conjugated donkey anti-rabbit IgG diluted in 1% BSA in TBS (1:200; Jackson ImmunoResearch) for 30 minutes at room temperature. After washing 3 times for 5 minutes each with TBS, slides were mounted with SlowFade Gold Antifade Reagent (Invitrogen) + DAPI (1 μg/mL).

1.14. TAT-Pep5 treatment

Freshly isolated wild-type HSCs were seeded onto 8 well chamber slides (1.5 – 2.5 x 10^5 cells/well) and treated every day with TAT-Pep5 (1 μM) [36] or vehicle (DMSO) for 7 days. HSC activation was examined by αSMA staining and Rho activation was examined by phospho-cofilin staining as described.

1.15. HGF ELISA

The amount of HGF in liver samples was measured by an enzyme-linked immunosorbent assay (ELISA) kit (Institute of Immunology, Tokyo, Japan) according to the manufacturer's instructions and as described in Yamada *et al.* [131]. Briefly, 0.2-0.6 g of frozen liver tissue was homogenized on ice in 4 volumes of extraction buffer (20 mM Tris buffer, pH 7.5, 2 M NaCl, 0.1% Tween-80, 1 mM EDTA, and 1 mM PMSF) and then centrifuged at 19,000x*g* for 30 minutes at 4°C. The supernatants were collected, diluted 1:4 with sample diluent (extraction buffer without NaCl) and passed over a HiTrap Heparin column (Amersham Biosciences) to bind HGF. The HGF-enriched fractions were eluted with extraction buffer, and 50 µL applied to the HGF ELISA.

1.16. Hepatocyte isolation, co-culture with HSCs, and hepatocyte proliferation assay

For co-culture experiments, wild-type or *p75^NTR*-/- HSCs (day 7-21, passage 2-4) were seeded onto cell culture inserts (24-well format, PET membrane with 0.4µm pore size; BD Biosciences), 10,000 cells/insert, one day prior to hepatocyte isolation [79]. Primary hepatocytes were isolated from 2-4 month old wild-type C57BL/6 mice (Harlan Sprague Dawley) as described in Galijatovic *et al.* [132], with modifications. Briefly, mice were anesthetized with 2.5% Avertin injected i.p. The inferior vena cava was canulated and the portal vein cut. The liver was perfused *in situ* with HBSS (Ca^{2+} and Mg^{2+}-free) containing 0.5 mM EGTA and 10 mM Hepes at pH 7.4, followed by

perfusion with collagenase solution [1 mg/mouse Liberase Blendzyme 3 (Roche) in HBSS, with Ca^{2+} and Mg^{2+}]. The liver was removed and washed with cold HSC medium (DMEM + 10% FBS + 1% penicillin/streptomycin + 0.25 ug/mL Amphotericin B). Hepatocytes were isolated by mechanical dissociation with forceps, filtered through a sterile 70 μm filter, and washed twice by centrifugation at 50x*g* for 2 minutes. Hepatocytes were cultured in 24-well plates coated with collagen type I from calf skin (Sigma), ~30,000 cells/well, in 0.5 mL of HSC medium. Four hours after plating, the hepatocytes were washed twice with co-culture medium (DMEM + 0.2% FBS + 1% penicillin/streptomycin + 0.25 ug/mL Amphotericin B), and then incubated in 0.7 mL co-culture medium with or without HGF (R&D Systems; 50 ng/mL). Concurrently, HSCs in inserts were washed twice with co-culture medium, incubated in 0.2 mL co-culture medium, and transferred to the hepatocyte-containing wells. After 24 hours, [*methyl*-^{3}H]Thymidine (Amersham Biosciences) was added to the hepatocyte medium (1 μCi/mL). Co-cultures were incubated for 48 hours total and hepatocyte proliferation was assessed by [*methyl*-^{3}H]Thymidine incorporation. Inserts were removed and hepatocytes were washed twice with cold PBS. [*methyl*-^{3}H]Thymidine incorporated into cellular DNA was precipitated with 10% trichloroacetic acid (TCA) for 15 minutes at room temperature, the TCA was aspirated, and the hepatocytes were solubilized with a 0.3 M sodium hydroxide (NaOH) + 1% sodium dodecyl sulfate (SDS) solution for 10 minutes at room temperature. Lysates were neutralized with an equal volume of 0.3 M hydrochloric acid (HCl) and assayed for β-emission on a liquid scintillation counter [133].

1.17. Statistics

Statistical significance was calculated using GraphPad Prism (GraphPad Software) by unpaired Student's *t* test for isolated pairs or by analysis of variance (one-way ANOVA, Bonferroni post-test) for multiple comparisons. Data are shown as the mean ± SEM.

2. p75^NTR/fibrinogen interactions

2.1. Preparation of fibrinogen fragment D

The fibrinogen proteolytic degradation product fragment D was kindly provided by Dr. Russell Doolittle (University of California San Diego). Additionally, some experiments were performed using fibrinogen fragment D that was produced in our lab by Ryan Adams using a protocol obtained from Dr. R. Doolittle [134]. Briefly, human fibrinogen (~5 mg/mL; Calbiochem) was digested for 4 hours at room temperature with plasmin (16 μg/mL; Chromogenix) to produce fibrinogen fragments D and E. Fragment D was purified by affinity chromatography using a Gly-Pro-Arg column and eluted with 1 M NaBr + 0.05 M NaOAc, pH 5.3. Fragment D was precipitated from solution by addition of ammonium sulfate, then resuspended and dialyzed in HBS-EP for Biacore binding studies. Protein concentration was determined by Bradford assay. Comparison of the fragment D from both sources was conducted using SDS-PAGE analysis, FPLC analysis, and Biacore binding analysis, and no significant differences were observed between the two lots.

2.2. Cloning of human p75^{NTR} extracellular domain into FLAG vector

The extracellular domain (residues 1-223) of human p75^{NTR} was obtained by PCR amplification from the full length cDNA (in plasmid "1.5J", kindly sent by M.V. Chao, New York University), with the addition of a 5' HindIII and a 3' XbaI restriction site to facilitate subcloning, as well as a C-terminal stop codon to terminate translation of the generated transcript. The following primers were used:

Forward: 5' − CGATGACGACAAGCTTGCCAAGGAGGCATGCCCC − 3'

Reverse: 5' − CCGGGATCCTCTAGATTAGTTGTCGGTGGTGCCTCGGG − 3'

The HindIII/XbaI-digested PCR product was subcloned into the pFLAG-CMV-3 expression vector (Sigma), generating a sequence which codes for a soluble, secreted protein with an N-terminal FLAG octapeptide tag followed by the entire human p75^{NTR} extracellular domain, dubbed FLAG-p75^{NTR} ECD FL (residues 1-223). Additionally, a truncated form of the human p75^{NTR} extracellular domain (residues 1-162; truncated after the fourth cysteine rich domain) was generated by HindIII/BstY1 digest of the PCR product. This digested fragment was subcloned into the HindIII/BamHI sites of pFLAG-CMV-3. Site-directed mutagenesis (QuickChange; Stratagene) was performed to create a C-terminal stop codon. The resulting sequence codes for an N-terminal FLAG tag followed by the truncated human p75^{NTR} extracellular domain, dubbed FLAG-p75^{NTR} ECD TR (residues 1-162) (Fig. 28B).

2.3. Expression and purification of FLAG-p75^{NTR} ECD

Both the FL and TR constructs were transfected into HEK 293 cells using Lipofectamine 2000 (Invitrogen) according to manufacturer's protocol. Stably transfected clones were selected for by their resistance to Geneticin (G418; Invitrogen). Highest-expressing clones were determined by FLAG western blot of conditioned culturing medium [DMEM + 10% FBS + 1% penicillin/streptomycin + 500 μg/mL Geneticin (all from Invitrogen)]. The truncated construct was expressed at higher levels than the full length ECD construct. Additionally, the truncated construct is similar to that used by He and Garcia, who performed crystallographic and structural analysis of the extracellular domain of p75^{NTR} [4]. For these reasons, we chose to continue on with the expression and purification of FLAG-p75^{NTR} ECD TR only (from now on simply referred to as "FLAG-p75^{NTR} ECD") for use in our binding studies.

FLAG-p75^{NTR} ECD was expressed in culturing medium containing 3% FBS and was purified by affinity chromatography using M2 anti-FLAG resin (Sigma). The column was washed with wash buffer (15 mM Hepes, pH 7.4, and 450 mM NaCl), then FLAG-p75^{NTR} ECD was eluted by competition with 100 μg/mL FLAG peptide in elution buffer (15 mM Hepes, pH 7.4, and 150 mM NaCl). The eluted protein was concentrated by centrifugation using a Centricon centrifugal filter device (Millipore), and protein concentration was determined by Bradford assay. Protein purity and integrity was determined by separation on an SDS-PAGE gel and staining with GelCode Blue Stain Reagent (Pierce).

2.4. Biacore binding studies

All Biacore binding experiments were carried out at 25°C in HBS-EP buffer [10 mM Hepes, pH 7.4, 150 mM NaCl, 3 mM EDTA, and 0.005% (v/v) surfactant P20] on a Biacore 3000 system. Approximately 200-300 RU of FLAG-p75^{NTR} ECD was covalently coupled using amine chemistry to the carboxymethylated dextran matrix of a CM5 sensor chip (Biacore) [135]. The first flow-cell was mock-coupled with buffer only to serve as a control for non-specific background binding. Specific binding data was obtained by subtracting the background signal from the control flow-cell from the total binding signal of the flow-cell coupled with FLAG-p75^{NTR} ECD. Injection of nerve growth factor, a previously characterized p75^{NTR} ligand [4], showed binding to FLAG-p75^{NTR} ECD, suggesting that the recombinant FLAG-p75^{NTR} ECD protein was functional. Fibrinogen fragment D was injected in random order over the FLAG-p75^{NTR} ECD surface as a set of 8 concentrations from 37 to 81000 nM in 3-fold dilutions at a flow rate of 20 or 30 μL/minute. After each injection, the binding surfaces were regenerated by injecting IUw solution [equal parts ionic solution I (0.46 M KSCN, 1.83 M MgCl$_2$, 0.92 M urea, and 1.83 M guanidine-HCl), non-polar solution U (equal volumes of DMSO, formamide, ethanol, acetonitrile, and 1-butanol), and deionized water] [136] for 30 seconds. Total binding of fragment D to FLAG-p75^{NTR} ECD at equilibrium was recorded and plotted as a function of fragment D concentration. The plots were then fit by nonlinear regression to calculate dissociation constants, K_d, using GraphPad Prism 3.0 (GraphPad software).

Chapter 3. Determining a function for p75[NTR] in liver injury and repair

1. Introduction

Despite the widespread expression of p75[NTR] in a variety of tissues throughout the body (Table 1), very little is known about the functions of p75[NTR] outside of the nervous system. Previous studies have reported that p75[NTR] is upregulated by hepatic stellate cells (HSCs) in the human cirrhotic liver and in animal models of toxic liver injury [19, 41], however the role that p75[NTR] plays in HSC function and liver pathology remains unclear. Prior studies have indicated that p75[NTR] may mediate HSC death *in vitro*, as treatment of rat HSCs with high concentrations of exogenous NGF can induce a small 1.5-fold increase in apoptosis [19, 42]. However, a very recent study reported that in chronically activated human HSCs, which are similar to those found in fibrotic and cirrhotic liver, NGF treatment is unable to cause apoptosis [77]. This group additionally showed that in general HSCs that are chronically activated, such as in cases of liver fibrosis and cirrhosis, are resistant to apoptosis due to their overexpression of the anti-apoptotic protein Bcl-2 [77]. Even though p75[NTR] may mediate HSC death *in vitro* through the application of high non-physiological concentrations of NGF, whether this actually occurs *in vivo* during liver disease remains to be proven. Because no studies had yet been performed to address the role of p75[NTR] in the liver *in vivo*, we wanted to determine a biological role for p75[NTR] in the liver and how p75[NTR] functions in liver injury and repair.

2. Genetic loss of p75^{NTR} causes exacerbated liver pathology in a mouse model of liver injury

To address the role of p75^{NTR} in liver disease *in vivo*, we crossed mice deficient for p75^{NTR} (*p75^{NTR}-/-*) with plasminogen deficient (*plg-/-*) mice. *plg-/-* mice spontaneously develop liver injury characterized by fibrin deposition, hepatocyte necrosis, and HSC activation [137, 138], characteristics that are observed in a variety of liver diseases of different etiologies [139]. *plg-/-p75^{NTR}-/-* mice were born at the expected Mendelian ratio. As early as 5 weeks of age, *plg-/-p75^{NTR}-/-* mice were noticeably smaller than littermate controls (Fig. 5A). *plg-/-p75^{NTR}-/-* mice also exhibited severe wasting (Fig. 5B). *plg-/-* mice have a median survival time of 6 months [137]. By contrast, *plg-/-p75^{NTR}-/-* mice had a median survival time of 2.5 months and did not live past 5 months (Fig. 5C), suggesting that genetic loss of p75^{NTR} exacerbates the phenotype of plasminogen deficiency.

We next examined the livers of the *plg-/-p75^{NTR}-/-* mice to determine the effects of p75^{NTR} deficiency on the liver pathology of the *plg-/-* mouse. *plg-/-p75^{NTR}-/-* mice showed prominent necrotic liver lesions macroscopically evident as early as 10 weeks of age (Fig. 6A). Histopathological analysis by Hematoxylin staining revealed large necrotic areas in the livers of *plg-/-p75^{NTR}-/-* mice not observed in either wild-type or 10 week old *plg-/-* control littermates (Fig. 6B). Examination of caspase activation, an indicator of apoptosis, showed no apoptosis in the livers of *plg-/-* mice, while *plg-/-p75^{NTR}-/-* had large regions containing apoptotic cells, determined by morphology to be hepatocytes (Fig. 6C). Taken together, these results show that loss

of p75^{NTR} exacerbates the liver pathology of the *plg-/-* mouse, and suggest that p75^{NTR} plays a protective role in liver disease.

3. Genetic loss of p75^{NTR} does not alter fibrin deposition in the *plg-/-* mouse

Two hypotheses could potentially account for the exacerbated liver pathology observed in the *plg-/-p75^{NTR}-/-* mouse. Hypothesis 1 would postulate that p75^{NTR} regulates fibrin deposition and degradation in the *plg-/-* mouse, and that loss of p75^{NTR} may lead to excess fibrin buildup, which is the causative agent that drives the liver pathology in the *plg-/-* mouse [137]. Hypothesis 2 would postulate that p75^{NTR} alters the pathophysiological characteristics of HSCs that are crucial for the progression of liver disease in the *plg-/-* mouse. To test the first hypothesis, we examined fibrin deposition in the livers of *plg-/-p75^{NTR}-/-* mice. Examination of fibrin deposition by immunochemical detection of fibrin(ogen) revealed no differences between *plg-/-* and *plg-/-p75^{NTR}-/-* mice (Fig. 7A). To examine fibrin levels in a more quantitative manner, we isolated fibrin from the livers of *plg-/-p75^{NTR}-/-* mice and control littermates at different timepoints and performed an immunoblot analysis for fibrin(ogen). We observed no differences between the levels of fibrin in the livers of the *plg-/- p75^{NTR}-/-* mice when compared to *plg-/-* mice of matching age (Fig. 7B). Taken together, these results suggest that the exacerbated liver pathology observed in the *plg-/- p75^{NTR}-/-* mice was not due to increased fibrin deposition.

4. Genetic loss of p75^{NTR} inhibits HSC activation *in vivo*

Once we determined that the exacerbated liver pathology of the *plg-/-p75^{NTR}-/-* mouse was not due to increased fibrin deposition, we wanted to next examine our alternative hypothesis, that p75^{NTR} regulates the function of HSCs in liver disease and this effect on HSC function is the cause of the exacerbated liver pathology observed in the *plg-/-p75^{NTR}-/-* mouse. We first examined p75^{NTR} expression in the liver by immunostaining for p75^{NTR} (Fig. 8). Wild-type *plg+/+p75^{NTR}+/+* control mice expressed low levels of p75^{NTR}, while livers of *plg-/-* mice exhibited a significant increase in p75^{NTR} expression in HSCs with characteristic spindle morphology and peri-hepatocyte localization (Fig. 8A). No immunoreactive staining was observed in the liver of *p75^{NTR}-/-* mice. Confocal double immunofluorescence for p75^{NTR} and the HSC marker desmin confirmed that p75^{NTR} is expressed by HSCs in the livers of *plg-/-* mice (Fig. 8B). Our results are in accordance with previous studies, which have found that quiescent HSCs express low levels of p75^{NTR} [19, 41] and that p75^{NTR} is upregulated after HSC activation into αSMA-positive myofibroblasts both *in vitro* [19] and *in vivo* [41].

Because a previous study had observed HSC activation in the *plg-/-* mouse [138], we were interested in determining if the exacerbated liver pathology of the *plg-/-p75^{NTR}-/-* mouse was due to effects on HSC activation caused by loss of p75^{NTR}. To determine if loss of p75^{NTR} alters HSC activation, we examined the expression of α-smooth muscle actin (*αSMA*) and collagen I (*col1α1*), which are the two major markers expressed in the liver by HSCs that have differentiated to myofibroblasts [50]. *plg-/-* mice had a nearly 7-fold increase in *αSMA* gene expression compared to wild-

type control animals (Fig. 9A), as well as a 2-fold increase in *col1α1* gene expression (Fig. 9B). By contrast, both *αSMA* and *col1α1* were significantly reduced in the livers of the *plg-/-p75^NTR^-/-* mice compared to *plg-/-* mice, suggesting that p75^NTR^ is required for the induction of activated HSC gene products *in vivo*. Total number of HSCs was similar in between *plg-/-* and *plg-/-p75^NTR^-/-* mice (Fig. 10), suggesting that the decrease in *αSMA* and *col1α1* was a result of their activation state and not differences in cell number. Additionally, examination of HSCs in adult wild-type and *p75^NTR^-/-* mice showed no differences in the number of total desmin-positive HSCs, suggesting that p75^NTR^ does not affect the developmental differentiation of HSCs (Fig. 10). Taken together, these results indicate that p75^NTR^ is necessary for HSC activation *in vivo*, and that the exacerbated liver pathology of the *plg-/-p75^NTR^-/-* mouse may be due to defects in HSC activation due to loss of p75^NTR^.

5. Loss of p75^NTR^ inhibits HSC activation *in vitro*

To examine whether p75^NTR^ might be directly involved in the regulation of HSC differentiation to myofibroblasts, we assessed the ability of primary HSCs isolated from *p75^NTR^-/-* mice to differentiate *in vitro*. Wild-type HSCs undergo activation within two weeks in culture and p75^NTR^ expression positively correlates with HSC activation [19]. After 3 weeks in culture, wild-type HSCs exhibited morphologic features of activated myofibroblasts, characterized by wide, spread out morphology and large round nuclei (Fig. 11A). By contrast, *p75^NTR^-/-* HSCs were mostly in a quiescent state and the few cells that were αSMA+ were arrested at an

intermediate stage of differentiation, characterized by small size and shrunken morphology (Fig. 11A). $p75^{NTR}$-/- HSCs showed an 8-fold decrease in the percentage of αSMA+ differentiated cells, as well as a 3-fold decrease in αSMA+ cell size, when compared to wild-type HSCs (Fig. 11, B and C). Additionally, genetic loss of p75^{NTR} in HSCs suppressed protein expression of αSMA and collagen I (Fig. 12A), as well as gene expression of both *col1α1* and transforming growth factor β-1 (*TGFβ-1*) (Fig. 12B), which are upregulated by HSCs in the myofibroblast state [49].

To further confirm that loss of p75^{NTR} inhibits HSC differentiation to myofibroblasts and that the defect in HSC activation observed in $p75^{NTR}$-/- HSCs was not due to gross developmental or signaling changes due to genetic depletion of p75^{NTR}, we decided to use a gene knockdown approach to deplete p75^{NTR} from wild-type HSCs. Because primary HSCs, like many other primary cells, are notoriously difficult to transfect using traditional lipid-based reagents for oligonucleotide transfection [140], we created a novel lentiviral vector encoding a short hairpin RNA (shRNA) against mouse $p75^{NTR}$ for use in lentivirus-mediated shRNA knockdown of $p75^{NTR}$ (Fig. 13). Lentiviral shRNA-mediated knockdown of $p75^{NTR}$ in wild-type HSCs resulted in a 4.4-fold reduction of αSMA+ cells compared to control (Fig. 14, A and B), suggesting that depletion of p75^{NTR} by RNA interference inhibits HSC activation similar to the genetic depletion of p75^{NTR} in HSCs. Taken together, these results suggest that p75^{NTR} is necessary for HSC activation, and that loss of p75^{NTR} inhibits HSC differentiation into myofibroblasts.

54

6. Adenoviral delivery of p75^{NTR} restores activation in *p75^{NTR}*-/- HSCs

Because we had observed that loss of p75^{NTR} causes an inhibition of HSC differentiation to myofibroblasts, we were interested in determining whether re-expression of *p75^{NTR}* in *p75^{NTR}*-/- HSCs could restore their activation. To examine this, we used an adenovirus containing *p75^{NTR}* [141] to deliver *p75^{NTR}* to *p75^{NTR}*-/- HSCs (Fig. 15). In *p75^{NTR}*-/- HSCs infected with adenovirus containing the full length *p75^{NTR}* gene (*p75^{NTR}*-/- Ad p75^{NTR} FL), we observed activation similar to wild-type HSCs infected with control adenovirus (wt Ad ctrl) (Fig. 15, A and B). Interestingly, we observed similar results in *p75^{NTR}*-/- HSCs infected with adenovirus containing just the intracellular domain of the *p75^{NTR}* gene (*p75^{NTR}*-/- Ad p75^{NTR} ICD) (Fig. 15, A and B), suggesting that expression of the ICD of p75^{NTR} alone is sufficient to promote HSC activation. Overall, our results suggest that the defects we observe in HSC activation *in vitro* are specifically due to loss of p75^{NTR}, as re-expression of *p75^{NTR}* is able to restore differentiation in *p75^{NTR}*-/- HSCs.

7. Loss of p75^{NTR} had no affect on HSC apoptosis or proliferation

Because we observed such a significant difference in HSC activation due to p75^{NTR} expression, we wanted to make sure that the affect of p75^{NTR} on HSC differentiation was not due to secondary effects from changes in HSC apoptosis or proliferation. Prior studies have shown a small 1.5-fold increase in HSC apoptosis upon induction with high non-physiological concentrations of exogenous NGF [19]. In our experiments, we confirmed that addition of exogenous NGF at high

concentrations caused a 1.6-fold increase of HSC apoptosis in wild-type cells (Fig. 16A). In the absence of exogenous NGF, wild-type and $p75^{NTR}$-/- HSCs showed no difference in apoptosis (Fig. 16A). Because the tissue culture conditions of the differentiation experiments (Figs. 11, 12, 14, 15) were performed in the absence of exogenous NGF, we believe that apoptosis cannot account for the large differences observed in HSC differentiation. Addionally, examination of proliferation of wild-type and $p75^{NTR}$-/- HSCs revealed no significant differences in cell proliferation, either in the presence or absence of NGF (Fig. 16B), suggesting that the differences observed in HSC differentiation are not due to differences in proliferation between wild-type and $p75^{NTR}$-/- HSCs. Overall, these results suggest that the major function of $p75^{NTR}$ in HSCs is the regulation of differentiation from quiescent cells into activated myofibroblasts.

8. $p75^{NTR}$-mediated HSC differentiation is neurotrophin- and Trk-independent

Once we identified that the major function of $p75^{NTR}$ in HSCs is regulation of differentiation, we next wanted to examine the signaling mechanisms involved in $p75^{NTR}$-mediated HSC activation. We first wanted to determine if $p75^{NTR}$-mediated HSC activation was dependent upon neurotrophins, which are the major physiological ligands that have been identified for $p75^{NTR}$ [5]. As already described, the effects of $p75^{NTR}$ on HSC differentiation that we observed occurred without the addition of exogenous neurotrophin ligand (Figs. 11, 12, 14, 15). Because there is some evidence in the literature that HSCs can express all four neurotrophins [41], we wanted to

determine if HSC-derived neurotrophins were able to promote HSC activation in an autocrine manner. To examine this, we observed HSC differentiation in the presence of neurotrophin-neutralizing agents. Neutralization of neurotrophins by either anti-NGF antibody, BDNF scavenger Fc-TrkB, or pan-neurotrophin scavenger Fc-p75^{NTR} had no effect on HSC differentiation (Fig. 17), suggesting that a neurotrophin autocrine loop is not responsible for HSC differentiation. Moreover, adenoviral delivery of the intracellular domain of p75^{NTR} alone restored differentiation of *p75^{NTR}*-/- HSCs similar to adenoviral delivery of full length p75^{NTR} (Fig. 15), suggesting that p75^{NTR}-mediated HSC activation can occur in a ligand-independent manner.

We additionally wanted to determine if p75^{NTR}-mediated HSC activation requires activation of the p75^{NTR} co-receptor Trk. Previous work has shown that HSCs express two of the three Trk isoforms [41], and other studies have shown that p75^{NTR}-mediated Trk activation plays a role in neuronal cell differentiation [142]. To examine whether Trk is involved in p75^{NTR}-mediated HSC differentiation, we treated HSCs with the Trk inhibitor K252a and observed its effects on differentiation. Inhibition of Trk activity with K252a had no effect on HSC activation (Fig. 17), suggesting that HSC differentiation occurs independently of Trk signaling.

9. p75^{NTR} signaling through Rho is responsible for p75^{NTR}-mediated HSC activation

After ruling out a role for neurotrophins and Trk in p75^{NTR}-mediated HSC differentiation, we hoped to identify other mediators involved in intracellular signaling

during this process. In general, the signal transduction mechanisms that promote and control HSC differentiation into myofibroblasts remain elusive. Previous studies have implicated the involvement of the small GTPase Rho in regulating myofibroblast morphology via reorganization of the actin cytoskeleton [143, 144]. A signaling relationship between p75[NTR] and Rho has been well documented in the nervous system, where p75[NTR]-mediated Rho signaling is involved in rearrangement of the actin cytoskeleton in neurons to control neurite outgrowth [36]. Since either p75[NTR] in the absence of ligand or the ICD of p75[NTR] alone can activate Rho through a direct interaction [9] and Rho is involved in promoting the myofibroblastic state of HSC [144], we examined whether p75[NTR] promotes HSC activation through Rho. We first examined Rho activity in wild-type and *p75[NTR]-/-* HSCs through immunostaining for phosphorylated cofilin (phospho-cofilin), a marker for Rho activation [145]. In contrast to wild-type HSCs, *p75[NTR]-/-* HSCs were negative for phospho-cofilin (Fig. 18), suggesting that Rho activation was reduced in *p75[NTR]-/-* HSCs. To determine if reduced Rho activity was causing the inhibited activation observed in *p75[NTR]-/-* HSCs, we next examined whether expression of constitutively activated *Rho* in *p75[NTR]-/-* HSCs could restore their activation. To examine this, we used an adenovirus to deliver constitutively activated *Rho* [146] to *p75[NTR]-/-* HSCs (Fig. 19, A and B). In *p75[NTR]-/-* HSCs infected with adenovirus containing constitutively activated *Rho* (*p75[NTR]-/-* Ad Rho), we observed activation similar to wild-type HSCs infected with control adenovirus (wt Ad ctrl) (Fig. 19B).

To determine if blocking p75[NTR]-mediated Rho signaling in wild-type HSCs would prevent their differentiation into myofibroblasts, we treated wild-type HSCs

with TAT-Pep5, a cell-permeable peptide inhibitor that specifically blocks the activation of Rho through p75^{NTR} [36] and observed their differentiation (Fig. 20). Control-treated HSCs exhibited the characteristic spread out myofibroblastic morphology. By contrast, the majority of the TAT-Pep5-treated cells showed an undifferentiated morphology (Fig. 20A) similar to *p75^{NTR}-/-* HSCs (Fig. 11A). Gene expression analysis revealed decreased *col1α1* and *TGFβ-1* expression in TAT-Pep5-treated cells compared to control (Fig. 20B), similar to the gene expression profile observed in *p75^{NTR}-/-* HSCs (Fig. 12B). Additionally, TAT-Pep5 reduced phospho-cofilin in wild-type cells (Fig. 21), further suggesting that p75^{NTR} is a major activator of Rho in HSCs. Overall, these results suggest that p75^{NTR} signaling through Rho promotes HSC differentiation to myofibroblasts.

10. Genetic loss of p75^{NTR} results in reduced liver cell proliferation and reduced levels of HGF in a mouse model of liver injury

Previous studies have shown the importance of HSC activation in promoting hepatocyte proliferation, as defective HSC activation results in impaired liver regeneration [78]. Therefore, we were interested in determining whether p75^{NTR} as a regulator of HSC activation could regulate hepatocyte proliferation and liver regeneration. To investigate this, we examined liver cell proliferation in *plg-/-* and *plg-/-p75^{NTR}-/-* mice to see whether loss of p75^{NTR} affects liver repair after injury. After *in vivo* labeling with the cell proliferation marker bromodeoxyuridine (BrdU), *plg-/-* mice showed an increased number of BrdU+ proliferating hepatocytes (126.6 ±

3.9) (Fig. 22, A and B), when compared to wild-type mice (95.2 ± 3.7), suggestive of the regenerative response in the liver after injury. By contrast, *plg-/-p75^NTR^-/-* mice displayed significantly decreased cell proliferation (74.2 ± 9.1) compared to *plg-/-* mice (Fig. 22, A and B), suggesting that expression of p75^NTR^ promotes hepatocyte proliferation in the *plg-/-* mouse. One of the key mediators in promoting hepatocyte proliferation and subsequent liver regeneration is hepatocyte growth factor (HGF) [49]. To determine if the differences in cell proliferation observed in the *plg-/-* and *plg-/-p75^NTR^-/-* mice were due to differences in HGF, we examined HGF levels in the livers of these mice. Strikingly, whole liver homogenates from *plg-/-p75^NTR^-/-* mice showed a 3-fold decrease in HGF protein compared to *plg-/-* livers (Fig. 23). Since HSCs are a major source of HGF in the liver [147, 148], the reduction in HGF in the *plg-/-p75^NTR^-/-* mouse is in accordance with the defective HSC activation observed after genetic loss of p75^NTR^ both *in vivo* (Fig. 9) and *in vitro* (Fig. 11). Taken together, these results suggest that expression of p75^NTR^ promotes expression of HGF and hepatocyte proliferation *in vivo*.

11. Genetic loss of p75^NTR^ in HSCs causes diminished levels of hepatocyte proliferation *in vitro*

Crosstalk of HSCs with hepatocytes is a major cellular mechanism that drives hepatocyte proliferation and liver repair [49, 78, 79]. We therefore examined whether p75^NTR^-mediated activation of HSCs was necessary to support hepatocyte proliferation. We used a previously established hepatocyte-HSC *in vitro* co-culture

system (Fig. 24A), where wild-type HSCs promote hepatocyte proliferation [79]. Primary wild-type hepatocytes were co-cultured with either wild-type or $p75^{NTR}$-/- HSCs. Hepatocytes in co-culture with $p75^{NTR}$-/- HSCs exhibited a 30% decrease in proliferation compared to those incubated with wild-type HSCs (Fig. 24B). This reduction in proliferation was rescued when additional HGF was added to the culture medium (Fig. 24B). Overall, these results suggest that p75^{NTR} expression by HSCs is necessary for their differentiation to repair-supporting, HGF-secreting cells which in turn can promote hepatocyte proliferation both *in vivo* (Fig. 22) and *in vitro* (Fig. 24).

12. Summary

With the goal of determining the function of p75^{NTR} in liver injury and repair, we discovered that the major function of p75^{NTR} in the liver is regulation of HSC differentiation from a quiescent lipocyte to a myofibroblast cell type, and that p75^{NTR}-mediated HSC activation is protective in liver injury and necessary for liver repair. In the *plg*-/- mouse model of liver injury, loss of p75^{NTR} resulted in exacerbated liver pathology and inhibited HSC activation *in vivo* (Figs. 6, 9). *In vitro*, $p75^{NTR}$-/- HSCs failed to differentiate, and adenoviral delivery of $p75^{NTR}$ restored activation in $p75^{NTR}$-/- HSCs, suggesting that p75^{NTR} is necessary for HSC differentiation (Figs. 11, 15). No differences in apoptosis or proliferation were observed between wild-type and $p75^{NTR}$-/- HSCs (Fig. 16), thus identifying regulation of differentiation as the major function of p75^{NTR} in HSCs. Neither neurotrophins nor Trk activity was required for HSC differentiation (Fig. 17), and in fact expression of the intracellular domain of

p75^{NTR} alone was sufficient to promote HSC activation (Fig. 15). *p75^{NTR}-/-* HSCs exhibited loss of Rho activation compared to wild-type HSCs (Fig. 18), and restoration of Rho activity completely rescued the differentiation of *p75^{NTR}-/-* HSCs (Fig. 19). Moreover, inhibition of p75^{NTR}-mediated Rho activation prevented activation of wild-type HSCs (Fig. 20), suggesting that p75^{NTR} signaling through Rho promotes HSC differentiation. In examining the role of p75^{NTR} in liver repair after injury, we found that the loss of p75^{NTR} resulted in diminished liver cell proliferation in the *plg-/-* mouse (Fig. 22), as well as decreased levels of hepatocyte growth factor in the liver (Fig. 23). In co-culture, *p75^{NTR}-/-* HSCs were unable to promote hepatocyte proliferation to the extent of wild-type HSCs, but hepatocyte proliferation was recovered by addition of HGF (Fig. 24). Overall, the results of our studies suggest that p75^{NTR} expression by HSCs is necessary for their differentiation to repair-supporting, HGF-secreting cells, which in turn can promote the hepatocyte proliferation necessary for liver repair after injury or disease.

13. Acknowledgments
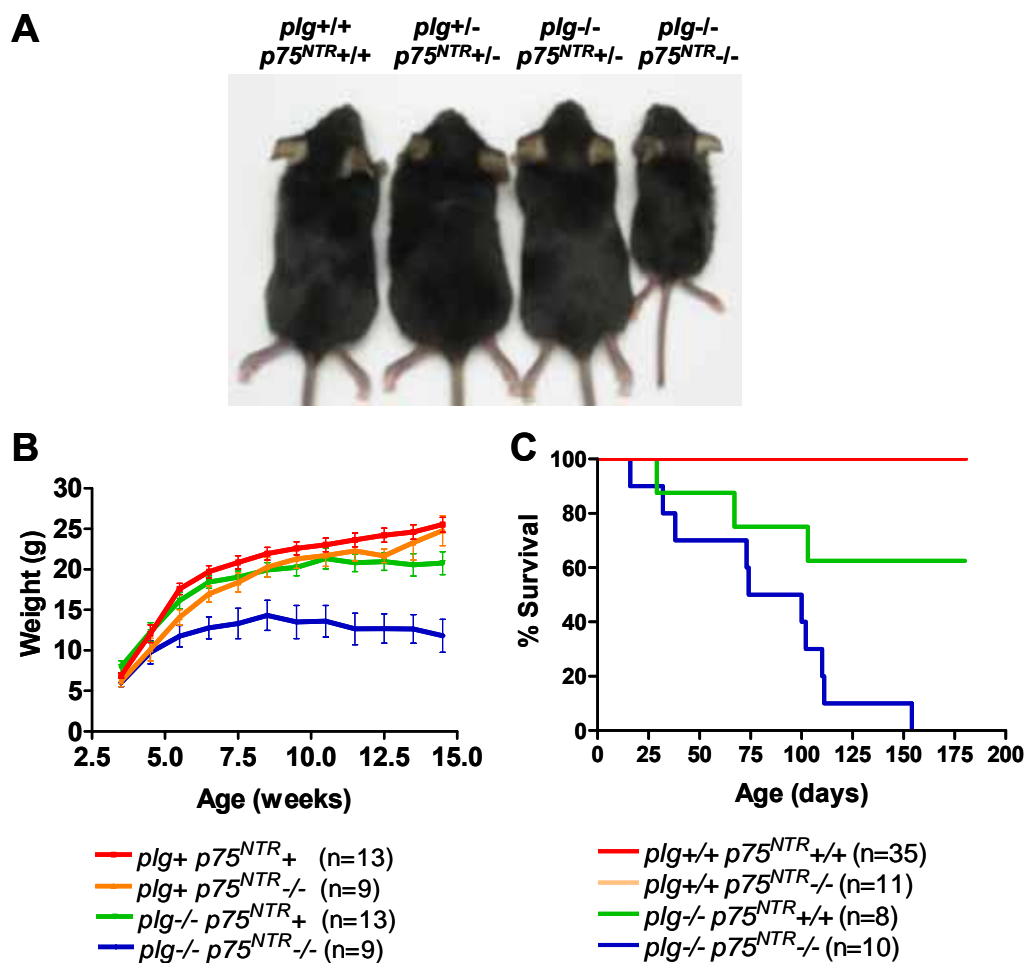
Figure 5. Exacerbated wasting and mortality caused by p75^NTR deficiency.

(A) Representative appearance of a *plg+/+p75^NTR+/+* mouse, a *plg+/-p75^NTR+/-* mouse, a *plg-/-p75^NTR+/-* mouse, and a *plg-/-p75^NTR-/-* mouse at 5 weeks of age. **(B)** Weight of *plg+p75^NTR+*, *plg+p75^NTR-/-*, *plg-/-p75^NTR+*, and *plg-/-p75^NTR-/-* mice. Because heterozygous (+/-) mice are phenotypically undistinguishable from homozygous (+/+) mice, mice with *plg+/+* or *plg+/-* genotype are designated *plg+*, and mice with *p75^NTR+/+* or *p75^NTR+/-* genotype are designated *p75^NTR+*. **(C)** Survival of *plg+/+p75^NTR+/+*, *plg+/+p75^NTR-/-*, *plg-/-p75^NTR+/+*, and *plg-/-p75^NTR-/-* mice. As both *plg+/+p75^NTR+/+* and *plg+/+p75^NTR-/-* mice exhibited 100% survival, the curves overlap and appear as a single line on the graph.
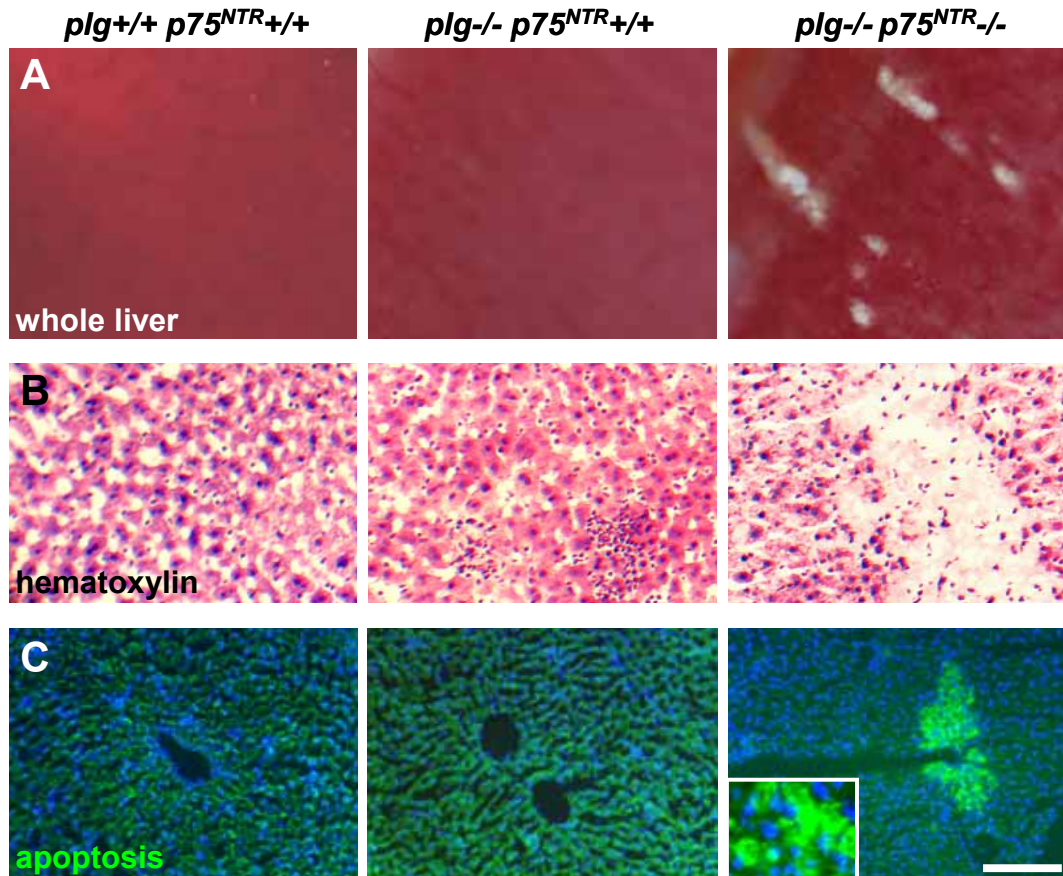
Figure 6. Exacerbated liver pathology caused by p75^{NTR} deficiency.

(A) Representative stereoscope images of the livers of 10 week old *plg+/+p75^{NTR}+/+*, *plg-/-p75^{NTR}+/+*, and *plg-/-p75^{NTR}-/-* mice. Note the appearance of lesions (white areas) in the *plg-/-p75^{NTR}-/-* mouse (right). Scale bar, 0.4 mm. **(B)** Hematoxylin staining of liver sections from mice described in (A). Note large area of necrosis in the *plg-/-p75^{NTR}-/-* mouse (right). Scale bar, 58 μm. **(C)** A FITC-conjugated inhibitor of active caspases was used to stain apoptotic cells (green) in liver sections from mice described in (A). Inset depicts apoptotic cells at a higher magnification, determined by morphology to be hepatocytes. Scale bar, 100 μm; inset, 35 μm.
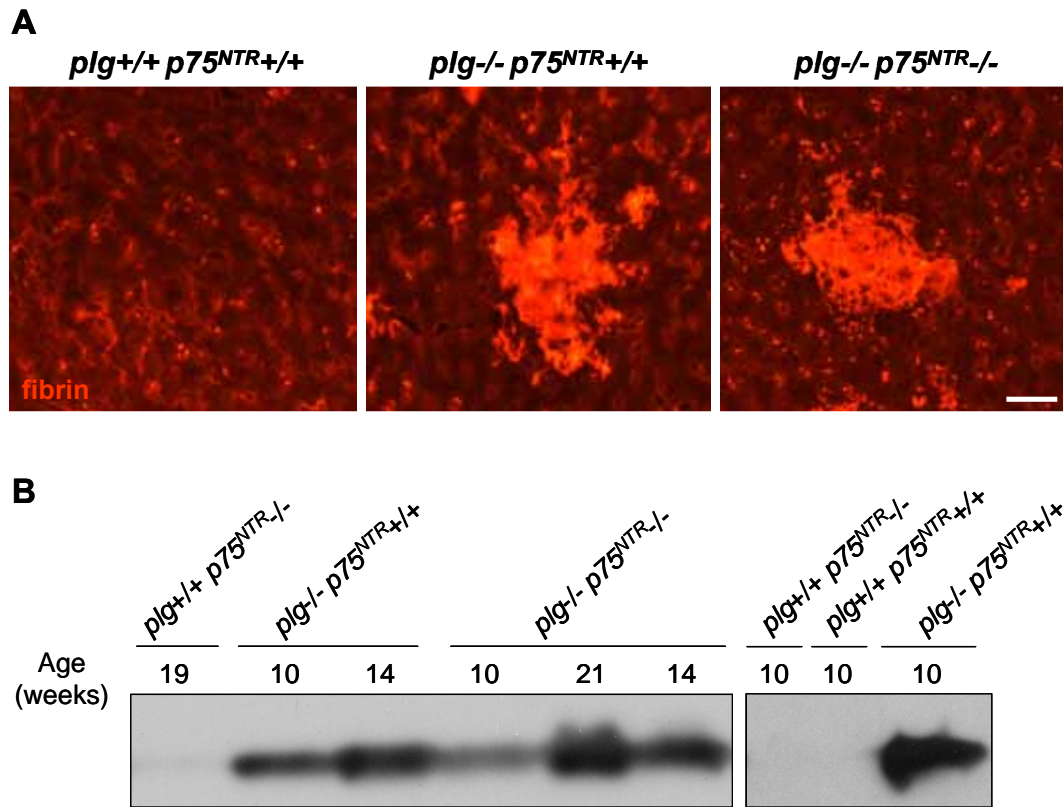
Figure 7. Genetic loss of p75^{NTR} does not change fibrin levels in the *plg-/-* mice.

(A) Immunochemical detection of fibrin(ogen) (red) in liver sections of 10 week old *plg+/+p75^NTR^+/+*, *plg-/-p75^NTR^+/+*, and *plg-/-p75^NTR^-/-* mice. Normal mice (left) exhibit granular fibrin(ogen) staining indicative of blood vessel morphology. Both *plg-/-p75^NTR^+/+* (middle) and *plg-/-p75^NTR^-/-* (right) liver contain large areas of fibrin deposition outside the vasculature. Scale bar, 31 μm. **(B)** Immunoblot detection of fibrin isolated from livers of *plg+/+p75^NTR^+/+*, *plg+/+p75^NTR^-/-*, *plg-/-p75^NTR^+/+*, and *plg-/-p75^NTR^-/-* mice, ages 10 to 21 weeks. Fibrin immunoblots performed by Jiang Han and Katerina Akassoglou.
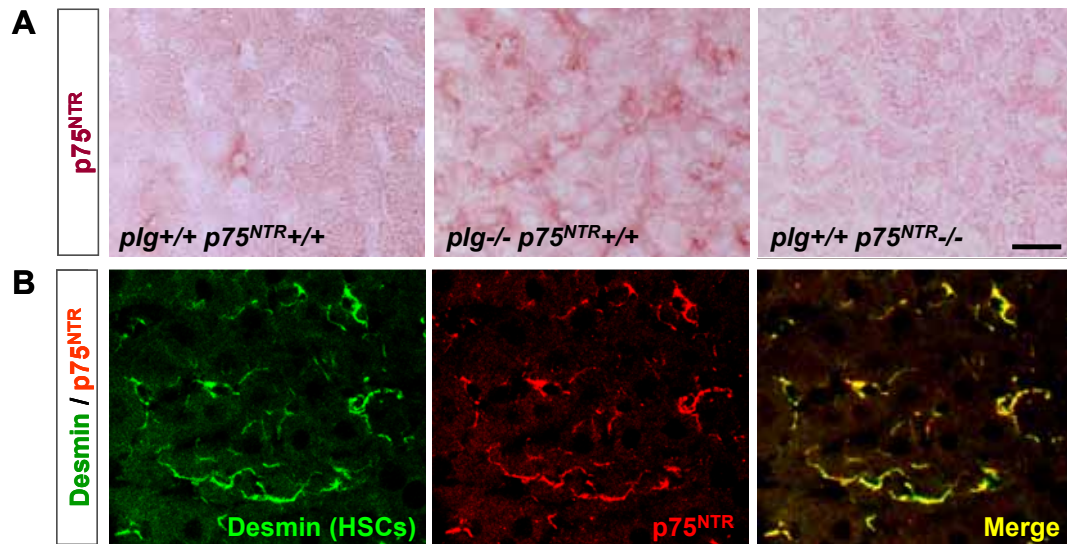
Figure 8. p75^{NTR} expression in liver.

(A) Immunochemical detection of p75^{NTR} (dark red) in livers of 10 week old *plg+/+p75^{NTR}+/+*, *plg-/-p75^{NTR}+/+*, and *plg+/+p75^{NTR}-/-* (negative control) mice. Immunoreactive cells show spindle morphology and peri-hepatocyte localization characteristic of HSCs. Scale bar, 19 μm. **(B)** Confocal double immunofluorescence in *plg-/-* liver shows colocalization (yellow) of the HSC marker desmin (green) with p75^{NTR} (red). Scale bar, 25 μm. Confocal microscopy was performed by Katerina Akassoglou.
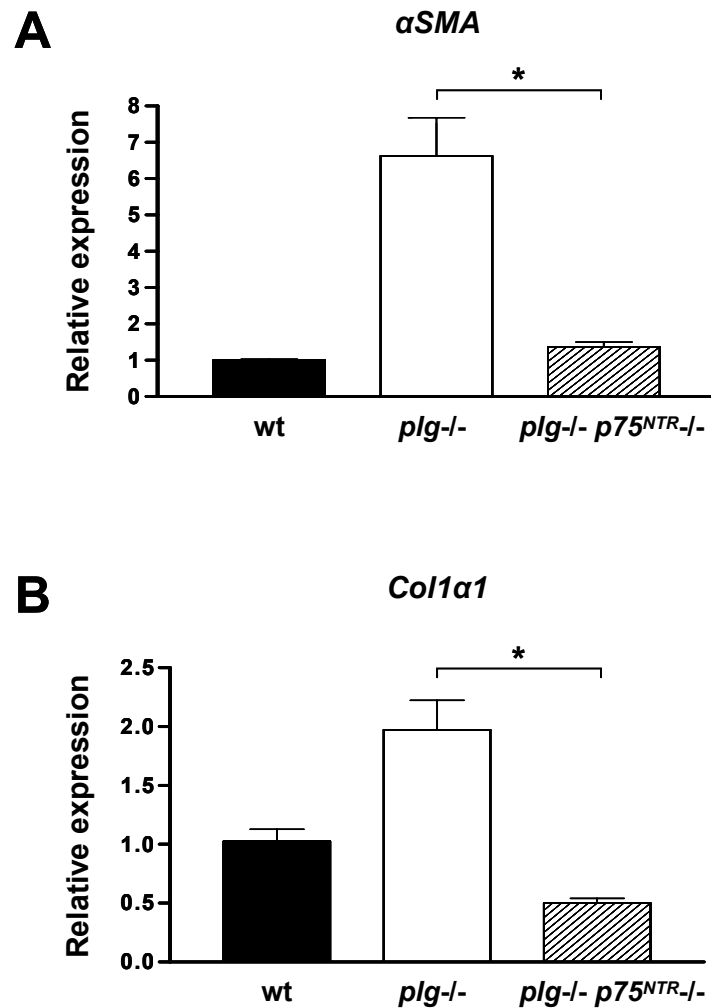
Figure 9. Genetic loss of p75^{NTR} inhibits HSC activation *in vivo*.

(A) *αSMA* and **(B)** *col1α1* gene expression was examined in 4 week old mice (*n* = 3 mice per genotype) by real-time polymerase chain reaction (PCR) analysis performed in duplicates. Bar graphs represent means ± SEM (*P<0.001; by one-way ANOVA).
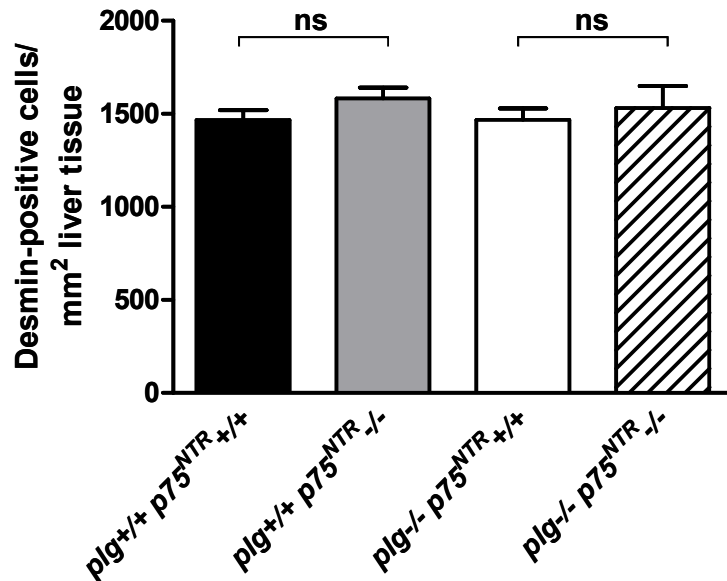
Figure 10. Genetic loss of p75^{NTR} does not affect developmental differentiation of HSCs.

Quantitation of HSC number *in vivo*. HSCs were visualized in liver sections of 10 week old *plg+/+p75^{NTR}+/+*, *plg+/+p75^{NTR}-/-*, *plg-/-p75^{NTR}+/+*, and *plg-/-p75^{NTR}-/-* mice by immunostaining for desmin, a HSC marker. HSC number was determined by counting the number of desmin-positive cells per field (*n* = 5 for *plg+/+p75^{NTR}+/+* and *plg+/+p75^{NTR}-/-*; *n* = 3 for *plg-/-p75^{NTR}+/+* and *plg-/-p75^{NTR}-/-*). Data are mean ± SEM (ns, not significant; by unpaired Student's *t* test).
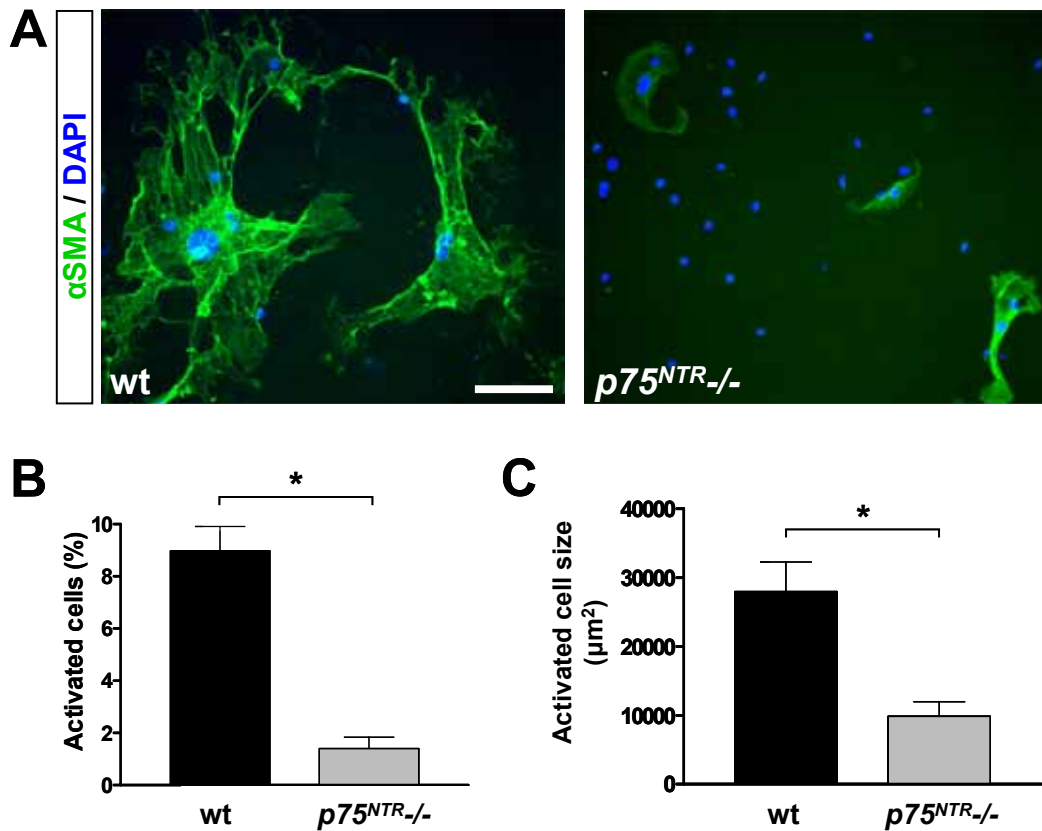
Figure 11. Genetic loss of p75^{NTR} inhibits HSC activation *in vitro*.

(A) αSMA immunostaining (green) of activated wild-type (wt) and *p75^NTR^-/-* HSCs after 21 days in culture. Wt HSCs are characterized by wide, spread out morphology and large round nuclei. *p75^NTR^-/-* HSCs are unable to differentiate and the few cells that showed immunostaining for αSMA are arrested at an intermediate stage of differentiation, characterized by small size and shrunken morphology. Nuclei are stained with DAPI (blue). Representative images are shown from 7 independent experiments. Scale bar, 93 μm. **(B)** Quantitation of percentage of activated wt and *p75^NTR^-/-* HSCs. Percentage of activated HSCs was quantified by counting the number of αSMA-immunopositive myofibroblasts per total number of nuclei per field. Experiments were performed four times in duplicates. Bar graph represents means ± SEM. (*$P<0.0001$; by unpaired Student's *t* test). **(C)** Quantitation of activated cell size of wt and *p75^NTR^-/-* HSCs. Activated cell size was quantitated by determining the area of αSMA-immunopositive cells in three independent experiments performed in duplicates. Bar graph represent means ± SEM (*$P<0.002$; by unpaired Student's *t* test).
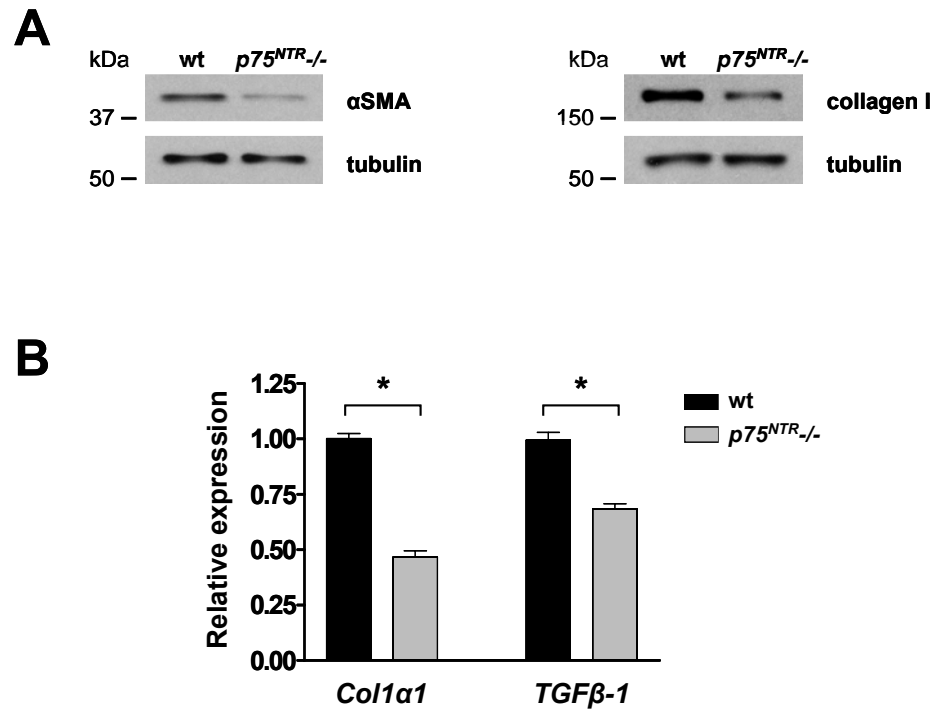
Figure 12. Genetic loss of p75^NTR diminishes expression of activated HSC markers in cultured HSCs.

(A) Western blot analysis of HSC protein extracts shows reduced expression of αSMA and collagen I in *p75^NTR-/-* HSCs when compared to control wild-type (wt) HSCs after 8 days in culture. Immunoblot for tubulin served as a loading control. **(B)** Real-time PCR analysis of gene expression of the myofibroblast markers *Col1α1* and *TGFβ-1* in wt and *p75^NTR-/-* HSCs after 14-21 days in culture. For each sample, gene expression data was normalized to HPRT gene expression and presented as fold change versus wt. Experiments were performed three times in duplicates. Graphs represent mean ± SEM (*$P<0.0001$; by unpaired Student's *t* test).
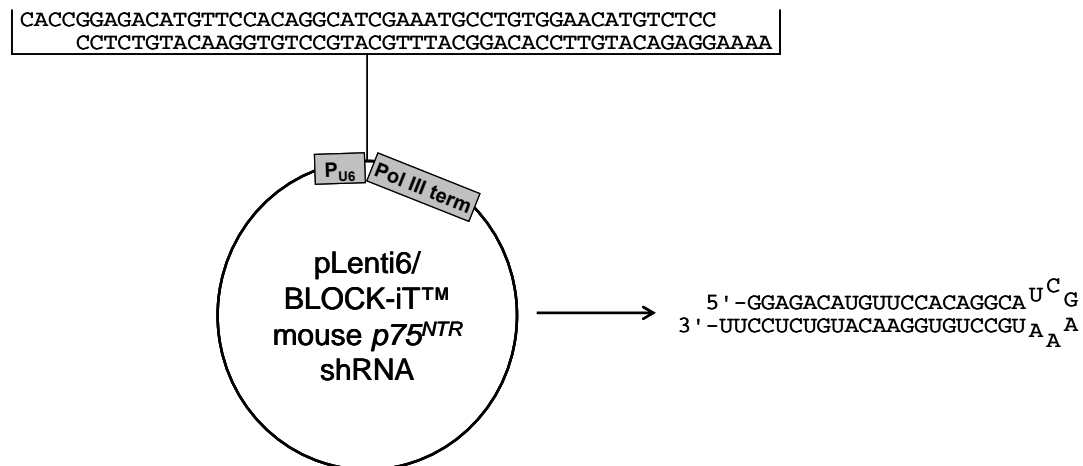
Figure 13. Vector map for the pLenti6/BLOCK-iT™ mouse *p75^NTR* shRNA vector.

Nucleotide sequence shown at top was inserted into the pLenti6/BLOCK-iT™ vector (Invitrogen). The predicted stem-loop structure of the mouse *p75^NTR* short hairpin RNA expressed from the vector is depicted at the right. Construction of vector and lentivirus expression were performed by Ryan Adams.
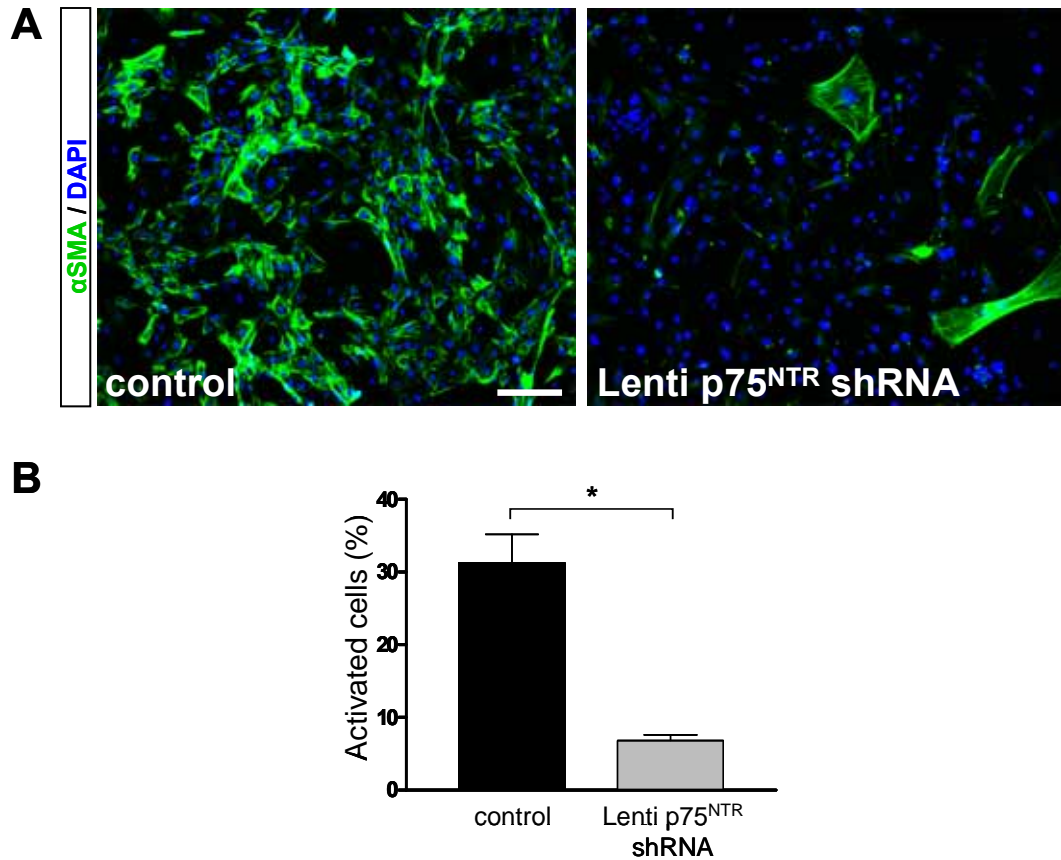
Figure 14. Lentiviral delivery of *p75^{NTR}* shRNA significantly decreases wild-type HSC activation.

(A) Representative images of control-treated (control) or *p75^{NTR}* shRNA lentivirus-treated (Lenti p75^{NTR} shRNA) HSCs. Freshly isolated wild-type (wt) HSCs were infected with lentivirus or control on day 2. αSMA immunostaining (green) was performed on day 10. Nuclei are stained with DAPI (blue). Scale bar, 123 μm. **(B)** Quantitation of percentage of activated HSCs. Percentage of activated HSCs was quantitated by counting the number of αSMA-immunopositive HSCs per total number of nuclei per field. Experiments were performed three times in duplicates. Data are mean ± SEM (*$P<0.009$; by unpaired Student's *t* test).
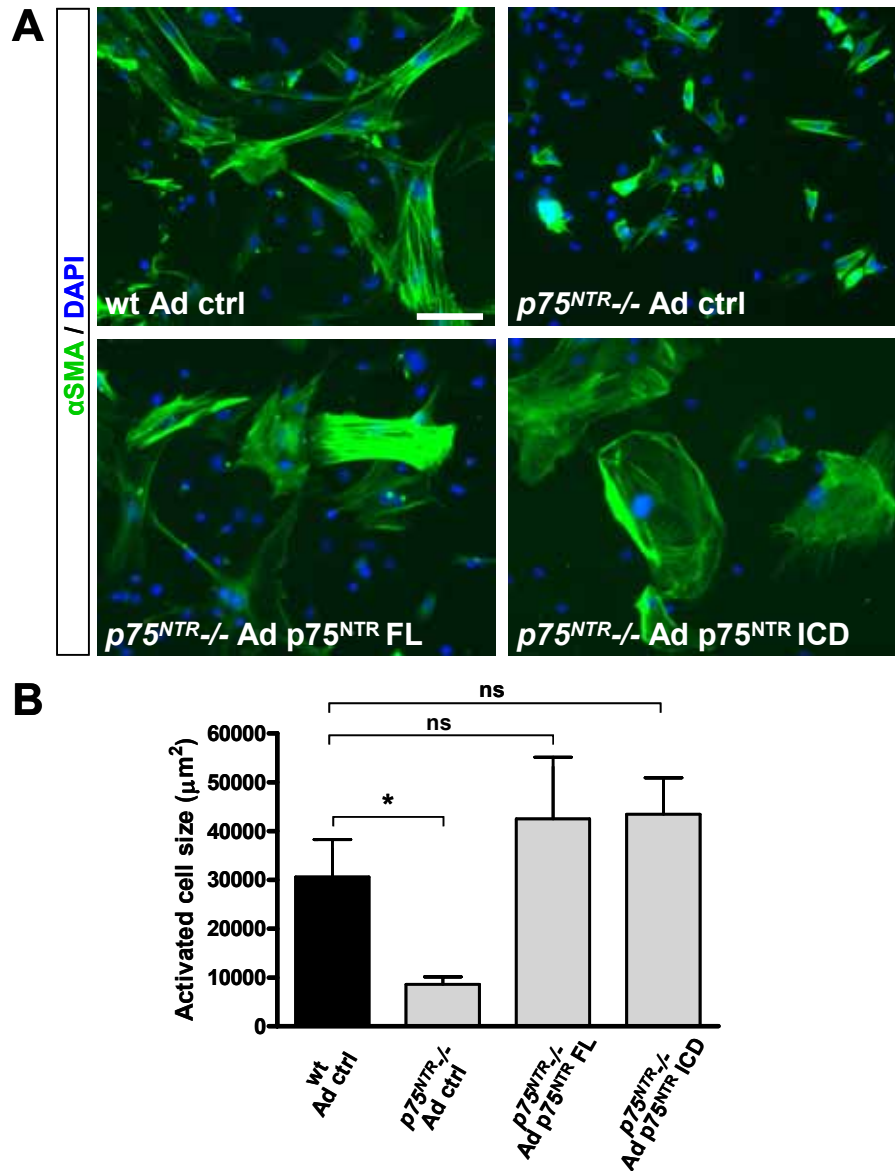
Figure 15. Adenoviral delivery of *p75^{NTR}* rescues the activation of *p75^{NTR}*-/- HSCs.

(A) Freshly isolated wild-type (wt) and *p75^{NTR}*-/- HSCs were infected on day 2 with adenovirus (control, Ad ctrl; full length *p75^{NTR}*, p75^{NTR} FL; or intracellular domain of *p75^{NTR}*, p75^{NTR} ICD). αSMA immunostaining (green) was performed on day 7. Nuclei were stained with DAPI (blue). Scale bar, 85 μm. **(B)** Quantitation of activated cell size of adenovirus-infected wt and *p75^{NTR}*-/- HSCs. Activated cell size was quantitated by determining the area of αSMA-immunopositive cells in three independent experiments performed in duplicates. Bar graphs represent means ± SEM (*$P<0.05$; ns, not significant; by one-way ANOVA). p75^{NTR} adenoviruses were kindly given by Philip Barker, McGill University.
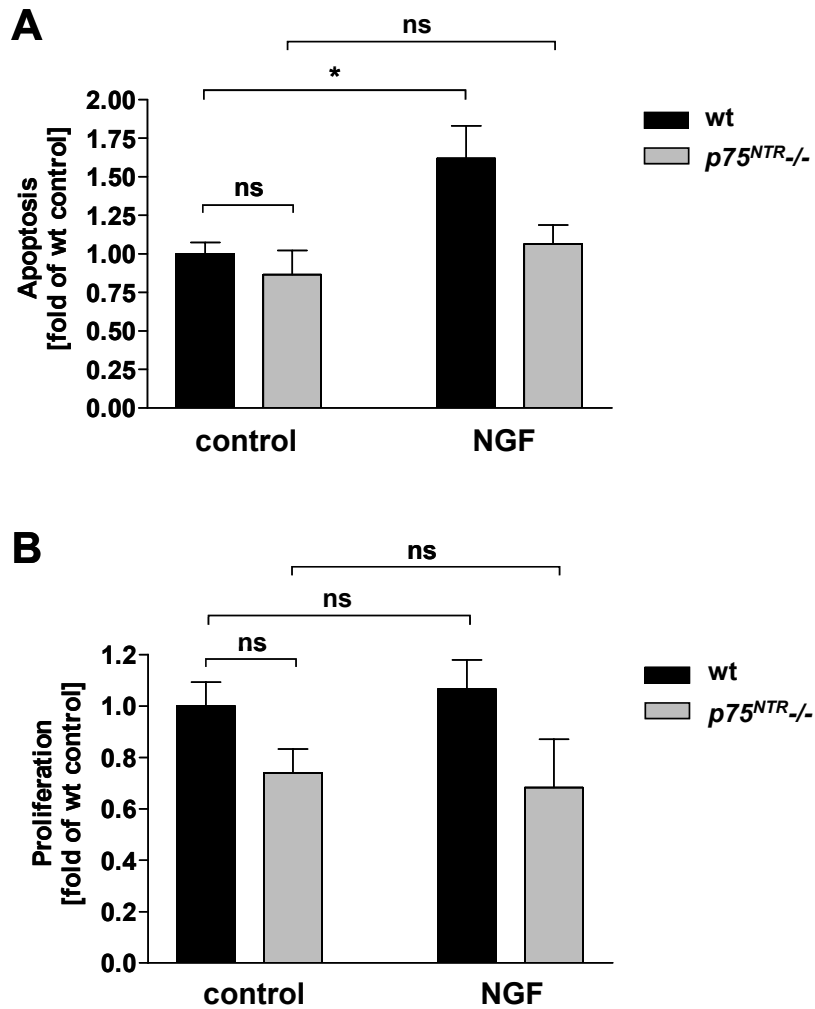
Figure 16. Genetic loss of p75^{NTR} does not affect apoptosis or proliferation of HSCs.

Wild-type (wt) and *p75^{NTR}-/-* HSCs (day 9-21) were incubated with or without 100 ng/mL NGF. **(A)** Apoptosis of HSCs *in vitro* after 24 hour treatment. Apoptosis, as measured by DNA fragmentation, was assayed by ELISA. Experiments were performed three times in duplicates. Data are mean ± SEM (*$P<0.05$; ns, not significant; by one-way ANOVA). **(B)** Proliferation of HSCs *in vitro* after 48 hour treatment. BrdU was added during the last 24 hours of treatment. Proliferation, as measured by BrdU incorporation, was assayed by ELISA. Experiments were performed three times in duplicates. Data are mean ± SEM (ns, not significant; by one-way ANOVA).
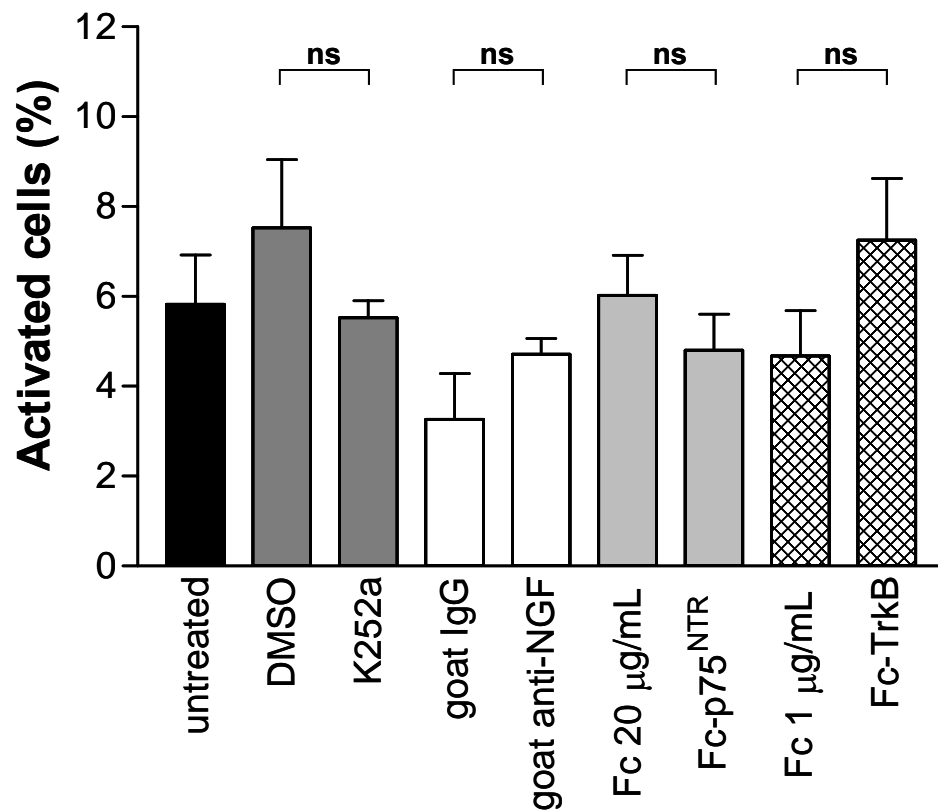
Figure 17. Trk inhibition or neurotrophin blocking have no effect on wild-type HSC differentiation.

Freshly isolated wild-type (wt) HSCs were treated on day 1 with the following: Trk inhibitor K252a (10 nM) or DMSO vehicle control; NGF-blocking antibody goat anti-NGF (2 μg/mL) or goat IgG control; neurotrophin scavenger Fc-p75^{NTR} or Fc fragment control (20 μg/mL); or BDNF scavenger Fc-TrkB or Fc fragment control (1 μg/mL). The medium was replaced with fresh medium containing treatments on days 3 and 5. αSMA immunostaining was performed on day 7 to assess activation. Percentage of activated HSCs was quantitated by counting the number of αSMA-immunopositive HSCs per total number of nuclei per field. Experiments were performed three times in duplicates. Data are mean ± SEM (ns, not significant; by unpaired Student's *t* test).
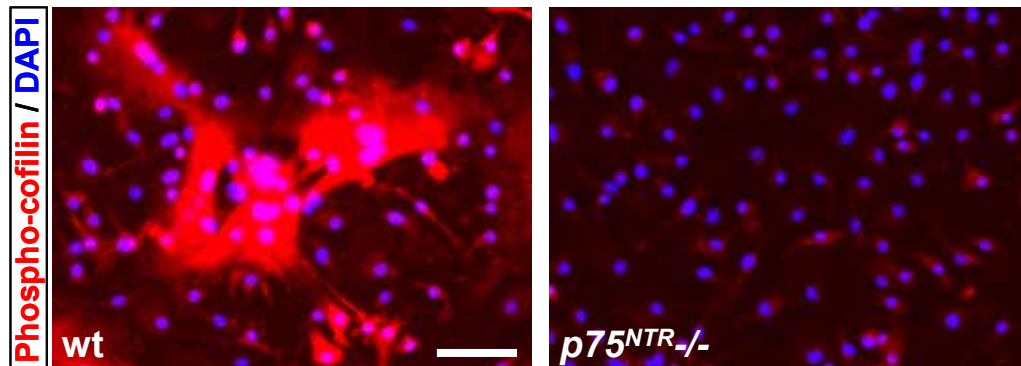
Figure 18. Loss of Rho activation in *p75^{NTR}*-/- HSCs.

Detection of phosphorylated cofilin (phospho-cofilin), a marker indicative of Rho activation, by immunostaining (red) in wild-type (wt) and *p75^{NTR}*-/- HSCs after 21 days in culture. Nuclei are stained with DAPI (blue). Scale bar, 70 μm.
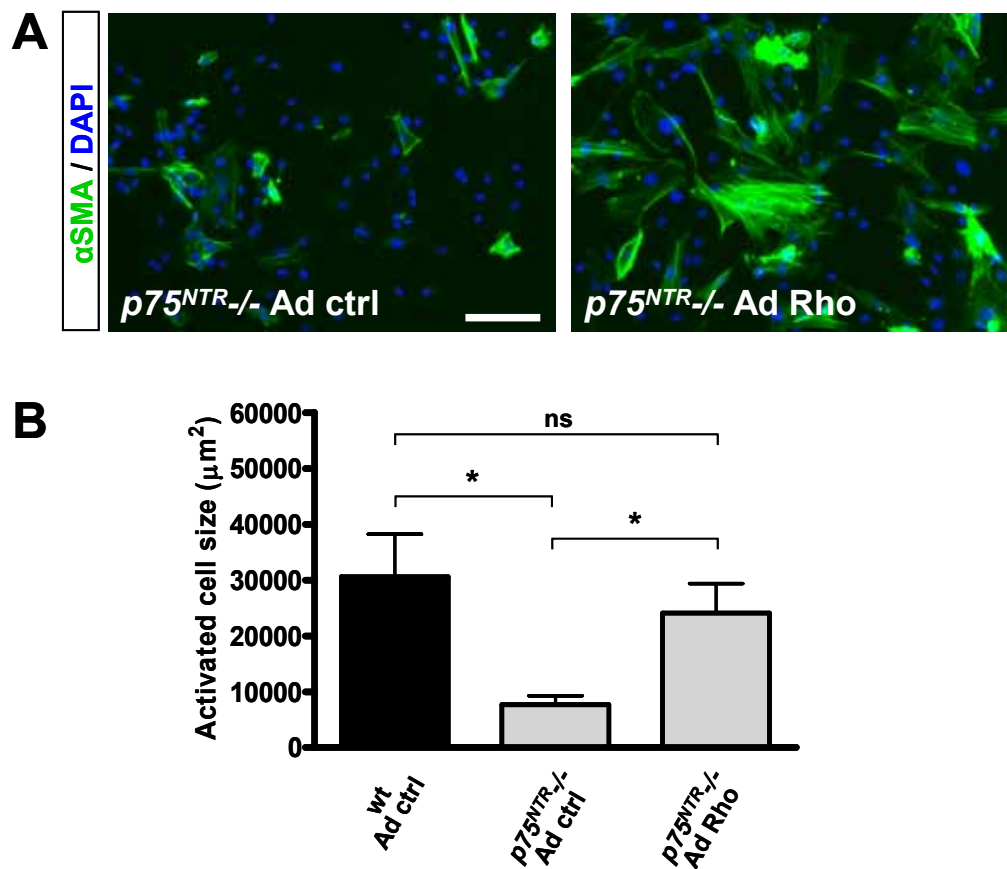
Figure 19. Adenoviral delivery of constitutively activated *Rho* rescues the activation of *p75^{NTR}*-/- HSCs.

Freshly isolated wild-type (wt) and **(A)** *p75^{NTR}*-/- HSCs were infected on day 2 with adenovirus (control, Ad ctrl; or constitutively activated *Rho*, Ad Rho). αSMA immunostaining (green) was performed on day 7. Nuclei were stained with DAPI (blue). Scale bar, 85 μm. **(B)** Quantitation of activated cell size of adenovirus-infected wt and *p75^{NTR}*-/- HSCs. Activated cell size was quantitated by determining the area of αSMA-immunopositive cells in three independent experiments performed in duplicates. Bar graph represent means ± SEM (*$P<0.05$; ns, not significant; by one-way ANOVA). Constitutively activated Rho adenovirus was kindly given by Joan Heller Brown, UCSD.
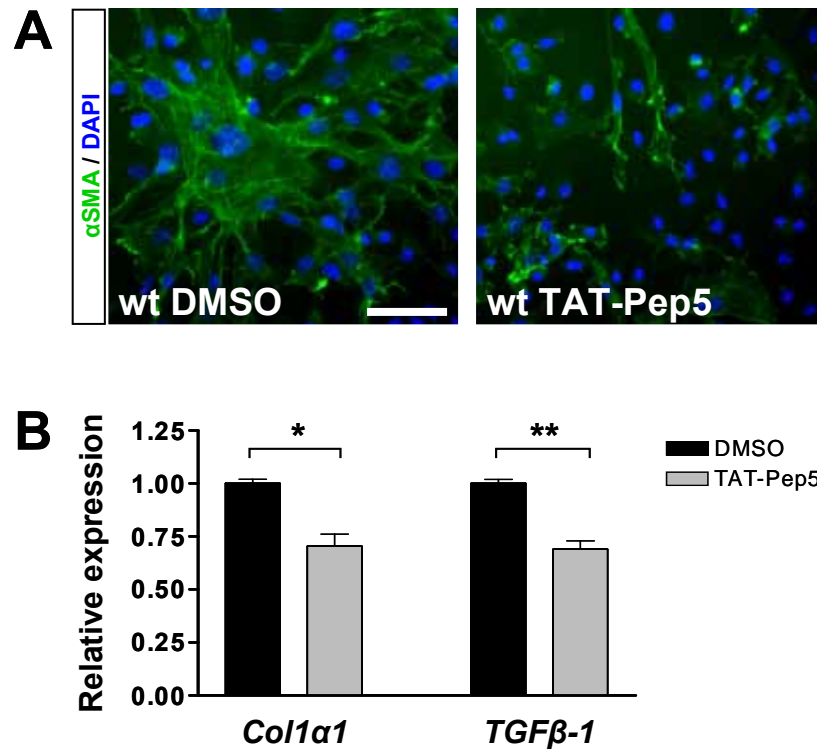
Figure 20. Inhibition of p75^{NTR}-mediated Rho activation blocks differentiation of wild-type HSCs.

(A) Representative images of wild-type (wt) HSCs after a 7 day treatment with either vehicle (DMSO) or TAT-Pep5, a cell-permeable peptide inhibitor that specifically blocks the activation of Rho through p75^{NTR}. Activated HSCs are identified by αSMA immunostaining (green). Nuclei are stained with DAPI (blue). Scale bar, 32 μm. **(B)** Expression of myofibroblast markers in wt HSCs (day 7-21) treated with DMSO or TAT-Pep5. *Col1α1* and *TGFβ-1* gene expression levels were quantitated using real-time PCR. For each sample, gene expression data was normalized to HPRT gene expression and presented as fold change versus DMSO-treated control. Experiments were performed three times in duplicates. Graph represents mean ± SEM (*$P<0.003$; **$P<0.001$; by unpaired Student's *t* test).
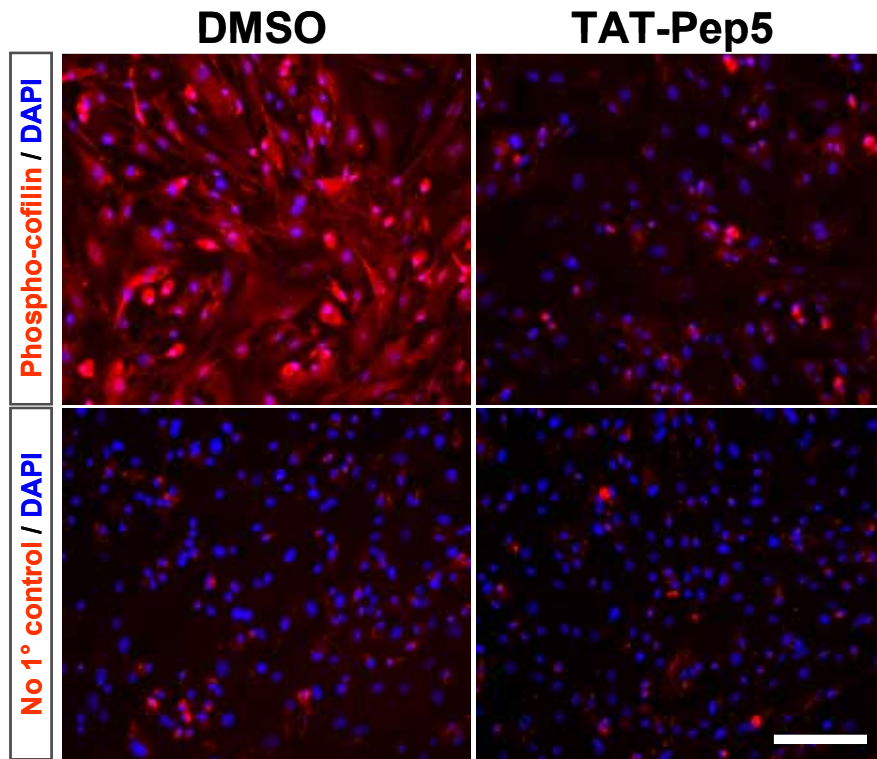
Figure 21. Loss of Rho activation in wild-type HSCs treated with TAT-Pep5.

Examination of Rho activation in wild-type (wt) HSCs treated with TAT-Pep5. Freshly isolated wt HSCs were treated every day starting at day 1 with either TAT-Pep5, a specific inhibitor of $p75^{NTR}$-mediated Rho activation, or DMSO (vehicle) control. Phosphorylated cofilin (phospho-cofilin), a marker indicative of Rho activation, was detected by immunostaining (red) on day 7 (top panels). Primary antibody omission served as an immunostaining control (bottom panels). Nuclei are stained with DAPI (blue). Scale bar, 175 μm.

A

B
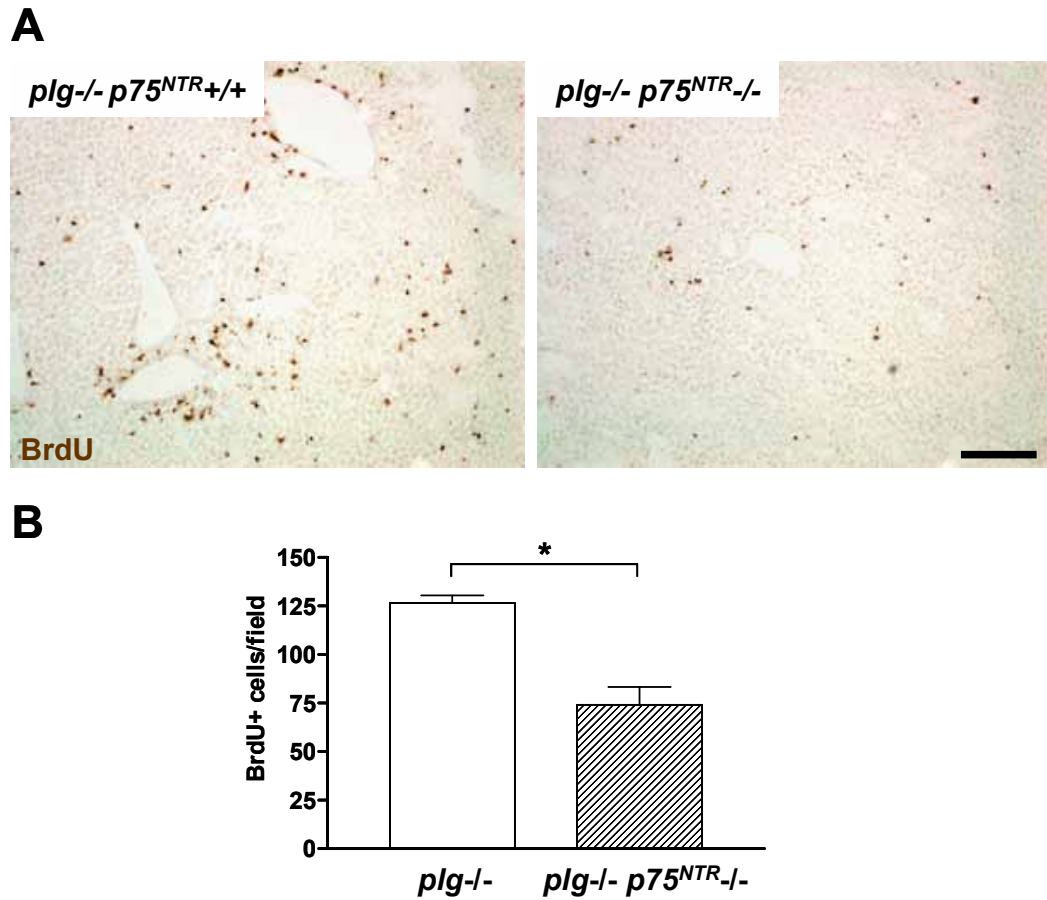
Figure 22. Genetic loss of p75^{NTR} inhibits liver cell proliferation *in vivo*.

(A) Liver cell proliferation in *plg-/-p75^{NTR}+/+* and *plg-/-p75^{NTR}-/-* mice. 10 week old mice were injected intraperitoneally with bromodeoxyuridine (BrdU) (100 mg/kg) daily for 3 days. Proliferating cells were visualized by immunochemical detection of BrdU. Scale bar, 198 μm. **(B)** Liver cell proliferation in mice described in (A) was quantified by counting the number of BrdU-immunopositive (BrdU+) cells per field (field corresponds to 1.5 mm^2). Graph represents mean ± SEM (*n* = 5 per genotype, *P<0.001; by unpaired Student's *t* test).
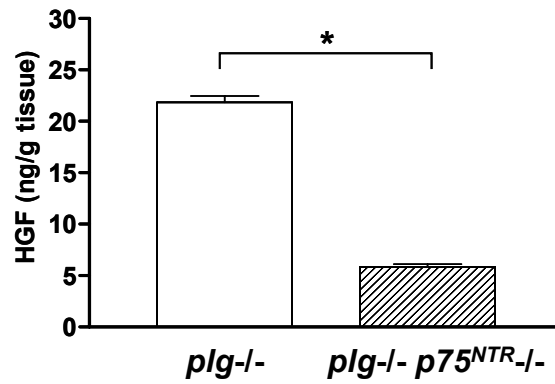
Figure 23. Genetic loss of p75^{NTR} causes diminished levels of hepatocyte growth factor in liver.

Hepatocyte growth factor (HGF) levels in the livers of *plg-/-* and *plg-/-p75^{NTR}-/-* mice as quantified by ELISA. Graph represents mean ± SEM ($n = 8$ for *plg-/-* and $n = 5$ for *plg-/-p75^{NTR}-/-*, *$P<0.0001$; by unpaired Student's *t* test).
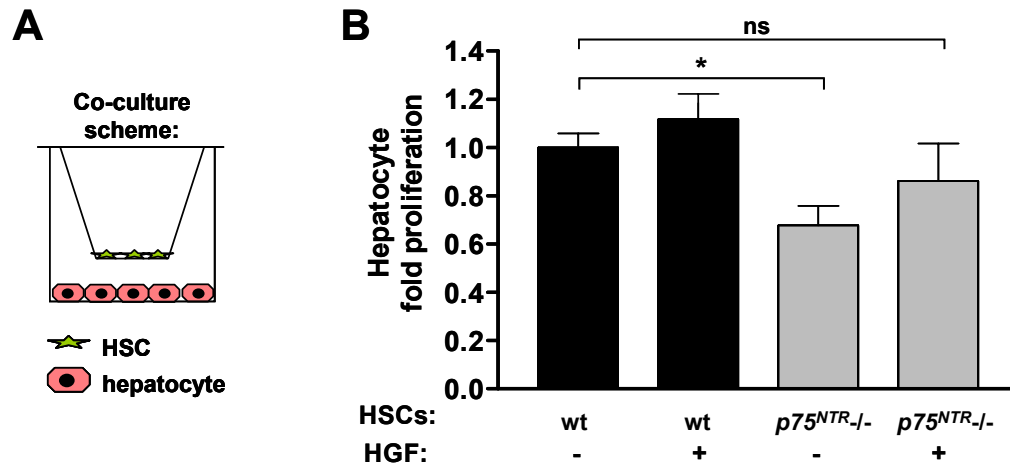
Figure 24. Genetic loss of p75$^{\text{NTR}}$ in HSCs causes diminished levels of hepatocyte proliferation *in vitro*.

(A) Scheme of co-culture of primary hepatocytes with HSCs. **(B)** Proliferation of hepatocytes in co-culture with HSCs. Hepatocytes were plated in the bottom of the well and incubated with HSCs grown on inserts placed within the well. Hepatocytes were cultured with wild-type (wt) or *p75$^{\text{NTR}}$-/-* HSCs (day 7-21, passage 2-4), with or without HGF (50 ng/mL). After 2 days, hepatocyte proliferation was assessed by [^{3}H]thymidine incorporation. Data are mean ± SEM from four independent experiments performed in duplicates (*$P<0.05$; ns, not significant; by one-way ANOVA).

Chapter 4. Examining interactions between p75^{NTR} and fibrinogen

1. Introduction

Many studies have shown a correlation between p75^{NTR} expression and sites of tissue injury and disease (Table 1), making the receptor an interesting potential drug target for a variety of conditions. Recent research has discovered that p75^{NTR} is able to bind ligands associated with specific pathologies, including β-amyloid, prion protein peptide, and rabies virus glycoprotein [27]. Because these interactions of pathological ligands with p75^{NTR} are highly specific for disease, targeting of these interactions could be very promising in developing therapeutic treatments. As p75^{NTR} is expressed in a variety of diseases and injury states, identification of other pathological ligands for p75^{NTR} and their biological effects could be important in pinpointing ideal drug targets for the treatment of specific conditions. Because other evidence in our lab has shown a potential relationship between p75^{NTR} and fibrinogen [99], another protein that is found at sites of injury and in diseased tissue, we were interested in determining whether p75^{NTR} and fibrinogen interact, and if fibrinogen can act a pathological ligand of p75^{NTR}.

2. Fibrinogen interacts with p75^{NTR}

Because both fibrinogen and p75^{NTR} are found at sites of injury and disease, we were interested to see if fibrinogen and p75^{NTR} were able to interact. To determine if an interaction occurs between fibrinogen and p75^{NTR}, we performed a

co-immunoprecipitation using sciatic nerve tissue. In a normal, uninjured sciatic nerve, p75^{NTR} expression is very minimal, and because the blood-nerve barrier is intact, the only fibrinogen one finds in the nerve is the small amount that is contained within the blood vessels (Fig. 25, lane 5). After crush injury of the sciatic nerve, p75^{NTR} expression is highly upregulated. Additionally, injury causes disruption of the blood-nerve barrier, and fibrinogen extravasates from the injured blood vessels, flooding into the nerve tissue (Fig. 25, lane 6). Immunoprecipitation with an anti-p75^{NTR} antibody showed very little p75^{NTR} expression in uninjured sciatic nerve, and minimal interaction with fibrinogen (Fig. 25, lane 1). In crush-injured sciatic nerve, immunoprecipitation with the same anti-p75^{NTR} antibody showed a high level of p75^{NTR} expression, and strikingly also pulled down a significant amount of fibrinogen, suggesting a p75^{NTR}-fibrinogen interaction in the injured nerve (Fig. 25, lane 3). Immunoprecipitation reactions using control IgG (Fig. 25, lanes 2 and 4) showed no binding of either p75^{NTR} or fibrinogen, suggesting that the interactions observed in the anti-p75^{NTR} immunoprecipitations were not merely non-specific background binding.

To further examine whether fibrinogen may interact with p75^{NTR}, we assessed the binding of fibrinogen to cells expressing p75^{NTR}. Fluorescently labeled fibrinogen was incubated with either NIH3T3 control cells or NIH3T3-p75^{NTR} cells which are stably transfected to constitutively express p75^{NTR}. No fibrinogen binding was observed in the control cells, while fibrinogen was able bind to the NIH3T3-p75^{NTR} cells (Fig. 26). Fibrinogen binding colocalized with p75^{NTR} expression. Taken together, these results suggest that interactions may occur between fibrinogen and p75^{NTR}.

3. Fibrinogen fragment D directly binds to the extracellular domain of p75^{NTR}

Although our results suggested that a p75^{NTR}-fibrinogen interaction is able to occur, the techniques used could not allow us to determine whether p75^{NTR} and fibrinogen are able to bind directly, or whether the interaction observed is an indirect binding interaction (i.e. the proteins interact as part of a complex of proteins). Therefore, to determine if a direct binding interaction occurs between p75^{NTR} and fibrinogen, we chose to use the Biacore surface plasmon resonance technique for examining molecule-molecule interactions. The Biacore system is comprised of an internal sensor chip surface to which a molecule (e.g. a protein) can be covalently coupled, an external injection system by which one can load sample solutions for injection into the machine, and an internal optical sensor to measure changes in refractive index ("response") due to binding interactions at the surface of the sensor chip. Because fibrinogen has the tendency to precipitate out of solution at temperatures below 37°C and could potentially clog the fine capillary tubing of the Biacore system, we decided to use the soluble fibrinogen fragment D for our Biacore binding experiments with p75^{NTR}. The fibrinogen molecule is composed of three domains: a central E domain and two symmetric D domains at either end [149] (Fig. 27). Proteolytic cleavage of fibrinogen by plasmin, the endogenous protease responsible for fibrinogen and fibrin degradation, yields two distinct products: fibrinogen fragment E and fibrinogen fragment D, in a 1:2 ratio, each so termed because it contains the domain of fibrinogen of the same name (Fig. 27) [150]. Fibrinogen's D domain, and thus fibrinogen fragment D, contain the majority of molecular and cellular binding epitopes that have so far been documented for the

fibrinogen molecule [149]. Therefore, we believed that the soluble fibrinogen fragment D would serve as a sufficient surrogate for fibrinogen for use in our Biacore binding studies.

To create a soluble p75^{NTR} protein for use in the Biacore binding experiments, we generated a construct that encodes for the extracellular domain of p75^{NTR}, truncated after the fourth cysteine-rich domain (Fig. 28A). This truncated p75^{NTR} extracellular domain is similar to that used by He and Garcia, who performed crystallographic and structural analysis of the extracellular domain of p75^{NTR} [4], and contains all ligand binding epitopes identified thus far. A construct was generated containing an N-terminal FLAG epitope tag followed by the truncated human p75^{NTR} extracellular domain, which we have named FLAG-p75^{NTR} ECD TR, or simply FLAG-p75^{NTR} ECD (Fig. 28B). This construct was stably transfected into HEK 293 cells for protein production, and soluble FLAG-p75^{NTR} ECD protein was purified from the media by FLAG affinity chromatography.

To verify that the FLAG-p75^{NTR} ECD protein is able to act as a reliable surrogate for the p75^{NTR} receptor in our Biacore binding studies, we assessed the ability of FLAG-p75^{NTR} ECD to bind the well-characterized p75^{NTR} ligand NGF. NGF was able to bind to the FLAG-p75^{NTR} ECD protein in a concentration-dependent and dissociable manner (Fig. 29), suggesting that the FLAG-p75^{NTR} ECD protein is properly folded and has retained its ligand-binding abilities. We then wanted to determine if fibrinogen fragment D could bind to FLAG-p75^{NTR} ECD. Injection of fibrinogen fragment D produced a specific binding response with FLAG-p75^{NTR} ECD, suggesting that fibrinogen fragment D can bind directly to p75^{NTR} (Fig. 30).

Once we determined that fibrinogen fragment D and p75^{NTR} can bind directly in a ligand-receptor manner, we wanted to further characterize the binding interaction by determining a dissociation constant (K_d) for the binding. To determine a K_d for the equilibrium binding reaction between fibrinogen fragment D and FLAG-p75^{NTR} ECD, we examined the maximum binding response at equilibrium over a range of fibrinogen fragment D concentrations (Fig. 30). Total binding of fibrinogen fragment D to FLAG-p75^{NTR} ECD at equilibrium was recorded and plotted as a function of fragment D concentration, and the plots were fit by nonlinear regression to calculate K_d (Fig. 31). We observed an estimated K_d of 3.3 ± 1.0 µM for the equilibrium binding reaction between fibrinogen fragment D and FLAG-p75^{NTR} ECD, based on three independent experiments. The K_d calculated for the equilibrium binding reaction assumes a 1:1 binding interaction between ligand and receptor. At high concentrations, some proteins can form multimeric complexes; if this occurs it can cause error in the calculation of a K_d for an interaction. Because fibrinogen fragment D was injected at high micromolar concentrations, we wanted to assess whether fragment D was forming multimeric complexes in solution. In order to determine the state of fibrinogen fragment D in solution, we performed fast performance liquid chromatography (FPLC) analysis of a 30 µM fibrinogen fragment D solution. FPLC analysis revealed that the majority of the fibrinogen fragment D was in monomeric form based on an apparent mass of 107 kDa (actual mass of fibrinogen fragment D is ~94 kDa [150]) (Fig. 32, peak 2), with only a small fraction of the solution consisting of multimeric protein (Fig. 32, peak 1). Based on these results, we believe the assumptions that our K_d was based upon are correct as far as we can determine.

4. Fibrinogen fragment D causes apoptosis of cells expressing p75^{NTR}

Once we determined that p75^{NTR} could bind to fibrinogen, and more specifically fibrinogen fragment D, we were interested in examining whether this ligand-receptor interaction could elicit a specific biological effect in cells. To determine the effects of fibrinogen fragment D on p75^{NTR}-expressing cells, we treated Neuro-2a cells, a neuroblastoma cell line that highly expresses p75^{NTR}, with fibrinogen fragment D. Treatment with fragment D caused apoptosis of Neuro-2a cells in a dose-dependent manner with a 5.5-fold increase in apoptosis at the highest dose tested (1000 nM) compared to untreated control (Fig. 33). These results are very interesting, as other pathological ligands of p75^{NTR} have been shown to induce cell death and are believed to be play an important role in neurodegenerative diseases [27].

5. Summary

With the goal of examining potential interactions between fibrinogen and p75^{NTR}, we performed experiments to address if these two proteins can interact *in vivo* and *in vitro*. We found that in the sciatic nerve crush model of tissue injury, fibrinogen and p75^{NTR} co-immunoprecipitate (Fig. 25), suggesting that these proteins interact in injured tissue. Additionally, we found that fibrinogen binds to cells expressing p75^{NTR}, while it does not bind to control cells not expressing p75^{NTR} (Fig. 26), suggesting that fibrinogen and p75^{NTR} may interact at the cell surface. To show that fibrinogen can bind directly to p75^{NTR}, we performed protein-protein binding analysis using the Biacore surface plasmon resonance technique, and determined that

the soluble fibrinogen fragment D can bind to the extracellular domain of p75^{NTR} in a ligand-receptor relationship (Fig. 30). Using equilibrium binding analysis, we found that the estimated dissociation constant for the fibrinogen fragment D-p75^{NTR} binding interaction is 3.3 ± 1.0 µM (Fig. 31). We also identified a novel function of fibrinogen fragment D in promoting apoptosis of p75^{NTR}-expressing cells (Fig. 33). Other members of the lab are currently pursuing studies to determine whether the effect of fibrinogen fragment D on promoting cell death is specifically occurring through interaction with p75^{NTR}, and are additionally examining whether fibrinogen fragment D-p75^{NTR} interactions are responsible for initiating similar or different functions in other cell types to further characterize the role of fibrinogen/fibrinogen fragment D as a pathological ligand for p75^{NTR}.

6. Acknowledgments
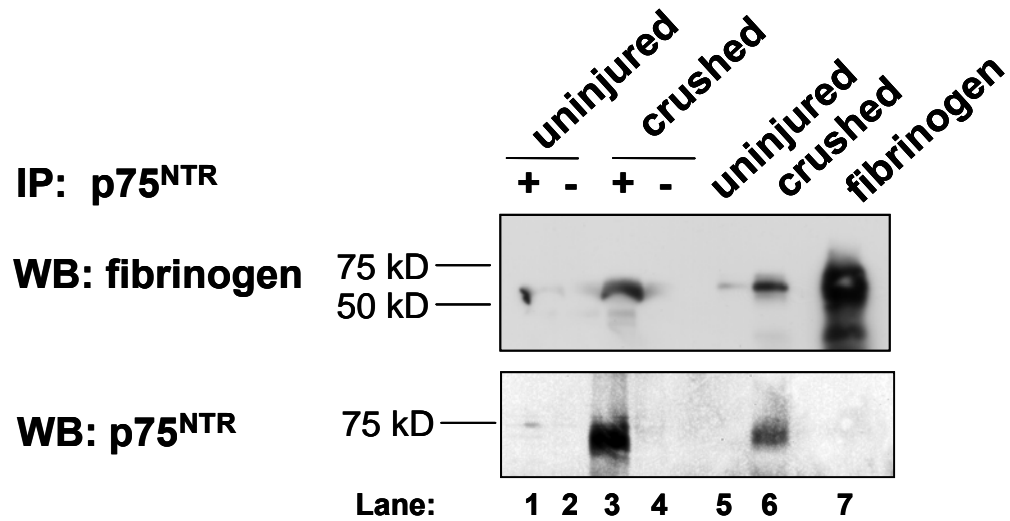
Figure 25. Fibrinogen co-immunoprecipitates with p75^NTR.

Lysates of uninjured or crush-injured sciatic nerves were precipitated with anti-p75^NTR antibody (lanes 1 and 3) or with pre-immune serum control (lanes 2 and 4). Precipitated proteins, lysates from uninjured or crushed nerves, and purified fibrinogen were separated by SDS-PAGE, transferred to nitrocellulose and immunoblotted for fibrinogen or p75^NTR. Input lysates (lanes 5 and 6) were used as controls for the presence total fibrinogen and p75^NTR, and purified fibrinogen (lane 7) was used as a control for fibrinogen antibody specificity. Experiment performed by Katerina Akassoglou.
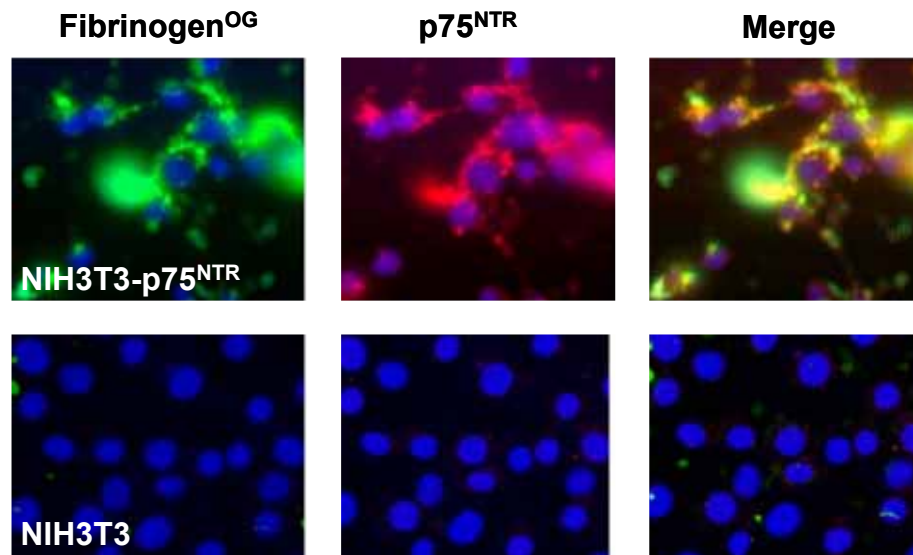
Figure 26. Fibrinogen binds to cells expressing p75^{NTR}.

NIH3T3 cells stably transfected with p75^{NTR} (NIH3T3-p75^{NTR}) or control NIH3T3 cells were incubated with Oregon Green-labeled fibrinogen (200 μg/ml) (green) for 2 hours before being washed, fixed, and immunostained for p75^{NTR} (red). Nuclei are stained with DAPI (blue). The merged image shows colocalization (yellow) of fibrinogen with p75^{NTR} expression. Experiment performed by Katerina Akassoglou.
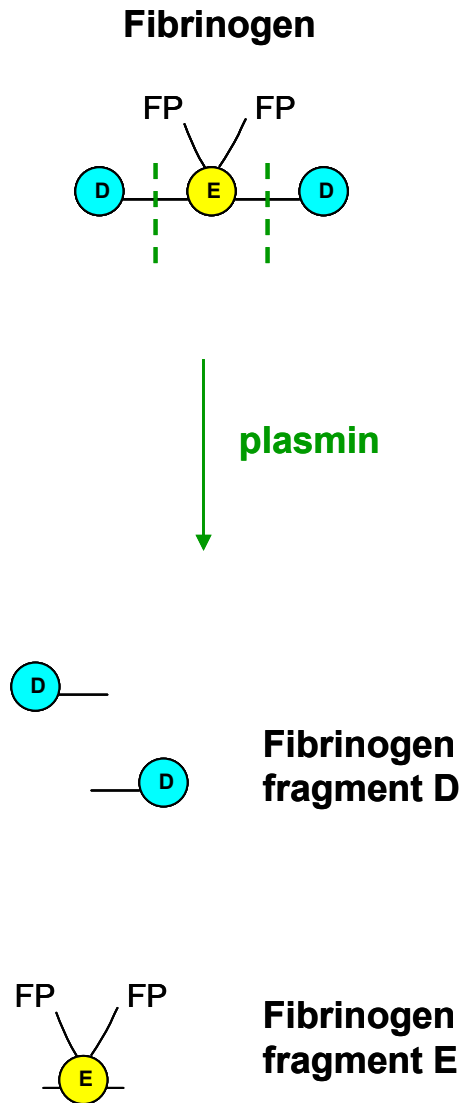
Figure 27. Generation of fibrinogen fragments D and E by plasmin cleavage.

Cartoon representation of fibrinogen cleavage by plasmin. Fibrinogen, comprised of two D domains (blue) and a central E domain (yellow), can be cleaved by the serine protease plasmin to generate two distinct products, fibrinogen fragment D (blue) and fibrinogen fragment E (yellow), produced at a 2:1 ratio.

A

CRD1
CRD2
CRD3
CRD4

p75^NTR ECD TR

B

FLAG-p75^NTR ECD TR

STOP
*

F ECD

HindIII BstY1
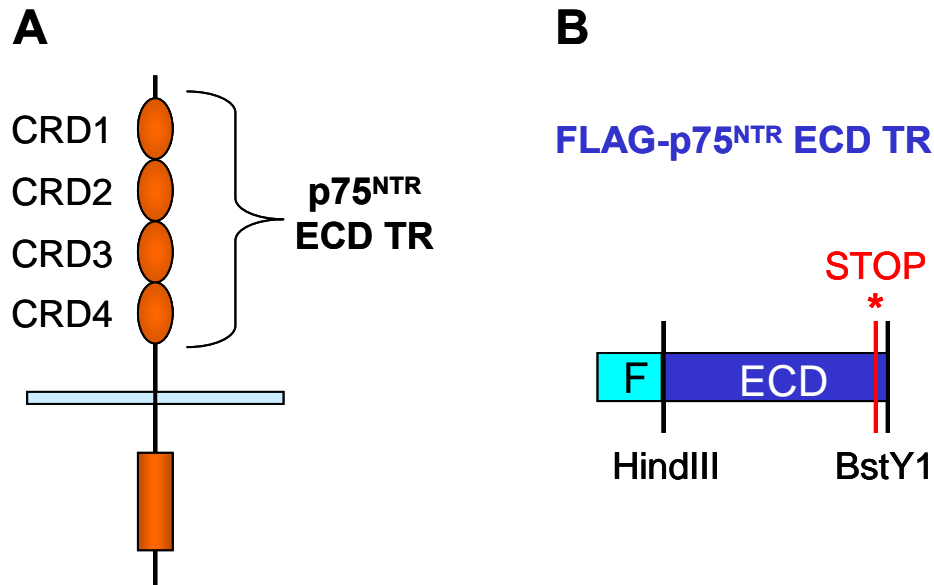
Figure 28. Construction of FLAG-p75^NTR ECD vector.

(A) Cartoon representation of p75^NTR depicting the region that is included in the FLAG-p75^NTR ECD TR construct. **(B)** Cartoon representation of FLAG-p75^NTR ECD TR construct. The N-terminal portion of p75^NTR, which contains the extracellular domain (ECD), was amplified by PCR and inserted into the pFLAG-CMV-3 expression vector 3' to a FLAG sequence (F) at HindIII and BstY1/BamHI restriction sites. A stop codon (STOP) was generated by site-directed mutagenesis to create the FLAG-p75^NTR ECD TR construct, which contains the ECD of p75^NTR truncated after the fourth cysteine-rich domain (CRD) (aa 1-162).
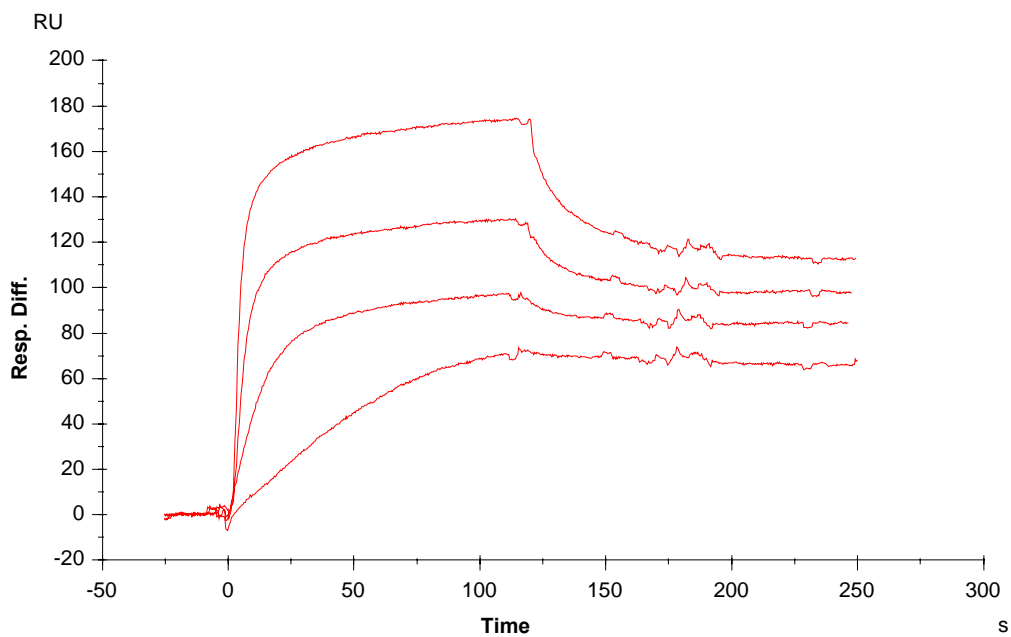
Figure 29. FLAG-p75^NTR ECD binds nerve growth factor.

Biacore surface plasmon resonance analysis of nerve growth factor (NGF) binding to FLAG-p75^{NTR} ECD. NGF (14 – 385 nM) was injected over the FLAG-p75^{NTR} ECD surface (450 RU) at a flow rate of 5 μL/minute. After each injection, the binding surfaces were regenerated by injecting a high salt/detergent solution (1 M NaCl, 0.5% surfactant P20).
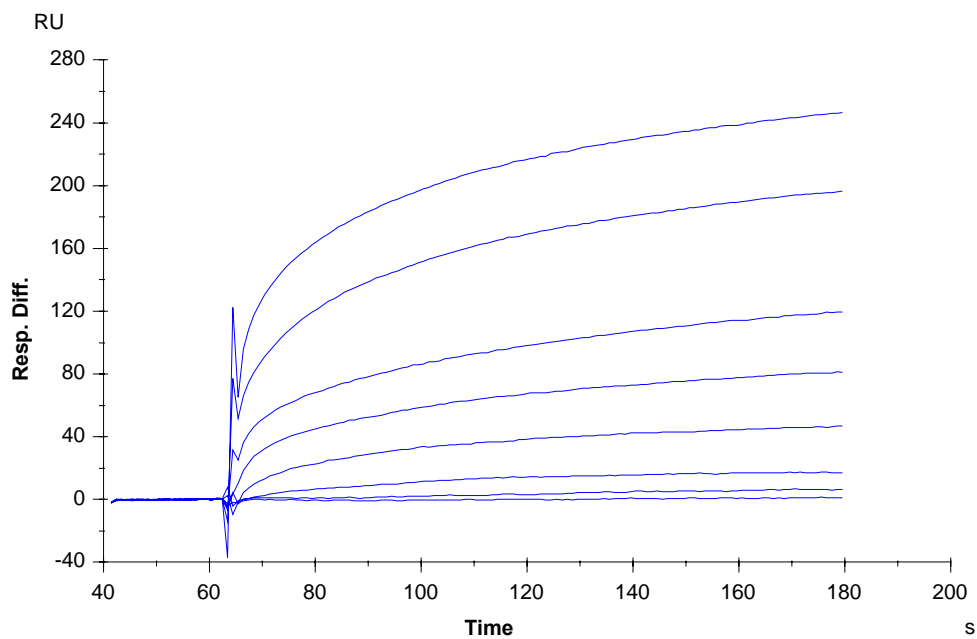
Figure 30. FLAG-p75^{NTR} ECD binds fibrinogen fragment D in a dose-dependent manner.

Representative binding curves from Biacore surface plasmon resonance analysis of fibrinogen fragment D binding to FLAG-p75^{NTR} ECD. Fibrinogen fragment D was injected in random order over the FLAG-p75^{NTR} ECD surface (200-300 RU) as a set of 8 concentrations from 37 to 81000 nM in 3-fold dilutions at a flow rate of 20 or 30 μL/minute. After each injection, the binding surfaces were regenerated by injecting an ionic/non-polar mixed solution as described in the Methods chapter.

$K_d = 3.3 \pm 1.0\ \mu M$
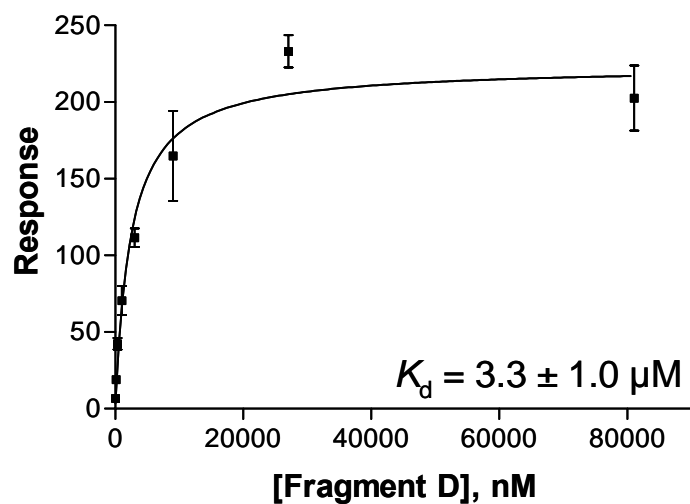
Figure 31. Equilibrium binding analysis of FLAG-p75[NTR] ECD/fibrinogen fragment D binding interaction.

Representative equilibrium binding analysis plot for FLAG-p75[NTR] ECD/fibrinogen fragment D binding interaction. Total binding of fragment D to FLAG-p75[NTR] ECD at equilibrium was recorded from Biacore surface plasmon resonance response and plotted as a function of fragment D concentration. The plots were then fit by nonlinear regression to calculate the dissociation constant, K_d. The K_d observed (3.3 μM ± 1.0 SD) is calculated from three independent experiments performed in duplicate.
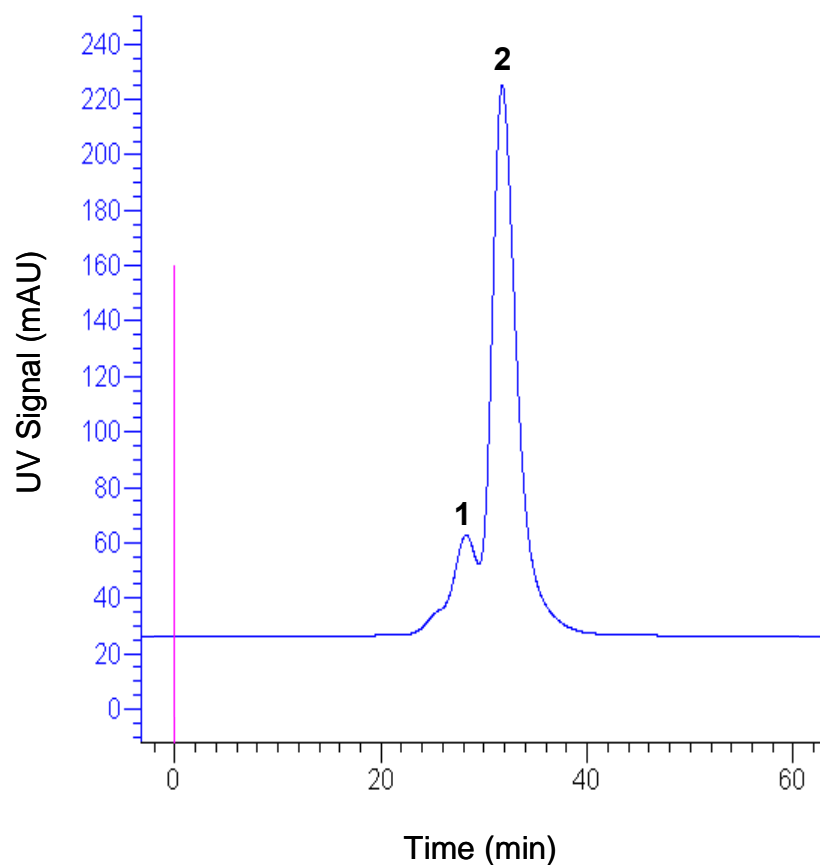
Figure 32. Fibrinogen fragment D is primarily monomeric in solution.

Representative curve from FPLC analysis of fibrinogen fragment D. Fragment D (30 μM) was analyzed by FPLC by separation over a size-exclusion column (Superose 6 GL) with 10 mM Hepes, pH 7.4, 150 mM NaCl as running buffer. Apparent molecule weights were determined by comparing elution times of peaks with those of molecular weight standards. Apparent molecular weights of peaks: **1**, 392 kDa; **2**, 107 kDa.
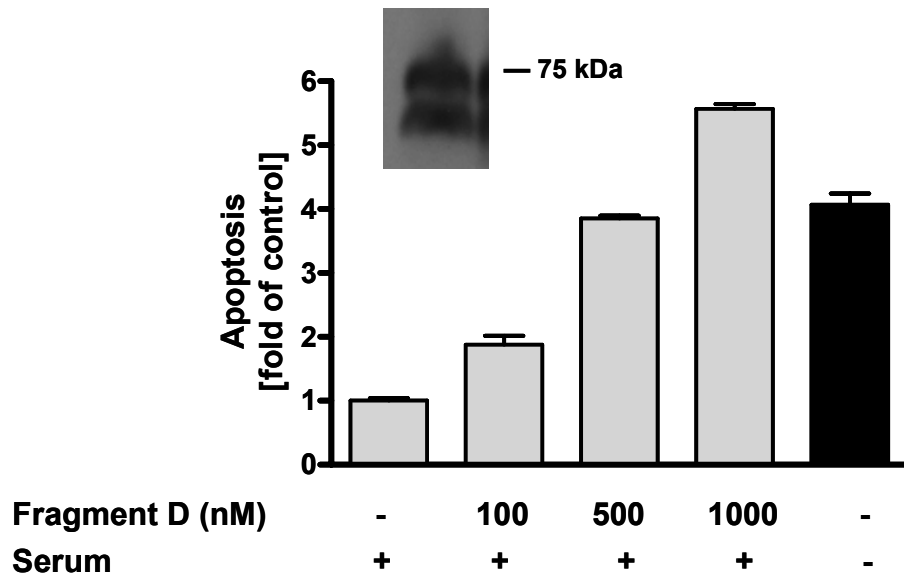
Figure 33. Fibrinogen fragment D causes apoptosis of Neuro-2a neuroblastoma cells.

Neuro-2a cells were treated for 16 hours with fibrinogen fragment D (100-1000 nM) in medium containing 10% FBS. Serum-free medium treatment was used as a positive control. Apoptosis, as measured by DNA fragmentation, was assayed by ELISA. Inset shows p75[NTR] expression in Neuro-2a cells as determined by immunoblot for p75[NTR]. Apoptosis assay performed by Christian Schachtrup. Western blot performed by Ryan Adams.

Chapter 5. Discussion

In the previous chapters I have presented the research I have performed for my dissertation studies in investigating novel functions and ligands for p75^{NTR}. These investigations have led to the identification of a novel function for p75^{NTR} in the liver in regulating hepatic stellate cell activation, as well as the identification of fibrinogen as a new pathological ligand for p75^{NTR}. In this chapter I would like to discuss the implications of our results and present suggestions for future studies that may be undertaken to further expand upon the findings of my dissertation research.

1. p75^{NTR} in liver injury and repair

1.1. Identification of a novel non-neuronal function of p75^{NTR}

Despite the fact that p75^{NTR} is an appealing therapeutic target due to its specific upregulation during injury and disease states, and multiple studies have been published depicting widespread expression of p75^{NTR} throughout many tissues and cell types in the body after injury (Table 1), p75^{NTR} has been primarily studied for its functions in the nervous system in neuronal cells and glia. Even though p75^{NTR} expression has been documented in a variety of non-nervous system tissues, including the liver, lung, kidney, pancreas, and immune system, the only known functions for p75^{NTR} outside of the nervous system are in myoblast survival [20] and keratinocyte and vascular smooth muscle cell apoptosis [21, 22]. Previous studies had shown that p75^{NTR} is upregulated in the liver in HSCs after liver injury or in fibrotic or cirrhotic disease [19, 41], but the function of p75^{NTR} in the liver and in HSCs remained unclear.

The results of my dissertation research demonstrate for the first time that p75^{NTR} is a major regulator of HSC differentiation from a quiescent lipocyte state to an activated myofibroblast state, and that p75^{NTR}-mediated HSC differentiation and HGF secretion plays a critical role in promoting hepatocyte proliferation and liver repair.

The role for p75^{NTR} in regulation of HSC differentiation is the first evidence for a role for p75^{NTR} in non-neuronal cell differentiation. Past studies of p75^{NTR} in the nervous system have implicated p75^{NTR} in both neuronal and glial cell differentiation. Previous work has found that p75^{NTR}, working in conjunction with Trk and in the presence of NGF, is able to promote the differentiation of neuronal precursor cells to neurons [142]. Additionally, others have shown that in the peripheral nervous system, p75^{NTR} is necessary to promote the differentiation of Schwann cells from a non-myelinating state to an actively myelinating cell type, and that this process requires the presence of the neurotrophin ligand BDNF [151]. Our discovery of p75^{NTR}'s role in HSC differentiation is unique, not only in that it is the first evidence for such a role in a non-nervous system cell type, but also because p75^{NTR}-mediated HSC differentiation does not require Trk as a co-receptor (Fig. 17), nor does it require the presence of a neurotrophin ligand (Figs. 15 and 17).

In addition, our discovery that p75^{NTR}-mediated HSC differentiation is critical to liver repair after injury is the first time that p75^{NTR} has been implicated in having a role in tissue repair outside of the nervous system. Many studies have documented the inhibitory role of p75^{NTR} in nerve regeneration after injury in the central nervous system [152]. Neurite outgrowth, a key process in promoting neuronal regeneration after injury, is inhibited by p75^{NTR} in conjunction with its co-receptors NogoR and

LINGO-1. In contrast to the nervous system, where p75^{NTR} plays a negative and inhibitory role in nerve regeneration, our results indicate that p75^{NTR} has a positive and protective role in the liver by promoting liver regeneration after injury (Fig. 22).

1.2. Identification of a novel ligand-independent function p75^{NTR}

Although there are many studies published describing the neurotrophin ligand-dependent functions of p75^{NTR}, more recent studies have unraveled that p75^{NTR} is not merely a neurotrophin receptor, but contributes to many different biological functions and signaling pathways independent of neurotrophins [24, 153-155]. For example, expression of p75^{NTR} or the intracellular domain of p75^{NTR} alone may signal in a neurotrophin-independent manner to induce apoptosis [8, 14], as well as activation of PI3 kinase [141] and Rho [9]. Moreover, the functions of p75^{NTR} and its co-receptor NogoR are neurotrophin-independent [24, 154, 156]. Our studies have identified a novel neurotrophin ligand-independent function for p75^{NTR}, as the effects of p75^{NTR} on HSC differentiation were observed in the absence of exogenous neurotrophin ligands (Figs. 11, 12, 14-21).

In addition, p75^{NTR} can promote signaling and regulate cell function in a completely ligand-independent manner. For example, expression of the ICD of p75^{NTR} alone can promote Akt signaling and regulate survival in a variety of cell types [38]. Similarly, we found that expression of the ICD of p75^{NTR} alone was sufficient to rescue the differentiation of *p75^{NTR}*-/- HSCs, identifying p75^{NTR}-mediated HSC differentiation as another potential ligand-independent function of p75^{NTR}. Although

one would believe that a ligand would be necessary for receptor activation, there are several examples of well-established ligand-independent signaling pathways in other receptor systems. For example, steroid hormone receptors [157], scavenger receptors [158], viral G-protein-coupled receptors [159], androgen receptors [160], and B-cell receptors [161] have all been shown to signal in a ligand-independent manner. Since p75^{NTR} is not constitutively expressed, but is upregulated at sites of liver injury, its expression itself could function as the signal to trigger a signaling pathway and thus regulate a cell's biological function.

1.3. p75^{NTR} in HSC activation

With our identification of p75^{NTR} as a regulator of HSC differentiation, we provide the first evidence for a specific receptor that regulates this important cellular process. Although regulation of HSC differentiation might seem an unexpected function for a neurotrophin receptor, it is actually in accordance with the neural/neuroendocrine characteristics of HSCs [162]. In addition to p75^{NTR}, HSCs express a variety of neuronal-related molecules, such as synaptophysin, GFAP, nestin, NCAM, α-B-crystallin, norepinephrine, and all four neurotrophins [162], and also respond to neurotransmitters such as acetylcholine [163]. Not only because of their gene expression similarities to neuronal cells, but also because of their functional response to injury, HSC activation has been compared to reactive gliosis in the nervous system. Our identification of p75^{NTR} as a major neuronal-related molecule

expressed by HSCs after injury that can act as a promoter of liver regeneration supports and expands upon the concept of neurogenic regulation of liver repair [162].

Although a variety of factors are believed to be involved in affecting HSC differentiation, evidence as to how they may all interact is disjointed at best. Thus, it is difficult to assess how p75^{NTR} may fit in with what is currently known about HSC differentiation. Unfortunately, examination of the current literature to find a connection between p75^{NTR} and TGFβ, the major factor that has thus far been implicated in promoting HSC differentiation, yields no results. Additionally, no studies have been performed to determine if there is a link between p75^{NTR} and the Smad transcription factor proteins, which are the primary downstream effectors of TGFβ signaling in HSCs. Whether potential interactions occur between p75^{NTR} and TGFβ remains an intriguing and wide open question; as both of these proteins are implicated in a variety of fibrotic diseases, examination of a relationship between p75^{NTR} and TGFβ could provide very interesting results with potentially important therapeutic implications.

A very recent study has shown that under conditions of hypo-osmolar stress, which can occur in instances of tissue edema caused by injury or disease-related inflammation, p75^{NTR} expression can be upregulated by activation of the transcription factor Sp1 [40]. Interestingly, Sp1 has also been implicated in regulating the transcription of HGF [164] and MMP-9 [165], two major proteins that are associated with HSC differentiation to myofibroblasts. Because it is unclear how p75^{NTR} expression is regulated in HSCs after liver injury, it would be interesting to examine Sp1 as a potential link between the upregulation of p75^{NTR}, HGF, and MMPs in HSCs

undergoing differentiation. Furthermore, in addition to its role in the liver, HGF has been shown to play an important role in the nervous system, where it is secreted by neurons and acts as a neurotrophic factor and can promote axonal growth [166, 167]. It would be of interest to determine whether p75^{NTR} is involved regulating HGF not only in the liver but in the nervous system as well.

We have observed that p75^{NTR}-mediated HSC differentiation occurs through the activation of the small GTPase Rho. Prior studies have shown that Rho activation can directly cause changes in the structure of the actin cytoskeleton to regulate HSC differentiation [143, 144]. Additionally, through activation of the transcription factor SRF (serum response factor), active Rho can also indirectly upregulate genes, including α-smooth muscle actin (αSMA), that are associated with the smooth muscle cell phenotype similar to the activated HSC myofibroblast state [168, 169]. Thus, Rho may be a key signaling molecule for mediating the changes that occur in αSMA during p75^{NTR}-mediated HSC differentiation.

In addition to its major function in the regulation of HSC differentiation, we have found that *in vitro* p75^{NTR} can cause a small increase HSC apoptosis in the presence of exogenous NGF (Fig. 16A). The possibility that p75^{NTR} may regulate both of these functions in HSCs in not without precedent. p75^{NTR} has been shown to have a pluripotent signaling capacity in neuronal cells, where it can mediate diverse cellular functions such as survival, apoptosis, and inhibition of neurite outgrowth, depending on the bioavailability of and levels of ligands, co-receptors, intracellular signal transduction pathways and levels of p75^{NTR} expression [24, 155]. However, although p75^{NTR} may mediate HSC apoptosis *in vitro*, whether this actually occurs *in*

vivo during liver disease remains to be determined, as chronically activated HSCs are resistant to NGF-induced cell death [77]. Therefore, we believe that the major and most important function of p75^{NTR} in HSCs *in vivo* is the regulation of differentiation.

1.4. Future studies

The main results of my dissertation studies have identified that p75^{NTR} is a major regulator of HSC activation and that p75^{NTR} plays a protective role in the *plg-/-* genetic mouse model of **liver injury and repair**. In the future, it would be interesting to examine the role of p75^{NTR} in other models of liver injury and regeneration to determine specific time points and other potential mechanisms whereby p75^{NTR} may exert its affects in the liver. A common injury model that is used for examining liver injury and repair in rodents is carbon tetrachloride (CCl$_4$) toxicity. The advantages of using CCl$_4$ to induce liver injury is that it is easily administered by i.p. injection and that the dosage can be varied to provide either an acute liver injury model (i.e. a single high dose of CCl$_4$) or a chronic injury model (i.e. several moderate doses of CCl$_4$ administered over a few weeks). As the liver undergoes repair processes after cessation of CCl$_4$ treatment, this model is also useful for examining liver repair. Examination and comparison of the effects of CCl$_4$ toxicity in wild-type and *p75^{NTR}-/-* mice would allow one to determine if p75^{NTR} also plays a protective role in this model of liver injury, as well as determining at what stages in liver injury and repair p75^{NTR}-mediated HSC activation is important. To specifically examine the role of p75^{NTR} in liver regeneration, one could use the two-thirds partial hepatectomy (PHx) model of

liver regeneration. In this model, approximately 70% of the liver tissue is surgically removed. The remaining liver lobules undergo growth and expansion to regenerate the liver mass that was lost, and within 7-8 days (in mice) the liver tissue is at 100% of its original mass. The advantages of using the PHx model is that one can specifically look at the effects of a certain gene/protein (in our case, p75^{NTR}) on hepatocyte proliferation, a key process in liver repair after injury or disease. Performing the PHx model on wild-type and *p75^{NTR}-/-* mice would allow one to ascertain how p75^{NTR}-mediated HSC activation is important to hepatocyte proliferation and liver regrowth after injury.

In addition to the liver, previous studies have shown that the *plg-/-* mouse exhibits disease pathology in other tissues, including the lung, pancreas, and gastrointestinal tract [137, 170]. Because p75^{NTR} can be expressed in all of these tissues (Table 1), it is of interest to examine p75^{NTR} expression in these tissues in the *plg-/-* mouse, and to determine how these tissues, in addition to the liver, may contribute to the severe pathology (i.e. wasting and decreased survival) observed in the *plg-/-p75^{NTR}-/-* mouse.

My dissertation work has focused on the role p75^{NTR} in promoting HSC **differentiation** from a quiescent lipocyte to a myofibroblast. Recent work has suggested that promoting HSC de-differentiation (i.e. reverting the activated myofibroblast back into a quiescent lipocyte) may be beneficial in the resolution of liver fibrosis caused by chronic HSC activation [55]. Therefore, it is of great interest to determine whether p75^{NTR} may play a role in HSC de-differentiation. If one is able to knockdown p75^{NTR} expression or block p75^{NTR}-mediated signaling once HSCs are

activated, are we able to reverse the differentiation? Obtaining an answer to this question is very important, as it may further implicate the therapeutic potential of manipulating p75^{NTR} to treat liver disease.

The research I have performed for my dissertation has focused on the role of p75^{NTR} in the liver in promoting HSC activation to **myofibroblasts**. Myofibroblasts are not only present in the liver, but also in other tissues, including the intestine, lung, and vasculature, and are major contributors to a variety fibrotic diseases [48]. p75^{NTR} is also expressed in tissues containing myofibroblasts (Table 1), but the cell types that express p75^{NTR} have only been definitively identified in some of these tissues. Because our study reveals that p75^{NTR} can act as a modulator of HSC differentiation to myofibroblasts, it would be interesting to determine if myofibroblasts in other tissues express p75^{NTR}, and if so, whether p75^{NTR} functions as a general regulator of tissue repair by regulating myofibroblast differentiation. Performing experiments to address these questions could identify p75^{NTR} as a specific target in fibrotic diseases and promote the therapeutic potential of targeting p75^{NTR} in fibrotic disease.

1.5. Implications and significance

HSC differentiation is a hallmark of fibrotic liver disease of different etiologies, such as viral hepatitis and chronic alcohol consumption [171]. Initiation of HSC differentiation results in secretion of HGF and ECM synthesis that are critical mediators for the restoration of normal liver structure, hepatocyte proliferation and liver regeneration [49]. However, perpetuation of HSC activation to a myofibroblastic

state leads to excessive collagen and ECM deposition that result in liver fibrosis. Therefore, sustained differentiation of HSCs is considered a target for the treatment of liver fibrosis [50]. At late stages of liver disease resolution of fibrosis depends on HSC apoptosis [171]. Our studies have showed that p75^{NTR} induces HSC differentiation, and have demonstrated that the mild *in vitro* effect of NGF on HSC apoptosis [19, 42] is mediated by p75^{NTR}. These results suggest that in liver injury p75^{NTR} might function both as a regulator of HSC differentiation and depending on the bioavailability of neurotrophins might also participate together with other apoptotic mediators in orchestrating the resolution of fibrosis. Identification of p75^{NTR} as a molecular link between HSC activation and hepatocyte proliferation could provide a therapeutic target for manipulating the stages of HSC activation during the progression of chronic liver disease.

2. Interactions between p75^{NTR} and fibrinogen

2.1. Fibrinogen fragment D as a novel pathological ligand for p75^{NTR}

Prior studies have shown that in addition to its physiological neurotrophin ligands, p75^{NTR} can bind to several pathological ligands that are involved in neurodegenerative diseases, including β-amyloid, prion protein peptide, and rabies virus glycoprotein (Fig. 2). Our current studies are the first to identify the blood protein fibrinogen as a new pathological ligand for p75^{NTR}. The results of my Biacore binding experiments have allowed us to calculate a dissociation constant (K_d) for the binding reaction between the extracellular domain of p75^{NTR} and fibrinogen fragment

D, with a K_d of approximately 3 μM (Fig. 31). To put this K_d value in context, it is necessary to compare it with K_d values that are known for p75^{NTR} and its other ligands, as well as for fibrinogen and its other receptors. First, how does this compare to the K_d values known for other p75^{NTR}/ligand interactions? Recent work has estimated that p75^{NTR} binds to the neurotrophin ligand NGF with a K_d of 1-2 nM, and to the proneurotrophin ligand proNGF with a K_d of 15-20 nM [26]. Thus, the pathological ligand fibrinogen fragment D has a binding affinity for p75^{NTR} that is 100 to 1000 times lower than the binding affinity of p75^{NTR} for its physiological ligands. Studies examining the binding of p75^{NTR} to its pathological ligands have estimated a K_d of 20 nM for the p75^{NTR}/β-amyloid binding interaction; a K_d of 30 pM for the p75^{NTR}/rabies virus glycoprotein binding interaction; and a K_d of 5 mM for the p75^{NTR}/prion peptide binding interaction [27]. These studies reveal that the pathological β-amyloid protein and rabies virus glycoprotein have binding affinities on the same order of magnitude as the physiological ligands of p75^{NTR}. The prion peptide binding affinity may seem low in comparison to the other ligands, but in general binding interactions with short peptides (as opposed to larger proteins) have K_d values in the micromolar or millimolar range, thus a K_d of 5 mM is not unreasonable. With an approximate K_d of 3 μM, the binding reaction between p75^{NTR} ECD and fibrinogen fragment D appears to have a low affinity compared to the other known pathological ligands of p75^{NTR}. Secondly, how does the K_d for the p75^{NTR}/fibrinogen fragment D compare to the K_d values known for other fibrinogen/receptor interactions? The binding interaction between fibrinogen and its platelet receptor, the αIIbβ3 integrin, has a K_d of ~50 nM when the receptor is reconstituted in planar lipid bilayers [172]. Binding between

fibrinogen and the integrin Mac-1 CD11b subunit domain has an estimated K_d of ~220 nM [173]. Thus, like p75^{NTR} and its ligands, fibrinogen and its known receptors have binding affinities in the nanomolar range. Therefore, the estimated K_d of 3 μM between p75^{NTR} ECD and fibrinogen fragment D is about 10 to 100 times lower than fibrinogen and its other receptors.

If fibrinogen is a pathological ligand for p75^{NTR}, what can account for the relatively low binding affinity between the two proteins in comparison to the interactions with their other protein binding partners? It is well documented that p75^{NTR} can interact with other receptors on the cell surface in a co-receptor relationship (Fig. 3) [24]. We believe that p75^{NTR} may interact with another fibrinogen receptor, such as an integrin receptor, in a co-receptor relationship, and it is plausible that on the cell surface p75^{NTR} interaction with an additional fibrinogen receptor could markedly increase its binding affinity for fibrinogen. Whether the p75^{NTR}/fibrinogen binding interaction requires a co-receptor remains to be discovered, but could provide additional biochemical and functional evidence into the nature of the p75^{NTR}/fibrinogen binding interaction.

Even though p75^{NTR} is known to induce apoptosis, our discovery that fibrinogen fragment D can promote cell death is unique, as no previous studies examining the biological effects of fragment D have indicated that it may play a role in apoptosis. There are only about a handful of published reports examining the effects of fibrinogen fragment D on cells, as most studies look more specifically at the effects fibrinogen or fibrin. The main cell type examined in previous fragment D studies is endothelial cells, since these cells line the interior of blood vessels and in the

researchers' opinion would be most likely to come in contact with fibrinogen proteolytic degradation products such as fragment D. The studies examining the effects of fibrinogen fragment D on endothelial cells relate mainly to control of vascular integrity. Fragment D has been shown to increase endothelial monolayer permeability [174], as well as aid in the adhesion of granulocytes to endothelial cells [175]. Additionally, fibrinogen fragment D can elicit vascular constriction *in vivo*, most likely through the binding to ICAM-1 on vascular endothelial cells [176]. Thus, identification of cell death as a fibrinogen fragment D-mediated function is completely novel and unexpected, and deserves to be studied further as it could have significant implications in many pathological conditions where fibrinogen extravasation occurs.

2.2. Future studies

The results of my dissertation studies have identified fibrinogen as a novel pathological ligand for $p75^{NTR}$, and I have determined a K_d for the $p75^{NTR}$/fibrinogen fragment D binding interaction. In the future, it would be of interest to further characterize the binding interaction between $p75^{NTR}$ and fibrinogen and fibrinogen fragment D on both a biochemical and functional level. In my studies, I determined a K_d for the $p75^{NTR}$/fibrinogen fragment D binding interaction using Biacore binding analysis of immobilized FLAG-$p75^{NTR}$ ECD and injection of fibrinogen fragment D in solution at a variety of concentrations. Typically, to verify the binding results in such an analysis, one would repeat the experiment by switching binding conditions, i.e. immobilize fibrinogen fragment D and inject FLAG-$p75^{NTR}$ ECD in solution. In

performing these experiments, the immobilized protein is needed in only microgram quantities, while the injected protein is needed in milligram quantities. Unfortunately I was unable to perform the latter experiment due to the inability to obtain the significant milligram amounts of FLAG-p75^{NTR} ECD protein that would be necessary to meet experimental conditions for injections. This is due to problems with the FLAG affinity purification of FLAG-p75^{NTR} ECD. While the stably-transfected cells were able to express the FLAG-p75^{NTR} ECD protein at very high levels (5-15 mg/L of medium), during the affinity purification process FLAG-p75^{NTR} ECD bound very poorly to the anti-FLAG chromatography resin, thus inhibiting us from purifying our protein from the culture medium. We were unable to determine the cause of the poor resin binding, but believe it may be due to a conformational issue of the FLAG-p75^{NTR} ECD protein that causes the N-terminal FLAG epitope to be "hidden" and thus inaccessible to binding by the FLAG antibody on the resin. To solve this problem, in the future we will optimize the p75^{NTR} ECD protein purification procedure by creating new p75^{NTR} ECD constructs with different epitope tags (e.g. 6X His, 3X FLAG) at either the N- or C-terminus, expressing the new proteins, and determining which epitope tag is optimum for purification of milligram quantities of the p75^{NTR} ECD protein. Once we are able to obtain substantial amounts of p75^{NTR} ECD protein, we will be able to perform the Biacore binding analysis experiment described above to verify the K_d value we have already calculated for p75^{NTR} ECD and fibrinogen fragment D.

In addition, obtaining milligram quantities of p75^{NTR} ECD protein will allow us to perform additional experiments to further analyze the p75^{NTR}/fibrinogen

fragment D binding interaction. Similar to the Biacore binding analysis, one could perform a solid phase assay to determine the K_d where one protein is coated on the bottom of a well and the second is added in solution in varying concentrations. Unlike the Biacore, where one has to worry about the fibrinogen precipitating out of solution and interfering with the sensitive Biacore machinery, the solid phase binding assay has the advantage of being able examine p75^{NTR} binding to the entire fibrinogen molecule if one coats the bottom of the assay wells with fibrinogen. Additionally, it would be of interest to perform additional experiments to verify (or disprove) the 1:1 binding stoichiometry between p75^{NTR} and fibrinogen fragment D. Similar to the FPLC analysis performed on fragment D, FPLC analysis could be performed on p75^{NTR} ECD to examine potential p75^{NTR} ECD multimerization in solution. Furthermore, biophysical analytical techniques, such as analytical ultracentrifugation, could be used to examine p75^{NTR}/fibrinogen fragment D binding stoichiometry in solution.

In the future, we would also like to determine the specific binding sites involved in p75^{NTR}/fibrinogen fragment D binding. One means to accomplish this is to determine a crystal structure for the complex formed between the p75^{NTR} ECD and fibrinogen fragment D proteins. The crystallographic process requires milligram quantities of protein, however, and optimization of the protein purification procedure for p75^{NTR} ECD will be necessary to obtain the large amounts of protein needed to perform crystallography. Prior to undertaking the arduous process that is involved in obtaining a crystal structure, we can examine the interaction between p75^{NTR} and fibrinogen fragment D using a bioinformatics approach with the already-determined crystal structures for the individual molecules. Our collaborator has already created a

molecular docking model using the crystal structures of p75^{NTR} ECD [4] and fibrinogen fragment D [177] to predict a plausible binding conformation between these two proteins (Fig. 34). Using this model, one is able to predict specific binding regions and/or specific amino acids that may be involved in the binding interaction. The docking model suggests that the β-chain of fibrinogen fragment D may interact with a six amino acid-long loop region in CRD3 of p75^{NTR} ECD (Fig. 34). To examine whether this loop region of p75^{NTR} ECD is involved in the binding of fibrinogen fragment D, I created point mutants for specific amino acid residues in the loop, as well as a deletion mutant with the entire six amino acid loop deleted, for use in Biacore binding analysis. Unfortunately, due to the aforementioned problems with FLAG protein purification, I was unable to obtain a large enough amount of the mutant p75^{NTR} ECD proteins to sufficiently perform the Biacore binding analysis with fibrinogen fragment D. In the future, optimization of the protein purification procedure will allow us to obtain sufficient amounts of protein to perform binding analyses with the p75^{NTR} ECD mutants, and through comparison with wild-type p75^{NTR} ECD protein determine the significance of the loop region in the p75^{NTR}/fibrinogen fragment D binding interaction. Interestingly, the loop structure of p75^{NTR} ECD that may be involved in fibrinogen fragment D binding is on the opposite side of the p75^{NTR} molecule from the neurotrophin binding region [4]. It would be interesting to determine whether binding of fibrinogen or fibrinogen fragment D to p75^{NTR} ECD has any affect on neurotrophin binding, e.g. if the two ligands exhibit competitive binding, or if both molecules can bind simultaneously. If fibrinogen or fibrinogen fragment D blocks the binding of neurotrophins to p75^{NTR}, this could have

important implications in nervous system pathologies that depend upon neurotrophins for their resolution.

As already discussed in the previous section of this chapter, we believe that on the cell surface, binding of p75^{NTR} to fibrinogen or fibrinogen fragment D may occur with the involvement of a co-receptor, potentially an integrin that is already known to mediate fibrinogen binding. We are interested in performing experiments to determine whether a co-receptor is involved in p75^{NTR}/fibrinogen fragment D binding on cells, and if so, to identify specifically which co-receptor is involved. Initial experiments that could be undertaken include determining a K_d between fibrinogen fragment D and cells expressing p75^{NTR}. If the K_d observed using cells has a much higher affinity than the K_d observed between the isolated proteins, these results could suggest that an additional receptor may be involved in p75^{NTR}-mediated fibrinogen fragment D binding to the cell surface. Subsequent analysis could involve treating p75^{NTR}-expressing cells with fibrinogen fragment D, followed by p75^{NTR} immunoprecipitation and PAGE analysis to determine which other proteins interact with p75^{NTR} upon its binding to fibrinogen fragment D. If and when a co-receptor is identified, more specific biochemical analyses can be performed to examine the effects of the co-receptor on the K_d for the p75^{NTR}/fibrinogen fragment D binding interaction.

Work by other members of my lab has identified a novel and unexpected function in fibrinogen fragment D-induced neuronal cell death. In the future, we would like to further characterize this new function through analysis of signal transduction pathways involved in fibrinogen fragment D-induced cell death, as well

as to specifically identify p75^{NTR} as the receptor that is mediating this effect. We are additionally interested in examining whether fibrinogen fragment D has similar affects on other cell types *in vitro*, as well as determining if fibrinogen fragment D-mediated apoptosis plays a role *in vivo*. Identification of fibrinogen and fibrinogen fragment D-mediated events could have important implications in disease states where fibrinogen and its degradation products are present in tissues.

2.3. Implications and significance

Extravascular fibrinogen is found in a number of different tissues in disease and injury states involving loss of vascular integrity, and has been show to cause deleterious affects on tissue repair after injury. Thus, targeting of specific fibrinogen-receptor interactions is appealing for therapeutic purposes to alleviate the inhibitory affects of fibrinogen on tissue repair. Research has already led to the development of a drug against the fibrinogen/αIIbβ3 integrin binding interaction, ReoPro, which is used to prevent platelet aggregation and thrombus formation during coronary surgery. Developing therapeutics that specifically target other fibrinogen-receptor interactions is very attractive because it allows one to block fibrinogen's pathological functions without affecting its function in blood coagulation. Identification of fibrinogen/fibrinogen fragment D as a novel pathological ligand for p75^{NTR} that could potentially play a role in regulating cell death during pathogenesis may allow for the development of new therapeutics to treat diseases where vascular disruption and inflammation occur.

3. General conclusions

p75^{NTR} remains to be one of the most complicated proteins studied by scientific researchers today. It can bind to numerous physiological and pathological ligands, can interact with several co-receptors, and can signal through a variety of intracellular signaling pathways to promote cell functions as diverse as survival, apoptosis, and differentiation. Because of the importance of its expression in injury and disease, intimate understanding of all aspects relating to p75^{NTR} are critical in order to take advantage of this receptor's therapeutic potential. The work performed during my dissertation studies has led to the identification of a novel function for p75^{NTR} in regulating HSC differentiation and liver injury and repair, as well as the identification of fibrinogen fragment D as a new pathological ligand for p75^{NTR}. It is my hope that future studies will continue to address the role of p75^{NTR} in injury and disease and perhaps put my new discoveries in context so that we may finally elucidate the true nature of this enigmatic receptor.
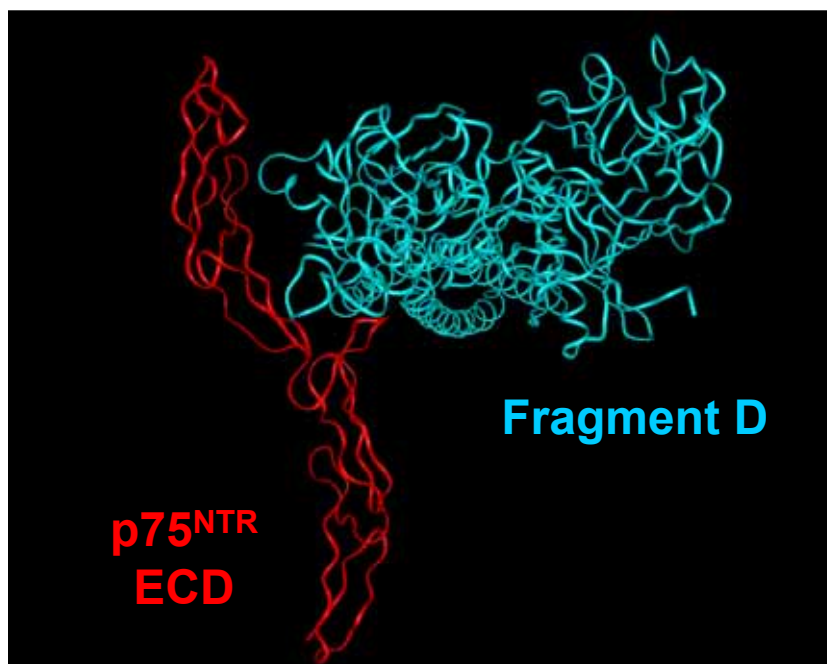
Figure 34. Molecular docking model for the p75^{NTR} ECD/fibrinogen fragment D interaction.

Crystal structures for p75^{NTR} ECD (red) [4] and fibrinogen fragment D (blue) [177] were subjected to molecular docking analysis to determine a potential binding conformation between the two proteins. Molecular docking analysis performed by Igor Tsigelny.

References

1.   Aloe, L., *Rita Levi-Montalcini: the discovery of nerve growth factor and modern neurobiology.* Trends Cell Biol, 2004. **14**(7): p. 395-9.

2.   Johnson, D., et al., *Expression and structure of the human NGF receptor.* Cell, 1986. **47**(4): p. 545-54.

3.   Roux, P.P. and P.A. Barker, *Neurotrophin signaling through the p75 neurotrophin receptor.* Prog Neurobiol, 2002. **67**(3): p. 203-33.

4.   He, X.L. and K.C. Garcia, *Structure of nerve growth factor complexed with the shared neurotrophin receptor p75.* Science, 2004. **304**(5672): p. 870-5.

5.   Dechant, G. and Y.A. Barde, *The neurotrophin receptor p75(NTR): novel functions and implications for diseases of the nervous system.* Nat Neurosci, 2002. **5**(11): p. 1131-6.

6.   Bothwell, M., *Tissue localization of nerve growth factor and nerve growth factor receptors.* Curr Top Microbiol Immunol, 1991. **165**: p. 55-70.

7.   Chao, M.V., *Neurotrophins and their receptors: a convergence point for many signalling pathways.* Nat Rev Neurosci, 2003. **4**(4): p. 299-309.

8.   Rabizadeh, S., et al., *Induction of apoptosis by the low-affinity NGF receptor.* Science, 1993. **261**(5119): p. 345-8.

9.   Yamashita, T., K.L. Tucker, and Y.A. Barde, *Neurotrophin binding to the p75 receptor modulates Rho activity and axonal outgrowth.* Neuron, 1999. **24**(3): p. 585-93.

10.   Chittka, A., et al., *The p75NTR-interacting protein SC1 inhibits cell cycle progression by transcriptional repression of cyclin E.* J Cell Biol, 2004. **164**(7): p. 985-96.

11.   Lee, K.F., et al., *Targeted mutation of the gene encoding the low affinity NGF receptor p75 leads to deficits in the peripheral sensory nervous system.* Cell, 1992. **69**(5): p. 737-49.

12.   Paul, C.E., et al., *A pro-apoptotic fragment of the p75 neurotrophin receptor is expressed in p75NTRExonIV null mice.* J Neurosci, 2004. **24**(8): p. 1917-23.

13.   von Schack, D., et al., *Complete ablation of the neurotrophin receptor p75NTR causes defects both in the nervous and the vascular system.* Nat Neurosci, 2001. **4**(10): p. 977-8.

14.   Majdan, M., et al., *Transgenic mice expressing the intracellular domain of the p75 neurotrophin receptor undergo neuronal apoptosis.* J Neurosci, 1997. **17**(18): p. 6988-98.

15.   Beattie, M.S., et al., *ProNGF induces p75-mediated death of oligodendrocytes following spinal cord injury.* Neuron, 2002. **36**(3): p. 375-86.

16.   Scott, A.L., J.F. Borisoff, and M.S. Ramer, *Deafferentation and neurotrophin-mediated intraspinal sprouting: a central role for the p75 neurotrophin receptor.* Eur J Neurosci, 2005. **21**(1): p. 81-92.

17.   Copray, S., et al., *Deficient p75 low-affinity neurotrophin receptor expression exacerbates experimental allergic encephalomyelitis in C57/BL6 mice.* J Neuroimmunol, 2004. **148**(1-2): p. 41-53.

18.   Soilu-Hanninen, M., et al., *Treatment of experimental autoimmune encephalomyelitis with antisense oligonucleotides against the low affinity neurotrophin receptor.* J Neurosci Res, 2000. **59**(6): p. 712-21.

19.   Trim, N., et al., *Hepatic stellate cells express the low affinity nerve growth factor receptor p75 and undergo apoptosis in response to nerve growth factor stimulation.* Am J Pathol, 2000. **156**(4): p. 1235-43.

20.   Reddypalli, S., et al., *p75NTR-mediated signaling promotes the survival of myoblasts and influences muscle strength.* J Cell Physiol, 2005. **204**(3): p. 819-29.

21.   Kraemer, R., *Reduced apoptosis and increased lesion development in the flow-restricted carotid artery of p75(NTR)-null mutant mice.* Circ Res, 2002. **91**(6): p. 494-500.

22.   Botchkarev, V.A., et al., *A role for p75 neurotrophin receptor in the control of apoptosis-driven hair follicle regression.* Faseb J, 2000. **14**(13): p. 1931-42.

23.   Kerzel, S., et al., *Pan-neurotrophin receptor p75 contributes to neuronal hyperreactivity and airway inflammation in a murine model of experimental asthma.* Am J Respir Cell Mol Biol, 2003. **28**(2): p. 170-8.

24.   Barker, P.A., *p75NTR is positively promiscuous: novel partners and new insights.* Neuron, 2004. **42**(4): p. 529-33.

25. Rodriguez-Tebar, A., et al., *Binding of neurotrophin-3 to its neuronal receptors and interactions with nerve growth factor and brain-derived neurotrophic factor.* Embo J, 1992. **11**(3): p. 917-22.

26. Nykjaer, A., et al., *Sortilin is essential for proNGF-induced neuronal cell death.* Nature, 2004. **427**(6977): p. 843-8.

27. Butowt, R. and C.S. von Bartheld, *Connecting the dots: trafficking of neurotrophins, lectins and diverse pathogens by binding to the neurotrophin receptor p75NTR.* Eur J Neurosci, 2003. **17**(4): p. 673-80.

28. Yaar, M., et al., *Binding of beta-amyloid to the p75 neurotrophin receptor induces apoptosis. A possible mechanism for Alzheimer's disease.* J Clin Invest, 1997. **100**(9): p. 2333-40.

29. Della-Bianca, V., et al., *Neurotrophin p75 receptor is involved in neuronal damage by prion peptide-(106-126).* J Biol Chem, 2001. **276**(42): p. 38929-33.

30. Tuffereau, C., et al., *Low-affinity nerve-growth factor receptor (P75NTR) can serve as a receptor for rabies virus.* Embo J, 1998. **17**(24): p. 7250-9.

31. Wehrman, T., et al., *Structural and mechanistic insights into nerve growth factor interactions with the TrkA and p75 receptors.* Neuron, 2007. **53**(1): p. 25-38.

32. Yamashita, T., H. Higuchi, and M. Tohyama, *The p75 receptor transduces the signal from myelin-associated glycoprotein to Rho.* J Cell Biol, 2002. **157**(4): p. 565-70.

33. Wang, K.C., et al., *P75 interacts with the Nogo receptor as a co-receptor for Nogo, MAG and OMgp.* Nature, 2002. **420**(6911): p. 74-8.

34. Wong, S.T., et al., *A p75(NTR) and Nogo receptor complex mediates repulsive signaling by myelin-associated glycoprotein.* Nat Neurosci, 2002. **5**(12): p. 1302-8.

35. Domeniconi, M., et al., *MAG induces regulated intramembrane proteolysis of the p75 neurotrophin receptor to inhibit neurite outgrowth.* Neuron, 2005. **46**(6): p. 849-55.

36. Yamashita, T. and M. Tohyama, *The p75 receptor acts as a displacement factor that releases Rho from Rho-GDI.* Nat Neurosci, 2003. **6**(5): p. 461-7.

37. Mi, S., et al., *LINGO-1 is a component of the Nogo-66 receptor/p75 signaling complex.* Nat Neurosci, 2004. **7**(3): p. 221-8.

38. Roux, P.P., et al., *The p75 neurotrophin receptor activates Akt (protein kinase B) through a phosphatidylinositol 3-kinase-dependent pathway.* J Biol Chem, 2001. **276**(25): p. 23097-104.

39. Raile, K., et al., *Glucose regulates expression of the nerve growth factor (NGF) receptors TrkA and p75NTR in rat islets and INS-1E beta-cells.* Regul Pept, 2006. **135**(1-2): p. 30-8.

40. Ramos, A., et al., *Hypo-osmolar stress induces p75NTR expression by activating Sp1-dependent transcription.* J Neurosci, 2007. **27**(6): p. 1498-506.

41. Cassiman, D., et al., *Human and rat hepatic stellate cells express neurotrophins and neurotrophin receptors.* Hepatology, 2001. **33**(1): p. 148-58.

42. Oakley, F., et al., *Hepatocytes express nerve growth factor during liver injury: evidence for paracrine regulation of hepatic stellate cell apoptosis.* Am J Pathol, 2003. **163**(5): p. 1849-58.

43. Kupffer, K., *Ueber Sternzellen der Leber. Briefliche Mitteilung an Professor Waldeyer.* Archiv fur mikroscopische Anatomie und Entwicklungsmechanick, 1876. **12**: p. 353-358.

44. Ito, T. and M. Nemoto, *Uber die Kupfferschen Sternzellen und die "Fettspeicherungszellen" (fat storing cells) in der Blutkapillarenwand der menschlichen Leber.* Okajimas Folia Anat Jpn, 1952. **24**(4): p. 243-58.

45. Wake, K., *"Sternzellen" in the liver: perisinusoidal cells with special reference to storage of vitamin A.* Am J Anat, 1971. **132**(4): p. 429-62.

46. Geerts, A., *History, heterogeneity, developmental biology, and functions of quiescent hepatic stellate cells.* Semin Liver Dis, 2001. **21**(3): p. 311-35.

47. Reeves, H.L. and S.L. Friedman, *Activation of hepatic stellate cells--a key issue in liver fibrosis.* Front Biosci, 2002. **7**: p. d808-26.

48. Tomasek, J.J., et al., *Myofibroblasts and mechano-regulation of connective tissue remodelling.* Nat Rev Mol Cell Biol, 2002. **3**(5): p. 349-63.

49. Taub, R., *Liver regeneration: from myth to mechanism.* Nat Rev Mol Cell Biol, 2004. **5**(10): p. 836-47.

50. Bataller, R. and D.A. Brenner, *Hepatic stellate cells as a target for the treatment of liver fibrosis.* Semin Liver Dis, 2001. **21**(3): p. 437-51.

51.   Baer, H.U., et al., *Transforming growth factor betas and their receptors in human liver cirrhosis.* Eur J Gastroenterol Hepatol, 1998. **10**(12): p. 1031-9.

52.   Schnabl, B., et al., *The role of Smad3 in mediating mouse hepatic stellate cell activation.* Hepatology, 2001. **34**(1): p. 89-100.

53.   Uemura, M., et al., *Smad2 and Smad3 play different roles in rat hepatic stellate cell function and alpha-smooth muscle actin organization.* Mol Biol Cell, 2005. **16**(9): p. 4214-24.

54.   Hellerbrand, C., et al., *The role of TGFbeta1 in initiating hepatic stellate cell activation in vivo.* J Hepatol, 1999. **30**(1): p. 77-87.

55.   Tsukamoto, H., et al., *Anti-adipogenic regulation underlies hepatic stellate cell transdifferentiation.* J Gastroenterol Hepatol, 2006. **21 Suppl 3**: p. S102-5.

56.   She, H., et al., *Adipogenic transcriptional regulation of hepatic stellate cells.* J Biol Chem, 2005. **280**(6): p. 4959-67.

57.   Ikejima, K., et al., *Leptin receptor-mediated signaling regulates hepatic fibrogenesis and remodeling of extracellular matrix in the rat.* Gastroenterology, 2002. **122**(5): p. 1399-410.

58.   Galli, A., et al., *Antidiabetic thiazolidinediones inhibit collagen synthesis and hepatic stellate cell activation in vivo and in vitro.* Gastroenterology, 2002. **122**(7): p. 1924-40.

59.   Friedman, S.L., *Transcriptional regulation of stellate cell activation.* J Gastroenterol Hepatol, 2006. **21 Suppl 3**: p. S79-83.

60.   Mann, J., et al., *Regulation of myofibroblast transdifferentiation by DNA methylation and MeCP2: implications for wound healing and fibrogenesis.* Cell Death Differ, 2007. **14**(2): p. 275-85.

61.   Tox, U. and H.M. Steffen, *Impact of inhibitors of the Renin-Angiotensin-aldosterone system on liver fibrosis and portal hypertension.* Curr Med Chem, 2006. **13**(30): p. 3649-61.

62.   Hashmi, A.Z., et al., *Adenosine inhibits cytosolic calcium signals and chemotaxis in hepatic stellate cells.* Am J Physiol Gastrointest Liver Physiol, 2007. **292**(1): p. G395-401.

63.   Kruglov, E., et al., *Molecular Basis for Calcium Signaling in Hepatic Stellate Cells.* Am J Physiol Gastrointest Liver Physiol, 2007.

64.   Shimizu, I., et al., *Inhibitory effect of oestradiol on activation of rat hepatic stellate cells in vivo and in vitro.* Gut, 1999. **44**(1): p. 127-36.

65.   Oben, J.A., et al., *Hepatic fibrogenesis requires sympathetic neurotransmitters.* Gut, 2004. **53**(3): p. 438-45.

66.   Nieto, N., *Oxidative-stress and IL-6 mediate the fibrogenic effects of rodent Kupffer cells on stellate cells.* Hepatology, 2006. **44**(6): p. 1487-501.

67.   Han, Y.P., et al., *Essential role of matrix metalloproteinases in interleukin-1-induced myofibroblastic activation of hepatic stellate cell in collagen.* J Biol Chem, 2004. **279**(6): p. 4820-8.

68.   March, S., et al., *Identification and functional characterization of the hepatic stellate cell CD38 cell surface molecule.* Am J Pathol, 2007. **170**(1): p. 176-87.

69.   Henderson, N.C., et al., *Galectin-3 regulates myofibroblast activation and hepatic fibrosis.* Proc Natl Acad Sci U S A, 2006. **103**(13): p. 5060-5.

70.   Canbay, A., et al., *Apoptotic body engulfment by a human stellate cell line is profibrogenic.* Lab Invest, 2003. **83**(5): p. 655-63.

71.   Boers, W., et al., *Transcriptional profiling reveals novel markers of liver fibrogenesis: gremlin and insulin-like growth factor-binding proteins.* J Biol Chem, 2006. **281**(24): p. 16289-95.

72.   Jiang, F., C.J. Parsons, and B. Stefanovic, *Gene expression profile of quiescent and activated rat hepatic stellate cells implicates Wnt signaling pathway in activation.* J Hepatol, 2006. **45**(3): p. 401-9.

73.   Senoo, H., et al., *Molecular mechanisms in the reversible regulation of morphology, proliferation and collagen metabolism in hepatic stellate cells by the three-dimensional structure of the extracellular matrix.* J Gastroenterol Hepatol, 1998. **13 Suppl**: p. S19-32.

74.   Gaca, M.D., et al., *Basement membrane-like matrix inhibits proliferation and collagen synthesis by activated rat hepatic stellate cells: evidence for matrix-dependent deactivation of stellate cells.* Matrix Biol, 2003. **22**(3): p. 229-39.

75.   Hazra, S., et al., *Peroxisome proliferator-activated receptor gamma induces a phenotypic switch from activated to quiescent hepatic stellate cells.* J Biol Chem, 2004. **279**(12): p. 11392-401.

76.   Gabele, E., D.A. Brenner, and R.A. Rippe, *Liver fibrosis: signals leading to the amplification of the fibrogenic hepatic stellate cell.* Front Biosci, 2003. **8**: p. d69-77.

77.   Novo, E., et al., *Overexpression of Bcl-2 by activated human hepatic stellate cells: resistance to apoptosis as a mechanism of progressive hepatic fibrogenesis in humans.* Gut, 2006. **55**(8): p. 1174-82.

78.   Balabaud, C., P. Bioulac-Sage, and A. Desmouliere, *The role of hepatic stellate cells in liver regeneration.* J Hepatol, 2004. **40**(6): p. 1023-6.

79.   Uyama, N., et al., *Regulation of cultured rat hepatocyte proliferation by stellate cells.* J Hepatol, 2002. **36**(5): p. 590-9.

80.   Mabuchi, A., et al., *Role of Hepatic Stellate Cells in the Early Phase of Liver Regeneration in Rat: Formation of Tight Adhesion to Parenchymal Cells.* Comp Hepatol, 2004. **3 Suppl 1**: p. S29.

81.   Mabuchi, A., et al., *Role of hepatic stellate cell/hepatocyte interaction and activation of hepatic stellate cells in the early phase of liver regeneration in the rat.* J Hepatol, 2004. **40**(6): p. 910-6.

82.   Kalinichenko, V.V., et al., *Foxf1 +/- mice exhibit defective stellate cell activation and abnormal liver regeneration following CCl4 injury.* Hepatology, 2003. **37**(1): p. 107-17.

83.   Sidelmann, J.J., et al., *Fibrin clot formation and lysis: basic mechanisms.* Semin Thromb Hemost, 2000. **26**(6): p. 605-18.

84.   Sobel, R.A. and M.E. Mitchell, *Fibronectin in multiple sclerosis lesions.* Am J Pathol, 1989. **135**(1): p. 161-8.

85.   Akassoglou, K., et al., *Tissue plasminogen activator-mediated fibrinolysis protects against axonal degeneration and demyelination after sciatic nerve injury.* J Cell Biol, 2000. **149**(5): p. 1157-66.

86.   Akassoglou, K., et al., *Fibrin inhibits peripheral nerve remyelination by regulating Schwann cell differentiation.* Neuron, 2002. **33**(6): p. 861-75.

87.   Valenzuela, R., et al., *Immunoelectrophoretic and immunohistochemical characterizations of fibrinogen derivatives in atherosclerotic aortic intimas and vascular prosthesis pseudo-intimas.* Am J Pathol, 1992. **141**(4): p. 861-80.

88.   Imokawa, S., et al., *Tissue factor expression and fibrin deposition in the lungs of patients with idiopathic pulmonary fibrosis and systemic sclerosis.* Am J Respir Crit Care Med, 1997. **156**(2 Pt 1): p. 631-6.

89.   Carthew, P. and A.G. Smith, *Pathological mechanisms of hepatic tumour formation in rats exposed chronically to dietary hexachlorobenzene.* J Appl Toxicol, 1994. **14**(6): p. 447-52.

90.   Couser, W.G., *Glomerulonephritis.* Lancet, 1999. **353**(9163): p. 1509-15.

91.   Rybarczyk, B.J. and P.J. Simpson-Haidaris, *Fibrinogen assembly, secretion, and deposition into extracellular matrix by MCF-7 human breast carcinoma cells.* Cancer Res, 2000. **60**(7): p. 2033-9.

92.   Adams, R.A., et al., *Fibrin mechanisms and functions in nervous system pathology.* Mol Interv, 2004. **4**(3): p. 163-76.

93.   Dowling, P., et al., *Up-regulated p75NTR neurotrophin receptor on glial cells in MS plaques.* Neurology, 1999. **53**(8): p. 1676-82.

94.   Park, J.A., et al., *Co-induction of p75NTR and p75NTR-associated death executor in neurons after zinc exposure in cortical culture or transient ischemia in the rat.* J Neurosci, 2000. **20**(24): p. 9096-103.

95.   Wang, S., et al., *p75(NTR) mediates neurotrophin-induced apoptosis of vascular smooth muscle cells.* Am J Pathol, 2000. **157**(4): p. 1247-58.

96.   Tokuoka, S., et al., *Disruption of antigen-induced airway inflammation and airway hyper-responsiveness in low affinity neurotrophin receptor p75 gene deficient mice.* Br J Pharmacol, 2001. **134**(7): p. 1580-6.

97.   Donovan, M.J., et al., *Identification of the neurotrophin receptors p75 and trk in a series of Wilms' tumors.* Am J Pathol, 1994. **145**(4): p. 792-801.

98.   Krygier, S. and D. Djakiew, *The neurotrophin receptor p75NTR is a tumor suppressor in human prostate cancer.* Anticancer Res, 2001. **21**(6A): p. 3749-55.

99.   Sachs, B.D., et al., *p75 neurotrophin receptor regulates tissue fibrosis through inhibition of plasminogen activation via a PDE4/cAMP/PKA pathway.* J Cell Biol, submitted.

100.   Casaccia-Bonnefil, P., et al., *Death of oligodendrocytes mediated by the interaction of nerve growth factor with its receptor p75.* Nature, 1996. **383**(6602): p. 716-9.

101. Soilu-Hanninen, M., et al., *Nerve growth factor signaling through p75 induces apoptosis in Schwann cells via a Bcl-2-independent pathway.* J Neurosci, 1999. **19**(12): p. 4828-38.

102. Ricci, A., et al., *Neurotrophin and neurotrophin receptor protein expression in the human lung.* Am J Respir Cell Mol Biol, 2004. **30**(1): p. 12-9.

103. Alpers, C.E., et al., *Nerve growth factor receptor expression in fetal, mature, and diseased human kidneys.* Lab Invest, 1993. **69**(6): p. 703-13.

104. Teitelman, G., et al., *Islet injury induces neurotrophin expression in pancreatic cells and reactive gliosis of peri-islet Schwann cells.* J Neurobiol, 1998. **34**(4): p. 304-18.

105. Zhu, Z., et al., *Up-regulation of p75 neurotrophin receptor (p75NTR) is associated with apoptosis in chronic pancreatitis.* Dig Dis Sci, 2003. **48**(4): p. 717-25.

106. Aimi, Y., et al., *Immunohistochemical localization of low-affinity nerve growth factor receptor in the enteric nervous system of adult rats.* Histochem J, 1997. **29**(7): p. 529-37.

107. Kondyli, M., J. Varakis, and M. Assimakopoulou, *Expression of p75NTR and Trk neurotrophin receptors in the enteric nervous system of human adults.* Anat Sci Int, 2005. **80**(4): p. 223-8.

108. Pezzati, P., et al., *Expression of nerve growth factor receptor immunoreactivity on follicular dendritic cells from human mucosa associated lymphoid tissues.* Immunology, 1992. **76**(3): p. 485-90.

109. Jippo, T., et al., *Involvement of transcription factor encoded by the mouse mi locus (MITF) in expression of p75 receptor of nerve growth factor in cultured mast cells of mice.* Blood, 1997. **90**(7): p. 2601-8.

110. Hermes, B., et al., *Decreased cutaneous expression of stem cell factor and of the p75NGF receptor in urticaria.* Br J Dermatol, 2003. **148**(3): p. 411-7.

111. Flugel, A., et al., *Anti-inflammatory activity of nerve growth factor in experimental autoimmune encephalomyelitis: inhibition of monocyte transendothelial migration.* Eur J Immunol, 2001. **31**(1): p. 11-22.

112. Barouch, R., et al., *Nerve growth factor regulates TNF-alpha production in mouse macrophages via MAP kinase activation.* J Leukoc Biol, 2001. **69**(6): p. 1019-26.

113.   Nassenstein, C., et al., *The neurotrophins nerve growth factor, brain-derived neurotrophic factor, neurotrophin-3, and neurotrophin-4 are survival and activation factors for eosinophils in patients with allergic bronchial asthma.* J Exp Med, 2003. **198**(3): p. 455-67.

114.   Raap, U., et al., *Brain-derived neurotrophic factor is increased in atopic dermatitis and modulates eosinophil functions compared with that seen in nonatopic subjects.* J Allergy Clin Immunol, 2005. **115**(6): p. 1268-75.

115.   Perez-Pinera, P., et al., *Thymocyte depletion affects neurotrophin receptor expression in thymic stromal cells.* J Anat, 2006. **208**(2): p. 231-8.

116.   Mousavi, K. and B.J. Jasmin, *BDNF is expressed in skeletal muscle satellite cells and inhibits myogenic differentiation.* J Neurosci, 2006. **26**(21): p. 5739-49.

117.   Micera, A., et al., *The pro-fibrogenic effect of nerve growth factor on conjunctival fibroblasts is mediated by transforming growth factor-beta.* Clin Exp Allergy, 2005. **35**(5): p. 650-6.

118.   Popnikolov, N.K., et al., *Diagnostic utility of p75 neurotrophin receptor (p75NTR) as a marker of breast myoepithelial cells.* Mod Pathol, 2005. **18**(12): p. 1535-41.

119.   Kanai-Azuma, M., et al., *Nerve growth factor promotes giant-cell transformation of mouse trophoblast cells in vitro.* Biochem Biophys Res Commun, 1997. **231**(2): p. 309-15.

120.   Perez, M., et al., *Loss of low-affinity nerve growth factor receptor during malignant transformation of the human prostate.* Prostate, 1997. **30**(4): p. 274-9.

121.   Li, C., et al., *Expression of nerve growth factor (NGF), and its receptors TrkA and p75 in the reproductive organs of the adult male rats.* Zoolog Sci, 2005. **22**(8): p. 933-7.

122.   Weiler-Guettler, H., et al., *A Targeted Point Mutation in Thrombomodulin Generates Viable Mice with a Prethrombotic State.* J. Clin. Invest., 1998. **101**(9): p. 1983-1991.

123.   Livak, K.J. and T.D. Schmittgen, *Analysis of relative gene expression data using real-time quantitative PCR and the 2(-Delta Delta C(T)) Method.* Methods, 2001. **25**(4): p. 402-8.

124. Trogan, E., et al., *Laser capture microdissection analysis of gene expression in macrophages from atherosclerotic lesions of apolipoprotein E-deficient mice.* Proc Natl Acad Sci U S A, 2002. **99**(4): p. 2234-9.

125. Cui, C.-Y., et al., *EDA targets revealed by skin gene expression profiles of wild-type, Tabby and Tabby EDA-A1 transgenic mice.* Hum. Mol. Genet., 2002. **11**(15): p. 1763-1773.

126. Monteiro de Castro, G., et al., *Th1 and Th2 cytokine immunomodulation by gangliosides in experimental autoimmune encephalomyelitis.* Cytokine, 2004. **26**(4): p. 155-163.

127. Wang, X. and B. Seed, *A PCR primer bank for quantitative gene expression analysis.* Nucl. Acids Res., 2003. **31**(24): p. e154.

128. Swaney, J.S., et al., *Inhibition of cardiac myofibroblast formation and collagen synthesis by activation and overexpression of adenylyl cyclase.* Proc Natl Acad Sci U S A, 2005. **102**(2): p. 437-42.

129. Hoshijima, M., et al., *The low molecular weight GTPase Rho regulates myofibril formation and organization in neonatal rat ventricular myocytes. Involvement of Rho kinase.* J Biol Chem, 1998. **273**(13): p. 7725-30.

130. Higuchi, H., et al., *Functional inhibition of the p75 receptor using a small interfering RNA.* Biochem Biophys Res Commun, 2003. **301**(3): p. 804-9.

131. Yamada, A., et al., *Rapid and sensitive enzyme-linked immunosorbent assay for measurement of HGF in rat and human tissues.* Biomed Res, 1995. **16**: p. 105-114.

132. Galijatovic, A., et al., *The Human CYP1A1 Gene Is Regulated in a Developmental and Tissue-specific Fashion in Transgenic Mice.* J. Biol. Chem., 2004. **279**(23): p. 23969-23976.

133. Sun, D., et al., *Increasing cell membrane potential and GABAergic activity inhibits malignant hepatocyte growth.* Am J Physiol Gastrointest Liver Physiol, 2003. **285**(1): p. G12-19.

134. Everse, S.J., H. Pelletier, and R.F. Doolittle, *Crystallization of fragment D from human fibrinogen.* Protein Sci, 1995. **4**(5): p. 1013-6.

135. Johnsson, B., S. Lofas, and G. Lindquist, *Immobilization of proteins to a carboxymethyldextran-modified gold surface for biospecific interaction analysis in surface plasmon resonance sensors.* Anal Biochem, 1991. **198**(2): p. 268-77.

136.	Andersson, K., M. Hamalainen, and M. Malmqvist, *Identification and optimization of regeneration conditions for affinity-based biosensor assays. A multivariate cocktail approach.* Anal Chem, 1999. **71**(13): p. 2475-81.

137.	Bugge, T.H., et al., *Loss of fibrinogen rescues mice from the pleiotropic effects of plasminogen deficiency.* Cell, 1996. **87**(4): p. 709-19.

138.	Ng, V.L., et al., *Plasminogen deficiency results in poor clearance of non-fibrin matrix and persistent activation of hepatic stellate cells after an acute injury.* J Hepatol, 2001. **35**(6): p. 781-9.

139.	Bataller, R. and D.A. Brenner, *Liver fibrosis.* J Clin Invest, 2005. **115**(2): p. 209-18.

140.	Weiskirchen, R., et al., *Comparative evaluation of gene delivery devices in primary cultures of rat hepatic stellate cells and rat myofibroblasts.* BMC Cell Biol, 2000. **1**: p. 4.

141.	Roux, P.P., et al., *The p75 neurotrophin receptor activates Akt (protein kinase B) through a phosphatidylinositol 3-kinase-dependent pathway.* J Biol Chem, 2001. **276**(25): p. 23097-104.

142.	Verdi, J.M., et al., *p75LNGFR regulates Trk signal transduction and NGF-induced neuronal differentiation in MAH cells.* Neuron, 1994. **12**(4): p. 733-45.

143.	Yee, H.F., Jr., *Rho directs activation-associated changes in rat hepatic stellate cell morphology via regulation of the actin cytoskeleton.* Hepatology, 1998. **28**(3): p. 843-50.

144.	Kato, M., et al., *Role of Rho small GTP binding protein in the regulation of actin cytoskeleton in hepatic stellate cells.* J Hepatol, 1999. **31**(1): p. 91-9.

145.	Maekawa, M., et al., *Signaling from Rho to the actin cytoskeleton through protein kinases ROCK and LIM-kinase.* Science, 1999. **285**(5429): p. 895-8.

146.	Hoshijima, M., et al., *The Low Molecular Weight GTPase Rho Regulates Myofibril Formation and Organization in Neonatal Rat Ventricular Myocytes. INVOLVEMENT OF Rho KINASE.* J. Biol. Chem., 1998. **273**(13): p. 7725-7730.

147.	Hu, Z., et al., *Expression of hepatocyte growth factor and c-met genes during hepatic differentiation and liver development in the rat.* Am J Pathol, 1993. **142**(6): p. 1823-30.

148.   Maher, J.J., *Cell-specific expression of hepatocyte growth factor in liver. Upregulation in sinusoidal endothelial cells after carbon tetrachloride.* J Clin Invest, 1993. **91**(5): p. 2244-52.

149.   Mosesson, M.W., K.R. Siebenlist, and D.A. Meh, *The structure and biological features of fibrinogen and fibrin.* Ann N Y Acad Sci, 2001. **936**: p. 11-30.

150.   Gaffney, P.J., *Fibrin degradation products. A review of structures found in vitro and in vivo.* Ann N Y Acad Sci, 2001. **936**: p. 594-610.

151.   Cosgaya, J.M., J.R. Chan, and E.M. Shooter, *The neurotrophin receptor p75NTR as a positive modulator of myelination.* Science, 2002. **298**(5596): p. 1245-8.

152.   Yamashita, T., et al., *Multiple signals regulate axon regeneration through the nogo receptor complex.* Mol Neurobiol, 2005. **32**(2): p. 105-11.

153.   Zampieri, N. and M.V. Chao, *Mechanisms of neurotrophin receptor signalling.* Biochem Soc Trans, 2006. **34**(Pt 4): p. 607-11.

154.   Chao, M.V., *Neurotrophins and their receptors: a convergence point for many signalling pathways.* Nat Rev Neurosci, 2003. **4**(4): p. 299-309.

155.   Teng, K.K. and B.L. Hempstead, *Neurotrophins and their receptors: signaling trios in complex biological systems.* Cell Mol Life Sci, 2004. **61**(1): p. 35-48.

156.   Reichardt, L.F., *Neurotrophin-regulated signalling pathways.* Philos Trans R Soc Lond B Biol Sci, 2006. **361**(1473): p. 1545-64.

157.   Power, R.F., et al., *Dopaminergic and ligand-independent activation of steroid hormone receptors.* Science, 1991. **254**(5038): p. 1636-9.

158.   Li, X.A., et al., *A novel ligand-independent apoptotic pathway induced by scavenger receptor class B, type I and suppressed by endothelial nitric-oxide synthase and high density lipoprotein.* J Biol Chem, 2005. **280**(19): p. 19087-96.

159.   Vischer, H.F., R. Leurs, and M.J. Smit, *HCMV-encoded G-protein-coupled receptors as constitutively active modulators of cellular signaling networks.* Trends Pharmacol Sci, 2006. **27**(1): p. 56-63.

160.   Culig, Z., *Androgen receptor cross-talk with cell signalling pathways.* Growth Factors, 2004. **22**(3): p. 179-84.

161. Monroe, J.G., *Ligand-independent tonic signaling in B-cell receptor function.* Curr Opin Immunol, 2004. **16**(3): p. 288-95.

162. Roskams, T., et al., *Neuroregulation of the neuroendocrine compartment of the liver.* Anat Rec A Discov Mol Cell Evol Biol, 2004. **280**(1): p. 910-23.

163. Oben, J.A., et al., *Acetylcholine promotes the proliferation and collagen gene expression of myofibroblastic hepatic stellate cells.* Biochem Biophys Res Commun, 2003. **300**(1): p. 172-7.

164. Jiang, J.G., et al., *Transcriptional regulation of the hepatocyte growth factor (HGF) gene by the Sp family of transcription factors.* Oncogene, 1997. **14**(25): p. 3039-49.

165. Takahra, T., et al., *Induction of myofibroblast MMP-9 transcription in three-dimensional collagen I gel cultures: regulation by NF-kappaB, AP-1 and Sp1.* Int J Biochem Cell Biol, 2004. **36**(2): p. 353-63.

166. Ebens, A., et al., *Hepatocyte growth factor/scatter factor is an axonal chemoattractant and a neurotrophic factor for spinal motor neurons.* Neuron, 1996. **17**(6): p. 1157-72.

167. Yang, X.M., et al., *Autocrine hepatocyte growth factor provides a local mechanism for promoting axonal growth.* J Neurosci, 1998. **18**(20): p. 8369-81.

168. Pipes, G.C., E.E. Creemers, and E.N. Olson, *The myocardin family of transcriptional coactivators: versatile regulators of cell growth, migration, and myogenesis.* Genes Dev, 2006. **20**(12): p. 1545-56.

169. Rolfe, B.E., et al., *Rho and vascular disease.* Atherosclerosis, 2005. **183**(1): p. 1-16.

170. Bugge, T.H., et al., *Plasminogen deficiency causes severe thrombosis but is compatible with development and reproduction.* Genes Dev, 1995. **9**(7): p. 794-807.

171. Kisseleva, T. and D.A. Brenner, *Hepatic stellate cells and the reversal of fibrosis.* J Gastroenterol Hepatol, 2006. **21 Suppl 3**: p. S84-7.

172. Muller, B., et al., *Two-step binding mechanism of fibrinogen to alpha IIb beta 3 integrin reconstituted into planar lipid bilayers.* J Biol Chem, 1993. **268**(9): p. 6800-8.

173.   Zhou, L., et al., *Differential ligand binding specificities of recombinant CD11b/CD18 integrin I-domain.* J Biol Chem, 1994. **269**(25): p. 17075-9.

174.   Ge, M., et al., *Fibrinogen degradation product fragment D increases endothelial monolayer permeability.* Am J Physiol, 1991. **261**(4 Pt 1): p. L283-9.

175.   Fischer, E.G., et al., *Effect of fibrinogen fragments D and E on the adhesive properties of human granulocytes to venous endothelial cells.* Haemostasis, 1991. **21**(3): p. 141-6.

176.   Lominadze, D., et al., *Fibrinogen and fragment D-induced vascular constriction.* Am J Physiol Heart Circ Physiol, 2005. **288**(3): p. H1257-64.

177.   Spraggon, G., S.J. Everse, and R.F. Doolittle, *Crystal structures of fragment D from human fibrinogen and its crosslinked counterpart from fibrin.* Nature, 1997. **389**(6650): p. 455-62.